

Intestinal overgrowth of *Candida albicans* exacerbates bleomycin-induced pulmonary fibrosis in mice with dysbiosis

Short running title:

Effect of changes in the intestinal fungal microbiota on pulmonary fibrosis

Authors:

Takahiro Yamada¹, Taku Nakashima^{1*}, Takeshi Masuda¹, Shinjiro Sakamoto¹,
Kakuhiro Yamaguchi¹, Yasushi Horimasu¹, Shintaro Miyamoto¹, Hiroshi Iwamoto¹,
Kazunori Fujitaka¹, Hironobu Hamada², Nobuhiko Kamada^{3,4}, Noboru Hattori¹

Affiliations:

¹Department of Molecular and Internal Medicine, Graduate School of Biomedical and Health Sciences, Hiroshima University, Hiroshima, Japan

²Department of Physical Analysis and Therapeutic Sciences, Graduate School of Biomedical and Health Sciences, Hiroshima University, Hiroshima, Japan

³Division of Gastroenterology and Hepatology, Department of Internal Medicine, University of Michigan, Ann Arbor, MI, USA.

⁴Laboratory of Microbiology and Immunology, WPI Immunology Frontier Research Center, Osaka University, Suita, Osaka, Japan

***Corresponding author:**

Taku Nakashima, M.D., Ph.D.

Department of Molecular and Internal Medicine, Graduate School of Biomedical and Health Sciences, Hiroshima University, 1-2-3 Kasumi, Minami-ku, Hiroshima, 734-8551, JAPAN;

Phone: +81-(82)-257-5196

Fax: +81-(82)-255-7360

E-mail: tnaka@hiroshima-u.ac.jp

Co-authors :

Takahiro Yamada (E-mail: y3htk@yahoo.co.jp)

Takeshi Masuda (E-mail: ta-masuda@hiroshima-u.ac.jp)

Shinjiro Sakamoto (E-mail: s-sakamoto@hiroshima-u.ac.jp)

Kakuhiro Yamaguchi (E-mail: yamaguchikakuhiro@gmail.com)

Yasushi Horimasu (E-mail: yasushi17@hiroshima-u.ac.jp)

Shintaro Miyamoto (E-mail: miyamos@hiroshima-u.ac.jp)

Hiroshi Iwamoto (E-mail: iwamotohiroshig@gmail.com)

Kazunori Fujitaka (E-mail: fujikazu@hiroshima-u.ac.jp)

Hironobu Hamada (E-mail: hirohamada@hiroshima-u.ac.jp)

Nobuhiko Kamada (E-mail: nkamada@umich.edu)

Noboru Hattori (E-mail: nhattori@hiroshima-u.ac.jp)

Data availability statement:

The sequences generated in this study are available in the DDBJ Sequence Read Archive database (Accession Number: DRA015049 and DRA015055). The other data sets generated and analyzed during this study are included in this published article.

Funding:

This work was partially supported by Satake Technology Promotion Foundation grant.

The funders had no role in study design, data collection and analysis, decision to publish, or presentation of the manuscript.

Conflict of interest:

The authors declare that they have no competing interests.

Ethics approval:

All experimental procedures were approved by the Committee on Animal Research at Hiroshima University (approval no. A21-98) and were conducted in accordance with the Guide for the Care and Use of Laboratory Animals, 8th ed, 2010 (National Institutes of Health, Bethesda, MD, USA).

Word Count: 4106

ABSTRACT

Increasing evidence indicates an interaction between the intestinal microbiota and diseases in distal organs. However, the relationship between pulmonary fibrosis and the intestinal microbiota, especially intestinal fungal microbiota, is poorly understood. Thus, this study aimed to determine the effects of changes in the intestinal fungal microbiota on the pathogenesis of pulmonary fibrosis.

Mice with intestinal overgrowth of *Candida albicans* (*C. albicans*), which was established by oral administration of antibiotics plus *C. albicans*, showed accelerated bleomycin-induced pulmonary fibrosis relative to the control mice (i.e., without *C. albicans* treatment). In addition, the mice with intestinal overgrowth of *C. albicans* showed enhanced Th17-type immunity, and treatment with IL-17A neutralizing antibody alleviated pulmonary fibrosis in these mice but not in the control mice. This result indicates that IL-17A is involved in the pathogenesis of *C. albicans*-exacerbated pulmonary fibrosis. Even before bleomycin treatment, the expression of *Rorc*, the master regulator of Th17, was already upregulated in the pulmonary lymphocytes of the mice with intestinal overgrowth of *C. albicans*. Subsequent administration of bleomycin triggered these Th17-skewed lymphocytes to produce IL-17A, which enhanced endothelial–mesenchymal transition.

These results suggest that intestinal overgrowth of *C. albicans* exacerbates pulmonary fibrosis via IL-17A-mediated endothelial–mesenchymal transition. Thus, it might be a potential therapeutic target in pulmonary fibrosis. This study may serve as a basis for using intestinal fungal microbiota as novel therapeutic targets in pulmonary fibrosis.

Keywords: *Candida albicans*, pulmonary fibrosis, Th17, IL-17A, endothelial–mesenchymal transition, fungal microbiota, intestinal microbiota

INTRODUCTION

Idiopathic pulmonary fibrosis (IPF) is a refractory respiratory disease characterized by progressive collagen deposition in the lungs. Antifibrotic agents reduce the decline in forced vital capacity in patients with IPF [1–4]. However, the prognosis of these patients remains poor, with a reported average survival of 3–5 years. Effective treatment options for progressive pulmonary fibrosis are limited, and novel therapies need to be developed urgently.

The microbiota is a promising therapeutic target for refractory diseases. The interaction between gut microbiota and host immunity influences the progression and therapeutic responsiveness of underlying diseases in distal organs, including the lungs, via modification of immune cells and their cytokine production [5]. Furthermore, the lungs, previously thought to be sterile, have their own microbiota associated with various respiratory diseases [6,7]. The microbiota in bronchoalveolar lavage fluid (BALF) is altered in murine bleomycin (BLM)-induced pulmonary fibrosis and human IPF.

Relative to conventionally housed mice, germ-free mice show alleviated BLM-induced pulmonary fibrosis. Furthermore, IPF patients with low bacterial abundance in BALF have better prognosis than those with high bacterial abundance in BALF [8–10]. A recent study has shown that outer membrane vesicles produced by lung commensal bacteria exacerbate murine pulmonary fibrosis, and eliminating these bacteria with antibiotics alleviates the disease [11]. These studies suggest that targeting the microbiota is a promising therapeutic strategy to improve pulmonary fibrosis.

In addition to commensal bacteria, fungi also play important roles in the microbiota [12]. *Candida* species are prototypic fungal pathogens indigenous in the intestine.

Antibiotics can alter the bacterial and fungal microbiota; for example, antibiotic administration increases the proliferation of intestinal *Candida* [13]. Intestinal *Candida* proliferation can exacerbate murine allergic airway inflammation via M2 macrophages induction [14,15] and can induce Th17 immune reactions in human peripheral blood mononuclear cells and exacerbate fungus-related airway inflammation via cross-reactivity with other fungi [16]. These studies suggest that changes in the intestinal fungal microbiota affect the distal organs, as well as the bacterial microbiota. M2 macrophages are increased in fibrotic areas in murine pulmonary fibrosis and human IPF lungs and exacerbate fibrosis by producing IL-13 and TGF- β 1 [17]. Meanwhile, IL-17A exacerbates pulmonary fibrosis by mobilizing neutrophils and inducing inflammatory cytokines [18–21]. It also induces epithelial–mesenchymal transition (EMT) and fibroblast activation *in vitro* [20,22,23]. Thus, antibiotic-induced changes in the intestinal fungal microbiota, especially the genus *Candida*, may affect the pathogenesis of pulmonary fibrosis by increasing M2 macrophages or IL-17A. However, little is known about the association between the intestinal fungal microbiota and pulmonary fibrosis. We hypothesized that intestinal *Candida* proliferation exacerbates pulmonary fibrosis. This study aimed to determine the effects of antibiotic-induced changes in the intestinal fungal microbiota on the pathogenesis of pulmonary fibrosis.

MATERIALS AND METHODS

Mice and intestinal *Candida* proliferation

Specific pathogen-free male C57BL/6J mice (6–8 weeks old) were purchased from Charles River Laboratories, Japan (Yokohama, Japan). The mice were housed in a pathogen-free environment with free access to food and distilled water supplemented with or without cefoperazone (CPZ, 0.4 mg/ml, Tokyo Chemical Industry, Tokyo, Japan), clindamycin (CLDM, 0.5 mg/ml, Tokyo Chemical Industry), fluconazole (FLCZ, 0.5 mg/ml, Tokyo Chemical Industry), and *Candida albicans* (*C. albicans*). The drinking water bottles were changed every 3 days. *C. albicans* was obtained from the Infection Diseases Laboratory of Hiroshima University Hospital. *C. albicans* cultured on Sabouraud agar (2×10^8 colony forming units, Nissui Pharmaceutical, Tokyo, Japan) was mixed in 200 ml of sterile water and administered to the mice ad libitum. To confirm colonization, murine BALF and cecal contents were collected at the time of sacrifice and then cultured on CHROMagar (Kanto Chemical, Tokyo, Japan) for 48 h. Then, colony formation and color tone were evaluated.

All experimental procedures were approved by the Committee on Animal Research at Hiroshima University (approval no. A21-98) and were conducted in accordance with the Guide for the Care and Use of Laboratory Animals, 8th ed, 2010 (National Institutes of Health, Bethesda, MD, USA).

BLM-induced pulmonary fibrosis

After being intraperitoneally anesthetized with medetomidine hydrochloride (0.3 mg/kg body weight, Kyoritsu Seiyaku, Tokyo, Japan), midazolam (4.0 mg/kg body weight, Sandoz K.K., Tokyo, Japan), and butorphanol tartrate (5.0 mg/kg body weight, Meiji Seika Pharma, Tokyo, Japan), the mice were administered with BLM (2.0 mg/kg body weight, Nippon Kayaku, Tokyo, Japan) to induce pulmonary fibrosis. Except where indicated, the mice were sacrificed on day 14 after BLM administration, and blood, lung, BALF and intestinal samples were collected.

Histological examination

Murine lungs and ceca were fixed in a 2% formalin solution. After embedding in paraffin, the tissues were stained with hematoxylin–eosin, periodic acid Schiff (PAS), and Masson's Trichrome stain. Immunohistochemical staining was performed as follows: paraffin-embedded ceca tissues were stained with anti-ROR γ rabbit monoclonal antibody (Clone: EPR20006, Abcam, Cambridge, UK) as primary antibody, and peroxidase labeling anti-rabbit IgG polyclonal antibody (#424144, Nichirei, Tokyo, Japan) as secondary antibody.

Hydroxyproline assay

Hydroxyproline content was measured to evaluate the severity of pulmonary fibrosis. Murine left lungs were harvested and homogenized in 1 ml of PBS (Nacalai Tesque, Kyoto, Japan) and 1 ml of 12 N HCl and then hydrolyzed at 120°C for 16 h. In a 96-well plate, 5 μ L of the hydrolyzed sample, 10 μ L of citrate/acetate buffer (5% citric

acid, Sigma-Aldrich, St. Louis, MO, USA; 1.2% glacial acetic acid, Sigma-Aldrich; 7.25% sodium acetate, Sigma-Aldrich; and 3.4% sodium hydroxide, Nacalai Tesque), and 100 μ L of chloramine T solution (0.141 g chloramine T [Sigma-Aldrich] added to 8 ml of citrate/acetate buffer, 1 ml of 1-propanol [Sigma-Aldrich], and 1 ml of deionized distilled water) were mixed. After incubation at room temperature for 30 min, 100 μ L of Ehrlich's reagent (1.25 g p-dimethylaminobenzaldehyde [Sigma-Aldrich] in 4.65 ml of 1-propanol and 1.95 ml of 70% perchloric acid [Sigma-Aldrich]) was added, and the mixture was incubated at 65°C for 30 min. The absorbance of each sample was obtained at 540 nm on a plate reader (iMARK, Bio-Rad, Hercules, CA, USA).

Flow cytometry and fluorescence-activated cell sorting (FACS)

Single-cell suspensions were obtained as follows. The right lower lobe of the murine lung was excised, cut into small pieces, and then incubated in RPMI (Thermo Fisher Scientific, Waltham, MA, USA) supplemented with 1.0 mg/ml collagenase A (Roche, Basel, Switzerland) at 37°C for 30 min. After passing through a 70 μ m cell strainer, red blood cells were removed using RBC lysis buffer (Thermo Fisher Scientific). For mouse blood samples, erythrocyte lysis was repeated twice to obtain samples for flow cytometry. Cell suspensions were blocked with anti-CD16/32 antibody (Fc γ R, clone 93, BioLegend, San Diego, CA, USA) and then reacted with fluorescent antibodies diluted to the appropriate concentration. For intracellular staining, fixation and penetration were performed using the Cytofix/Cytoperm Kit (BD Biosciences, San Jose, CA, USA). For cytokine staining, the cells were added with GolgiStop (BD Biosciences) and then incubated for 4 h before antibody attachment. The fluorescent antibodies used are listed

in Table S1. Flow cytometry and FACS were performed using a FACS Aria II (BD Biosciences), and data were analyzed using FlowJo (BD Biosciences).

Quantitative PCR (qPCR)

The excised lungs were stored in RNA later (Thermo Fisher Scientific) at -80°C before use. Lungs or collected cells were homogenized with 1 ml of TRIzol Reagent (Life Technologies, Grand Island, NY, USA), and RNA was extracted using the RNeasy Mini Kit (QIAGEN, Venlo, Netherlands). RNA was reverse-transcribed to complementary DNA using the High-Capacity RNA-to-cDNA Kit (Thermo Fisher Scientific) in accordance with the manufacturer's protocol. mRNA expression was evaluated using the TaqMan Gene Expression Master Mix (Thermo Fisher Scientific) and Applied Biosystems 7500 Fast Real-Time PCR System (Thermo Fisher Scientific). The PCR conditions were as follows: 120 s at 94°C , 10 s at 98°C , 30 s at 60°C , 120 s at 68°C , repeated for 40 cycles. The primers used are listed in Table S2.

Enzyme-linked immunosorbent assay (ELISA)

Serum samples were centrifuged at $900 \times g$ for 30 min, and the supernatant was collected. The lower lobes of the right lung of each mouse were homogenized with 1 ml of PBS and then stored at -80°C before measurement. IL-17A levels in the serum and lungs were measured using the LEGEND MAX Mouse IL-17A ELISA Kit (BioLegend) in accordance with the manufacturer's protocol. TGF- β levels in the serum were

measured using Mouse TGF-beta 1 DuoSet ELISA (R&D Systems, Minneapolis, MN, USA).

Anti-IL-17A neutralizing antibody

To antagonize the effects of IL-17A, we intraperitoneally treated the mice with in vivo MAb anti-mouse IL-17 (200 µg/mouse, clone 17F3, Bio X Cell, Lebanon, NH, USA) three times a week from immediately before BLM administration until sacrifice [24]. The control group received the same dose of in vivo MAb mouse IgG1 isotype control (Bio X Cell).

Cell culture

The mouse microvascular endothelial cell line MS1 (MILE SVEN 1, ATCC CRL-2279) was purchased from ATCC (Manassas, VA, USA) and grown in DMEM (Thermo Fisher Scientific) supplemented with 10% fetal bovine serum (Sigma-Aldrich) and 1% penicillin–streptomycin (Thermo Fisher Scientific) at 37°C in a 5% CO₂ incubator. After being incubated with several concentrations of recombinant mouse IL-17A (BioLegend) for the indicated times, cells were harvested using trypsin-EDTA (Thermo Fisher Scientific) and subjected to qPCR, fluorescent immunocytochemistry, and flow cytometry.

Fluorescent immunocytochemistry

Cells were cultured in 48-well plates as described above. After removing the culture medium, the cells were fixed and permeabilized using the Cytfix/Cytoperm Kit (BD Biosciences), and then added with fluorescent antibodies. The antibodies used are listed in Table S1. The cells were stained with DAPI (DOJINDO LABORATORIES, Kumamoto, Japan) to identify the nuclei. All slides were examined under a fluorescence microscope BZ-9000 (KEYENCE, Osaka, Japan). Images were analyzed using ImageJ software.

DNA extraction and sequencing

For microbiological analysis, murine BALF, lungs, and cecal contents were collected under sterile conditions and promptly stored at -80°C . BALF pellets were centrifuged at $10000 \times g$ for 15 min, and the lungs were homogenized before use. Microbial DNA was obtained from each specimen using the NucleoSpin DNA Stool (Takara Bio, Shiga, Japan) in accordance with the manufacturer's protocol. The extracted DNA was measured using Nanodrop (Thermo Fisher Scientific) or Qubit (Thermo Fisher Scientific). Libraries were created for 16S rRNA genes for the bacterial microbiota and ITS for the fungal microbiota and sequenced using Miseq Reagent Kit v3 and MiSeq Reagent Kit v2 (Illumina, San Diego, CA, USA), respectively. The primers used for the sequencing are listed in Table S3. Data analysis was performed using QIIME 2 (<https://qiime2.org/>).

Statistical analyses

All statistical analyses were performed using JMP Pro 16 software (SAS Institute Inc., Cary, NC, USA). Data are presented as box plots. To compare the groups, we performed Mann–Whitney U tests. Statistical significance was set at $P < 0.05$.

RESULTS

Worsening of pulmonary fibrosis by intestinal *C. albicans* proliferation

To mimic intestinal *C. albicans* blooms in human, which requires intestinal dysbiosis, we fed the intervention group mice with water containing antibiotics and exogenous *C. albicans* from 1 week before BLM administration until sacrifice (*Candida* + group). In contrast, the control group mice were fed water containing antibiotics and anti-fungal drug (FLCZ) for the same period to eliminate the indigenous organisms (*Candida* – group) (Fig. 1A). The *Candida* + group mice showed no inflammatory cell infiltration in the intestinal tract, but PAS-positive yeast fungi were found in the mucosal lamina propria, suggesting colonization by *C. albicans* (Fig. 1B, S1A, S1B). In culture method, we observed increased *C. albicans* in the feces obtained from *Candida* + but not *Candida* – group (Fig. 1C). *C. albicans* was not detected in the BALF or lung homogenates from either group (data not shown).

To clarify the effect of intestinal *C. albicans* proliferation on pulmonary fibrosis, we compared hydroxyproline levels, the recommended indicator for lung collagen content, and histological findings (Fig. 1D, E, F). We confirmed that fibrosis was not seen when PBS was administered instead of BLM (Fig. S2). As indicated in the previous report [11], the antibiotic treatment suppressed pulmonary fibrosis (Fig. 1D, E, F: DW vs *Candida* –). The fibrosis ameliorating effect of antibiotics was reversed by intestinal overgrowth of *C. albicans* (Fig. 1D, E, F: *Candida* – vs *Candida* +). The severity of pulmonary fibrosis was significantly higher in the mice from the *Candida* + group than in the mice from the *Candida* – group. Comparison of BALF cell fractions showed a non-significant but increasing trend in neutrophils in the *Candida* + group (Fig. S3). To

exclude the possibility that FLCZ affected the severity of pulmonary fibrosis, we confirmed that FLCZ alone did not affect hydroxyproline levels (Fig. S4).

Analysis of intestinal and pulmonary microbiota

To evaluate the changes caused by antimicrobials, antifungals, and BLM administration, we analyzed the intestinal and pulmonary microbiota using samples obtained from these groups. Analysis of the fungal microbiota using DNA extracted from the specimens revealed that all fungi detected in the stool samples of the mice from the *Candida* + group were *Candida* spp., including *C. albicans*. By contrast, *Candida* spp. were rarely detected in the stool samples of the mice from the *Candida* – group, and various fungi, including *Saccharomyces* spp., were identified (Fig. 2A, B, S5A). Although *Candida* spp. were found in the BALF and lung samples of the mice from both groups, no significant difference in the percentage of *Candida* was detected (Fig. 2C, D, E, F, S5B, S5C). Sequencing analysis of the bacterial microbiota revealed the presence of *Firmicutes* spp. and *Proteobacteria* spp. in the stool samples of the mice from the *Candida* – and *Candida* + groups, and no significant difference in the abundance of these species was found between the two groups (Fig. S6A). The majority of bacteria were difficult to identify in the BALF and lungs, and no particular difference was observed (Fig. S6B, S6C).

Pulmonary fibrosis aggravated by *C. albicans* is mediated by Th17 (IL-17A)

We analyzed lung cell fractions through flow cytometry to determine the cell type that contributed to the exacerbation of pulmonary fibrosis in the *Candida* + group (Fig. S7A, S7B). No differences in M2 macrophage (CD45⁺/F4/80⁺/CD11c⁺/CD206⁺) or Treg (CD3⁺/CD4⁺/CD25⁺) fractions were found between the groups, whereas Th17 (CD3⁺/CD4⁺/IL-17A⁺) was markedly elevated in the *Candida* + group (Fig. 3A). Furthermore, there was a positive correlation between lung hydroxyproline content and Th17 (Fig. S8). Similarly, qPCR using lung tissues (Fig. 3B) and ELISA using serum and lung tissues (Fig. 3C) revealed that the expression of the Th17 cytokine IL-17A (*Il17a*) was significantly higher in the mice from the *Candida* + group than in those from the *Candida* – group. We found no difference in the expression of *Tbx21* and *Gata3*, the master regulators of Th1 and Th2 (Fig. S9A). TGF- β (*Tgfb*), one of the key profibrotic mediators, also did not differ between groups (Fig. S9B, S9C). Based on these results, we hypothesized that Th17/IL-17A mainly contributed to the difference in pulmonary fibrosis between the two groups. To test this hypothesis, we neutralized IL-17A using anti-IL-17A neutralizing antibodies (Fig. S10). In fecal cultures, there was no apparent difference in *Candida* colonization regardless of the neutralizing antibody administration (Fig. S11). However, results showed that the administration of IL-17A neutralizing antibody significantly decreased the hydroxyproline levels and pathological features in the mice from the *Candida* + group but not in those from the *Candida* – group (Fig. 3D, E, F), suggesting that the worsening of fibrosis in the mice from the *Candida* + group was mediated by IL-17A.

To confirm whether the induction of Th17 was associated with intestinal *C. albicans* proliferation, we evaluated the relationship between intestinal *C. albicans* detection and lung Th17 induction 14 days after BLM treatment under other settings. We compared

pulmonary fibrosis established in mice fed water alone (DW group) versus mice fed water containing *C. albicans* without antibiotics (*C. albicans* w/o ABx group) (Fig. S12A). In the *C. albicans* w/o ABx group, the *C. albicans* colony formation was not numerous but could be detected in fecal culture, and lung Th17 was significantly increased compared to DW group (Fig. S12B, S12C). However, no difference in hydroxyproline levels between the two groups was detected (Fig. S12D). When the mice were fed water containing antibiotics without *C. albicans*, fecal *C. albicans* was irregularly detected in some mice as shown ABx (*C. albicans* +) in Figure S13A, and lung Th17 levels tended to increase in these mice (Fig. S13B).

Mechanism by which intestinal overgrowth of *C. albicans* induces lung Th17

We examined the mechanism by which the intestinal overgrowth of *C. albicans* promotes Th17 in the lungs. Flow cytometric analysis of lung cells before BLM administration did not show an increase in the number of Th17 (CD3⁺/CD4⁺/IL-17A⁺) cells (Fig. 3G). *C. albicans* was not detected in the blood or BALF cultures (data not shown), which excluded the possibility that *C. albicans* migrated to the lungs. We also explored the possibility that lymphocytes transformed to Th17 in the gut migrated to the lungs through the bloodstream, but flow cytometry results revealed no IL-17A⁺ cells in the blood obtained before or after BLM administration (Fig. 3H). We then evaluated ROR γ t (*Rorc*), a master regulator of Th17 [25]. Lung CD4⁺ lymphocytes (CD3⁺/CD4⁺) were sorted before BLM administration, RNA was extracted, and qPCR was performed. The mice in the *Candida* + group showed significantly higher *Rorc* mRNA expression than those in the *Candida* – group, even though no difference in *Il17a* mRNA

expression was found between the mice from these two groups (Fig. 3I). To seek for the origin of ROR γ t-expressing cells, immunohistochemical staining of ceca tissue obtained from mice before BLM administration was performed. As a result, ROR γ t-positive cells were exclusively found in the *Candida* + group compared to the *Candida* – group (Fig. 3J).

Involvement of endothelial–mesenchymal transition in the exacerbation of pulmonary fibrosis mediated by IL-17A

We further investigated the mechanism by which IL-17A exacerbates pulmonary fibrosis. IL-17A reportedly exacerbates pulmonary fibrosis by mobilizing neutrophils, inducing inflammatory cytokines, promoting EMT, and activating fibroblasts *in vitro* [20,22,23]. To investigate whether these phenomena occurred in the present model, we conducted flow cytometry using lung cells obtained from mice 7 days after BLM treatment (Fig. S14A, S14B, S14C). In the *Candida* + group, the number of cells expressing epithelial markers decreased, whereas that of epithelial cells co-expressing mesenchymal markers tended to increase, suggesting that epithelial damage and EMT occurred (Fig. 4A). Similarly, the number of α SMA⁺/Col1A1⁺ fibroblasts increased, indicating that fibroblasts were converted to myofibroblasts, the activated form of fibroblasts (Fig. 4B). Furthermore, the number of endothelial cells decreased, whereas that of endothelial cells co-expressing mesenchymal markers increased, suggesting that endothelial damage and endothelial–mesenchymal transition (EndMT) occurred (Fig. 4C). Moreover, EndMT was suppressed when mice were treated with anti-IL-17A neutralizing antibody (Fig. 4D). To confirm whether this EndMT was caused by IL-

17A, we cultured murine endothelial cell line MS1 in a medium supplemented with various concentrations of IL-17A. Results of qPCR showed that the mRNA expression of mesenchymal markers (*Fn*, *Colla1*, and *Acta2*) and EndMT markers (*Snail1* and *Snail2*) increased in the cells cultured with IL-17A (Fig. 4E). Flow cytometry revealed that the supplementation of IL-17A decreased the expression of endothelial markers, but increased the expression of EndMT markers (Fig. 4F). Furthermore, fluorescent immunocytochemistry showed that the expression of α SMA and *Colla1* proteins was upregulated in the MS1 cells cultured with IL-17A (Fig. 4G, H), suggesting that IL-17A may exacerbate pulmonary fibrosis not only by promoting EMT and activating fibroblasts, as previously reported, but also by inducing EndMT. Figure 5 summarizes the findings of the current study.

DISCUSSION

Changes in the microbiota have been implicated not only in gastrointestinal diseases but also in diseases in various organs, including the lungs. Regarding pulmonary fibrosis, a high bacterial load in BALF is associated with a poor prognosis in patients with IPF, and removal of the pulmonary microbiota suppresses BLM-induced pulmonary fibrosis in mice [11]. However, the role of the intestinal microbiota, especially fungal microbiota, in the pathophysiology of pulmonary fibrosis remains unclear. In addition, a clinical trial involving antibiotics administration in patients with IPF failed to improve their prognosis [26]. In humans, administration of antibiotics causes yeast growth in stools [13], and intestinal yeast growth, including *Candida*, due to antibiotic administration may enhance pulmonary fibrosis, as we have shown in the present study. To achieve the microbiota-targeted treatment of IPF, further studies need not only to eliminate specific bacteria but also to consider intestinal dysbiosis, especially antibiotic-induced changes in the fungal microbiota, including *C. albicans*. The effects of the intestinal and fungal microbiota warrant further investigation.

Changes in the intestinal microbiota affect various pathophysiological conditions, such as the efficacy of anticancer chemotherapy. Some studies have reported microbiota-associated changes in T cell phenotype and cytokine production; however, the precise mechanisms by which the intestinal microbiota affects distant organs have not been fully elucidated. In a mouse model of allergic airway inflammation, intestinal overgrowth of *Candida* and its produced factors, such as prostaglandins, results in the activation of lung M2 macrophages [14], which was not observed in the current model. Similarly, no changes in Th1, Th2 or TGF- β were observed (Fig. S9A, S9B, S9C).

Instead, ROR γ t (*Rorc*) expressing Th17-skewed lymphocytes in the ceca and lungs increased even before induction of pulmonary fibrosis. Our results suggest that the proliferation of *C. albicans* in the gut causes *Rorc*-expressing Th17-skewed lymphocytes to patrol remote organs, including the lungs, and that BLM stimulates these cells to produce IL-17A. It has been shown that *C. albicans*-reactive T cells are involved in increased IL-17A expression via cross-reactivity with other fungi in the peripheral blood of asthma and COPD patients and in the lungs of cystic fibrosis patients [16]. Thus, the induction of IL-17A in the lung by intestinal *C. albicans* proliferation is not fibrosis-specific and may be a common mechanism in a variety of diseases. As we compared antibiotics +*C. albicans* (*Candida* + group) and antibiotics +FLCZ (*Candida* – group) in the current study, factors other than *C. albicans*, especially FLCZ administration or reduction of other specific fungi such as *Saccharomyces*, may have influenced the induction of Th17-skewed lymphocytes. However, in addition to the reported association between *C. albicans* and Th17 [27,28], more IL-17A-producing cells were found in the mice fed water containing *C. albicans* without antibiotics (Fig. S12C). Furthermore, mice in our facility have endogenous *C. albicans*, and we occasionally detect *C. albicans* even when fed water containing antibiotics only (Fig. S13A). We also showed that mice with *C. albicans* detected in the fecal culture tend to induce more Th17 than mice without *C. albicans* (Fig. S13B). These findings suggest that *C. albicans* contributes to the induction of Th17-skewed lymphocytes.

IL-17A has been associated with worsening of pulmonary fibrosis [18,21,29]. Reported mechanisms include promoting neutrophil mobilization through G-CSF induction, producing chemokines, inducing EMT in alveolar epithelial cells [20,22], stimulating

fibroblasts [23], and inhibiting autophagy [20]. The cell fractionation of BALF in the current model showed a non-significant but increasing trend in neutrophils in the *Candida* + group (Fig. S3). This neutrophilic tendency may be caused by an increase in IL-17A, which may partially contribute to enhanced fibrosis. In addition to these known mechanisms, we discovered that IL-17A can induce EndMT *in vitro* and *in vivo*.

Numerous studies have shown that EndMT aggravates pulmonary fibrosis [30–36], indicating that this pathway could also be a promising therapeutic target. IL-17A is involved in the pathogenesis of pulmonary fibrosis via several pathways, and IL-17A inhibitors are already clinically available for the treatment of autoimmune diseases, such as psoriasis. In patients with pulmonary fibrosis, inhibiting type 17 immunity has no established efficacy, but this strategy may be effective in certain populations.

As shown in Figure S12D, the reason why pulmonary fibrosis is not worsened in the mice fed water containing *C. albicans* but without antibiotics is unclear. The percentages of CD3⁺/CD4⁺/IL-17A⁺ cells in the *C. albicans* w/o ABx group (Fig. S12C) were increased at the same degree as that in the *Candida* + group (Fig. 3A), suggesting that commensal bacteria can counteract the effects of Th17. Both *C. albicans* proliferation and dysbiosis of the commensal microbiota seem necessary for *C. albicans* to exert its virulence in pulmonary fibrosis. The specific commensal bacteria counteracting *C. albicans* warrant further analyses.

In conclusion, this study shows that intestinal *C. albicans* proliferation exacerbates pulmonary fibrosis under dysbiosis with antibiotics by mobilizing Th17 cells to the lungs and enhancing IL-17A production by these mobilized cells. This response is regulated by a stepwise mechanism, in which the proliferation of *C. albicans* in the gut

first leads to the circulation of *Rorc*-expressing cells to distant organs, followed by the activation of *Rorc*-expressing cells triggered by a local stimulator such as BLM. Furthermore, IL-17A exacerbates fibrosis by inducing EndMT, in addition to its previously reported roles in promoting EMT and fibroblast activation. These findings contribute to elucidating the importance of the intestinal and fungal microbiota as therapeutic targets in pulmonary fibrosis.

ACKNOWLEDGEMENTS

We would like to thank Ms. Yukari Iyanaga (technical assistant from the Department of Molecular and Internal Medicine, Graduate School of Biomedical and Health Sciences, Hiroshima University) for providing technical assistance with the experiments and Ms. Yumiko Koba (Section of Infection Diseases Laboratory, Department of Clinical Support, Hiroshima University Hospital) for providing microbiological support. We would like to thank Mses. Yoko Hayashi, Nagisa Morihara and Shoko Hirano (technical staff from the Analysis Center of Life Science, Natural Science Center for Basic Research and Development, Hiroshima University) for their technical assistance with flow cytometric analysis and microbial profiling. We also would like to thank Editage (www.editage.com) for English language editing. A part of this work was carried out at Research Facilities for Laboratory Animal Science. This work was supported in part by the Natural Science Center for Basic Research and Development (NBARD-00093), and the Program of the Network-type Joint Usage/Research Center for Radiation Disaster Medical Science.

AUTHOR CONTRIBUTIONS

TY: collection of data, data analysis and interpretation, manuscript writing. TN: conception and design, collection of data, financial support, data analysis and interpretation, manuscript writing. TM, SS: data analysis and interpretation, reviewing the manuscript for important intellectual content. KY, YH, SM, HI, KF, HH: reviewing the manuscript for important intellectual content. NK: conception and design, data analysis and interpretation, reviewing the manuscript for important intellectual content.

NH: conception and design, financial support, reviewing the manuscript for important intellectual content. All authors read and approved the final manuscript.

CONSENT FOR PUBLICATION

Not applicable.

ABBREVIATIONS

IPF = Idiopathic pulmonary fibrosis

BALF = bronchoalveolar lavage fluid

BLM = bleomycin

EMT = epithelial–mesenchymal transition

CPZ = cefoperazone

CLDM = clindamycin

FLCZ = fluconazole

C. albicans = *Candida albicans*

PAS = periodic acid Schiff

FACS = fluorescence-activated cell sorting

MS1 = MILE SVEN 1

EndMT = endothelial–mesenchymal transition

REFERENCES

- 1 Richeldi L, Costabel U, Selman M, *et al.* Efficacy of a tyrosine kinase inhibitor in idiopathic pulmonary fibrosis. *N Engl J Med* 2011; **365**: 1079-1087
- 2 Glaspole I, Bonella F, Bargagli E, *et al.* Efficacy and safety of nintedanib in patients with idiopathic pulmonary fibrosis who are elderly or have comorbidities. *Respir Res* 2021; **22**: 1-10
- 3 Noble PW, Albera C, Bradford WZ, *et al.* Pirfenidone in patients with idiopathic pulmonary fibrosis (CAPACITY): Two randomised trials. *The Lancet* 2011; **377**: 1760-1769
- 4 King TE, Bradford WZ, Castro-Bernardini S, *et al.* A Phase 3 Trial of Pirfenidone in Patients with Idiopathic Pulmonary Fibrosis. *N Engl J Med* 2014; **370**: 2083-2092

- 5 Clemente JC, Manasson J, Scher JU. The role of the gut microbiome in systemic inflammatory disease. *BMJ* 2018; **360**: j5145
- 6 Budden KF, Shukla SD, Rehman SF, *et al.* Functional effects of the microbiota in chronic respiratory disease. *Lancet Respir Med* 2019; **2600**: 1-14
- 7 Chioma OS, Hesse LE, Chapman A, *et al.* Role of the Microbiome in Interstitial Lung Diseases. *Front Med (Lausanne)* 2021; **8**: 595522
- 8 O'Dwyer DN, Ashley SL, Gurczynski SJ, *et al.* Lung microbiota contribute to pulmonary inflammation and disease progression in pulmonary fibrosis. *Am J Respir Crit Care Med* 2019; **199**: 1127-1138
- 9 Takahashi Y, Saito A, Chiba H, *et al.* Impaired diversity of the lung microbiome predicts progression of idiopathic pulmonary fibrosis. *Respir Res* 2018; **19**: 34
- 10 Molyneaux PL, Cox MJ, Willis-Owen SAG, *et al.* The role of bacteria in the pathogenesis and progression of idiopathic pulmonary fibrosis. *Am J Respir Crit Care Med* 2014; **190**: 906-913
- 11 Yang D, Chen X, Wang J, *et al.* Dysregulated Lung Commensal Bacteria Drive Interleukin-17B Production to Promote Pulmonary Fibrosis through Their Outer Membrane Vesicles. *Immunity* 2019; **50**: 692-706.e7

- 12 Wheeler ML, Limon JJ, Bar AS, *et al.* Immunological Consequences of Intestinal Fungal Dysbiosis. *Cell Host Microbe* 2016; **19**: 865-873
- 13 Barza M, Giuliano M, Jacobus N v., *et al.* Effect of broad-spectrum parenteral antibiotics on composition of intestinal microflora of humans. *Antimicrob Agents Chemother* 1987; **31**: 723-727
- 14 Kim YG, Udayanga KGS, Totsuka N, *et al.* Gut dysbiosis promotes M2 macrophage polarization and allergic airway inflammation via fungi-induced PGE2. *Cell Host Microbe* 2014; **15**: 95-102
- 15 Noverr MC, Noggle RM, Toews GB, *et al.* Role of antibiotics and fungal microbiota in driving pulmonary allergic responses. *Infect Immun* 2004; **72**: 4996-5003
- 16 Bacher P, Hohnstein T, Beerbaum E, *et al.* Human Anti-fungal Th17 Immunity and Pathology Rely on Cross-Reactivity against *Candida albicans*. *Cell* 2019; **176**: 1340-1355.e15
- 17 Li D, Guabiraba R, Besnard AG, *et al.* IL-33 promotes ST2-dependent lung fibrosis by the induction of alternatively activated macrophages and innate

- lymphoid cells in mice. *Journal of Allergy and Clinical Immunology* 2014; **134**: 1422-1432
- 18 Wilson MS, Madala SK, Ramalingam TR, *et al.* Bleomycin and IL-1 β -mediated pulmonary fibrosis is IL-17A dependent. *Journal of Experimental Medicine* 2010; **207**: 535-552
- 19 Cipolla E, Fisher AJ, Gu H, *et al.* IL-17A deficiency mitigates bleomycin-induced complement activation during lung fibrosis. *FASEB Journal* 2017; **31**: 5543-5556
- 20 Mi S, Li Z, Yang H, *et al.* Blocking IL-17A promotes the resolution of pulmonary inflammation and fibrosis via TGF- β 1-dependent and -independent mechanisms. *J Immunol* 2011; **187**: 3003-3014
- 21 Gasse P, Riteau N, Vacher R, *et al.* IL-1 and IL-23 mediate early IL-17A production in pulmonary inflammation leading to late fibrosis. *PLoS One* 2011; **6**: e23185
- 22 Wang T, Liu Y, Zou JF, *et al.* Interleukin-17 induces human alveolar epithelial to mesenchymal cell transition via the TGF- β 1 mediated Smad2/3 and ERK1/2 activation. *PLoS One* 2017; **12**: 1-11

- 23 Zhang J, Wang D, Wang L, *et al.* Profibrotic effect of IL-17A and elevated IL-17RA in idiopathic pulmonary fibrosis and rheumatoid arthritis-associated lung disease support a direct role for IL-17A/IL-17RA in human fibrotic interstitial lung disease. *Am J Physiol Lung Cell Mol Physiol* 2019; **316**: L487-L497
- 24 Jin C, Lagoudas GK, Zhao C, *et al.* Commensal Microbiota Promote Lung Cancer Development via $\gamma\delta$ T Cells. *Cell* 2019; **176**: 998-1013.e16
- 25 Ivanov II, McKenzie BS, Zhou L, *et al.* The Orphan Nuclear Receptor ROR γ t Directs the Differentiation Program of Proinflammatory IL-17+ T Helper Cells. *Cell* 2006; **126**: 1121-1133
- 26 Martinez FJ, Yow E, Flaherty KR, *et al.* Effect of Antimicrobial Therapy on Respiratory Hospitalization or Death in Adults With Idiopathic Pulmonary Fibrosis: The CleanUP-IPF Randomized Clinical Trial. *JAMA* 2021; **325**: 1841-1851
- 27 van de Veerdonk FL, Marijnissen RJ, Kullberg BJ, *et al.* The macrophage mannose receptor induces IL-17 in response to *Candida albicans*. *Cell Host Microbe* 2009; **5**: 329-340

- 28 Smeekens SP, van de Veerdonk FL, van der Meer JWM, *et al.* The Candida Th17 response is dependent on mannan and β -glucan-induced prostaglandin E2. *Int Immunol* 2010; **22**: 889-895
- 29 Ramos-Martinez E, Falfán-Valencia R, Pérez-Rubio G, *et al.* Anti-Aminoacyl Transfer-RNA-Synthetases (Anti-tRNA) Autoantibodies Associated with Interstitial Lung Disease: Pulmonary Disease Progression has a Persistent Elevation of the Th17 Cytokine Profile. *J Clin Med* 2020; **9**: 1356
- 30 Singh S, Adam M, Matkar PN, *et al.* Endothelial-specific Loss of IFT88 Promotes Endothelial-to-Mesenchymal Transition and Exacerbates Bleomycin-induced Pulmonary Fibrosis. *Sci Rep* 2020; **10**: 1-14
- 31 Suzuki T, Tada Y, Gladson S, *et al.* Vildagliptin ameliorates pulmonary fibrosis in lipopolysaccharide-induced lung injury by inhibiting endothelial-to-mesenchymal transition. *Respir Res* 2017; **18**: 1-11
- 32 Pei B, Zhang N, Pang T, *et al.* Linagliptin ameliorates pulmonary fibrosis in systemic sclerosis mouse model via inhibition of endothelial-to-mesenchymal transition. *Mol Cell Biochem* 2022; **477**: 995-1007

- 33 Jiang Y, Zhou X, Hu R, *et al.* TGF- β 1-induced SMAD2/3/4 activation promotes RELM- β transcription to modulate the endothelium-mesenchymal transition in human endothelial cells. *International Journal of Biochemistry and Cell Biology* 2018; **105**: 52-60
- 34 Nataraj D, Ernst A, Kalluri R. Idiopathic pulmonary fibrosis is associated with endothelial to mesenchymal transition. *Am J Respir Cell Mol Biol* 2010; **43**: 129-130
- 35 Piera-Velazquez S, Mendoza FA, Jimenez SA. Endothelial to Mesenchymal Transition (EndoMT) in the pathogenesis of human fibrotic diseases. *J Clin Med* 2016; **5**: 1-22
- 36 Yun E, Kook Y, Yoo KH, *et al.* Endothelial to mesenchymal transition in pulmonary vascular diseases. *Biomedicines* 2020; **8**: 1-17

FIGURE LEGENDS

Figure 1

Exacerbation of pulmonary fibrosis by *Candida* proliferation in the intestine

(A) Experimental scheme and group naming for each antimicrobial treatment, fungal administration and induction of pulmonary fibrosis. BLM, bleomycin; CPZ, cefoperazone; CLDM, clindamycin; DW; distilled water; FLCZ, fluconazole.

(B) Periodic acid-Schiff staining of murine cecal tissue sections obtained from the *Candida* – and *Candida* + groups. The red arrows indicate *Candida* in the lamina propria.

(C) The evaluation of fecal culture on CHROMagar for 48 h. Green colonies indicate growth of *C. albicans*. The colonies were observed in *Candida* + group (middle) but not *Candida* – group. (left) Comparison of *C. albicans* CFUs in each group (n = 8–11/group). (right)

(D) Lung hydroxyproline content in each group (n = 4–5/group).

(E) Histological analysis using Masson's trichrome stain in lung tissue sections of each group.

(F) Quantification of fibrosis by Ashcroft score (n = 5/group).

Figure 2

Analysis of fungal microbiota

(A)(C)(E) Taxonomic distribution of fungal genus using ITS sequencing in fecal (A), BALF (C), and lung (E) samples collected from mice in the *Candida* – and *Candida* + groups. Four representative examples per group are shown.

(B)(D)(F) Percentages of ITS transcripts for the *Candida* genus in fecal (B), BALF (D), and lung (F) samples of each group (n = 5–8/group).

Figure 3

IL-17A-mediated exacerbation of pulmonary fibrosis

(A) Flow cytometric analysis (as shown in Fig. S7) for cell frequency of M2 macrophages, regulatory T cells (Treg), and T helper 17 cells (Th17). Lung cells are obtained from each mouse at 14 days after bleomycin administration (n = 4–5/group).

(B) Real-time quantitative PCR analysis for the mRNA expression levels of *Il17a* in lung tissues obtained at 14 days after bleomycin administration. Values are expressed relative to the expression of *18s* mRNA level (n = 4–5/group).

(C) Serum and lung protein levels of IL-17A at 14 days after bleomycin administration (n = 4–5/group).

(D) Lung hydroxyproline content in each group administrated with or without IL-17A neutralizing antibodies as shown in Fig. S10 (n = 6–12/group).

(E) Histological analysis using Masson's trichrome stain in lung tissue sections of each group.

(F) Quantification of fibrosis by Ashcroft score (n = 5–6/group).

- (G) Flow cytometric analysis of the percentages of Th17 in lung cells obtained from each mouse before bleomycin administration (n = 5/group).
- (H) Flow cytometric analysis of the percentages of Th17 in blood cells obtained from each mouse before or 14 days after bleomycin administration (n = 4–5/group).
- (I) Real-time quantitative PCR analysis of mRNA expression levels of *Rorc* and *Il17a*. Nucleic acids are extracted from CD3⁺/CD4⁺ cells sorted using fluorescence-activated cell sorting from each murine lung before bleomycin administration. Values are expressed relative to the expression of *18s* mRNA level (n = 6/group).
- (J) Representative images of RORγt immunostaining in ceca obtained from each mouse before bleomycin administration.

Figure 4

Endothelial–mesenchymal transition by IL-17A

- (A) Percentages of epithelial cells (EpCAM⁺ in CD45⁻/CD31⁻) and epithelial cells undergoing epithelial–mesenchymal transition (αSMA⁺/Colla1⁺ in EpCAM⁺/CD45⁻/CD31⁻) defined as Fig. S14.
- (B) Percentages of activated fibroblasts (myofibroblasts: αSMA⁺/Colla1⁺ in EpCAM⁻/CD45⁻/CD31⁻) defined as Fig. S14.
- (C) Percentages of endothelial cells (CD45⁻/CD31⁺) and endothelial cells undergoing endothelial–mesenchymal transition (αSMA⁺/Colla1⁺ in CD45⁻/CD31⁺) defined as Fig. S14.

(D) Percentages of endothelial cells undergoing endothelial–mesenchymal transition in mice treated with isotype control antibody or anti-IL-17A antibody as shown in Fig.

S10 (n = 6–7/group).

(E) Real-time quantitative PCR analysis of the mRNA expression levels of mesenchymal markers (*Fn*, *Colla1*, and *Acta2*) and endothelial–mesenchymal transition markers (*Snail1* and *Snail2*) in MS1 cells cultured under defined conditions. Values are expressed relative to the expression of *18s* mRNA level (n = 4/group).

(F) Flow cytometric analysis for CD31 expression in MS1 cells (lower) and $\alpha\text{SMA}^+/\text{Colla1}^+$ in CD31^+ MS1 cells (upper, MS1 undergoing endothelial–mesenchymal transition) (n = 3/group).

(G) Representative images of fluorescent immunocytochemistry of MS1. Cells are incubated for 30 h in medium with or without IL-17A. Expression levels of αSMA (red), *Colla1* (green), and nuclei (blue) are shown.

(H) Comparison of fluorescence intensity of each group (n = 6–11/group).

Figure 5

Graphical abstract of the current study

SUPPLEMENTAL FIGURE LEGENDS

Figure S1

Lack of inflammatory change in the cecum obtained from the *Candida* – and *Candida* + groups

(A) Hematoxylin–eosin staining of murine cecal tissue sections obtained from the *Candida* – and *Candida* + groups.

(B) Number of cells in the lamina propria of the cecum. Five high power fields for each sample were analyzed, and the average were plotted (n = 5/group).

Figure S2

***Candida* – and *Candida* + groups without bleomycin administration**

Experimental scheme for each antimicrobial treatment, fungal administration. CPZ, cefoperazone; CLDM, clindamycin; DW; distilled water; FLCZ, fluconazole.

Figure S3

Analysis of bronchoalveolar lavage fluid in the *Candida* – and *Candida* + groups

Cellular fractionation of BALF was examined and shown for macrophages (A), lymphocytes (B), and neutrophils (C). BALF is obtained from each mouse at 14 days after bleomycin administration (n = 5/group).

Figure S4

Effect of fluconazole administration on pulmonary fibrosis

(A) Experimental scheme for each antimicrobial treatment and induction of pulmonary fibrosis. BLM, bleomycin; DW, distilled water; FLCZ, fluconazole.

(B) Lung hydroxyproline content in each group (n = 5/group).

Figure S5

Analysis of fungal microbiota

Species-level phylogenetic classification in fecal (A), BALF (B), and lung (C) samples collected from mice in the *Candida* – and *Candida* + groups (n = 4/group).

Figure S6

Analysis of bacterial microbiota

Phylum-level phylogenetic classification in fecal (A), BALF (B), and lung (C) samples collected from mice in the *Candida* – and *Candida* + groups (n = 4/group). Microbial changes are analyzed by 16S rRNA gene sequencing.

Figure S7

Flow cytometric gating strategy

Gating strategy used to identify M2 macrophages (A), Treg and Th17 (B).

Figure S8

Correlation between lung hydroxyproline content and cell frequency of Th17 cells

Correlation between lung hydroxyproline content and cell frequency of IL-17A⁺ in lung CD3⁺/CD4⁺ cells. Lung cells are obtained from the *Candida* – and *Candida* + groups at 14 days after bleomycin administration (n = 8).

Figure S9

Factors other than Th17/IL-17A in *Candida* + and *Candida* – groups

(A) Real-time quantitative PCR analysis of the mRNA expression levels of *Tbx21* and *Gata3* in lung tissues obtained from the *Candida* – and *Candida* + groups at 14 days after bleomycin administration. Values are expressed relative to the expression of *I8s* mRNA level (n = 4–5/group).

(B) Real-time quantitative PCR analysis of the mRNA expression levels of *Tgfb* in lung tissues obtained from the *Candida* – and *Candida* + groups at 14 days after bleomycin administration. Values are expressed relative to the expression of *I8s* mRNA level (n = 4–5/group).

(C) Serum protein levels of TGF-β at 14 days after bleomycin administration (n = 4/group).

Figure S10

IL-17A neutralization

Experimental scheme of IL-17A neutralization using the anti-IL-17A antibodies. BLM, bleomycin; CPZ, cefoperazone; CLDM, clindamycin; DW, distilled water; FLCZ, fluconazole.

Figure S11

Effect of anti-IL-17A neutralizing antibody administration on intestinal *Candida* colonization

The evaluation of fecal culture on CHROMagar for 48 h. The box plots indicate comparison of *C. albicans* CFUs in each group (n = 2/group).

Figure S12

Intestinal *Candida* proliferation without antibiotic-induced dysbiosis

(A) Experimental scheme for each fungal administration and induction of pulmonary fibrosis. BLM, bleomycin; DW, distilled water.

(B) The evaluation of fecal culture on CHROMagar in *C. albicans* without ABx group.

(left) The box plots indicate comparison of *C. albicans* CFUs in DW and *C. albicans* without ABx group (n = 2–3/group). (right)

(C) Flow cytometric analysis for cell frequency of Th17. Lung cells are obtained from each mouse at 14 days after bleomycin administration (n = 4/group).

(D) Lung hydroxyproline content in each group (n = 4–6).

Figure S13

Changes in lung Th17 levels by whether or not *Candida albicans* is detected in fecal culture

(A) Experimental scheme for each antimicrobial treatment, fungal administration and induction of pulmonary fibrosis. BLM, bleomycin; CPZ, cefoperazone; CLDM, clindamycin; DW, distilled water.

(B) Flow cytometric analysis for cell frequency of Th17. Lung cells are obtained from each mouse at 14 days after bleomycin administration (n = 4/group).

Figure S14

Flow cytometric gating strategy

(A) Lung cell subsets and their surface markers in flow cytometric analysis. Murine lung cells were obtained at 7 days after bleomycin administration (n = 4–5/group).

(B)(C) Gating strategy used to identify fibroblasts, epithelial cells (B) and endothelial cells (C).

SUPPLEMENTAL TABLES

Table S1

Fluorescent antibodies used in this study

Fluorescence and molecule	Company	Clone
PE/Cyanine7 anti-CD3	BioLegend (San Diego, CA, USA)	17A2
FITC anti-CD4	BioLegend	RM4-5
PE anti-CD25	BioLegend	PC61
BV421 anti-ROR γ t	BD Biosciences (San Jose, CA, USA)	Q21-559
BV421 anti-mouse IgG2a, k	BD Biosciences	G155-178
APC anti-IL-17A	BioLegend	TC11-18H10.1
APC anti-rat IgG1, k	BioLegend	RTK2071
PerCP/Cyanine5.5 anti-CD45	BioLegend	30-F11
APC anti-CD11c	BioLegend	N418
FITC anti-F4/80	BioLegend	BM8
BV421 anti-CD80	BioLegend	BM8
PE anti-CD206/MMR	Thermo Fisher Scientific (Waltham, MA, USA)	MR6F3
PerCP/Cyanine5.5 anti-CD31	BioLegend	MEC13.3
Pacific Blue anti-mouse CD31	BioLegend	390
BV421 anti-CD326/EpCAM	BioLegend	G8.8
eFluor 660 anti-alpha smooth muscle actin	Thermo Fisher Scientific	1A4
eFluor 660 anti-mouse IgG2a, k	Thermo Fisher Scientific	eBM2a
FITC anti-collagen type 1	Rockland Immunochemicals	N/A

	(Pottstown, PA, USA)	
FITC anti-rabbit IgG	Bioss	N/A
	(Woburn, MA, USA)	

Table S2

Primers used in this study

Gene Name	Company	Assay ID
<i>Cdh1</i>	Thermo Fisher Scientific (Waltham, MA, USA)	Mm01247357_m1
<i>Fnl</i>	Thermo Fisher Scientific	Mm01256744_m1
<i>Acta2</i>	Thermo Fisher Scientific	Mm00725412_m1
<i>Vim</i>	Thermo Fisher Scientific	MM01333430_m1
<i>Pecam1</i>	Thermo Fisher Scientific	Mm01242576_m1
<i>Cdh5</i>	Thermo Fisher Scientific	Mm00486938_m1
<i>Colla1</i>	Thermo Fisher Scientific	Mm00801666_g1
<i>Il6</i>	Thermo Fisher Scientific	Mm00446190_m1
<i>Snail1</i>	Thermo Fisher Scientific	MM00441533_g1
<i>Snail2</i>	Thermo Fisher Scientific	Mm00441531_m1
<i>Twist1</i>	Thermo Fisher Scientific	Mm00442036_m1
<i>Twist2</i>	Thermo Fisher Scientific	MM00492147_m1
<i>Il17a</i>	Thermo Fisher Scientific	Mm00439619_m1
<i>Rorc</i>	Thermo Fisher Scientific	Mm01261022_m1
<i>Il17b</i>	Thermo Fisher Scientific	Mm01258783_m1

<i>Il6</i>	Thermo Fisher Scientific	Mm00446190_m1
<i>Il17f</i>	Thermo Fisher Scientific	Mm00521423_m1
<i>Tbx21</i>	Thermo Fisher Scientific	Mm00450960_m1
<i>Gata3</i>	Thermo Fisher Scientific	Mm00484683_m1
<i>Tgfb</i>	Thermo Fisher Scientific	Mm01178820_m1
<i>Candida a</i>	Thermo Fisher Scientific	Fn04646233_s1
<i>Actb</i>	Thermo Fisher Scientific	Mm02619580_g1
<i>Rn18s;R</i>	Thermo Fisher Scientific	Mm03928990_g1
<i>Gapdh</i>	Thermo Fisher Scientific	Mm99999915_g1

Table S3

Primers used for microbiological analysis

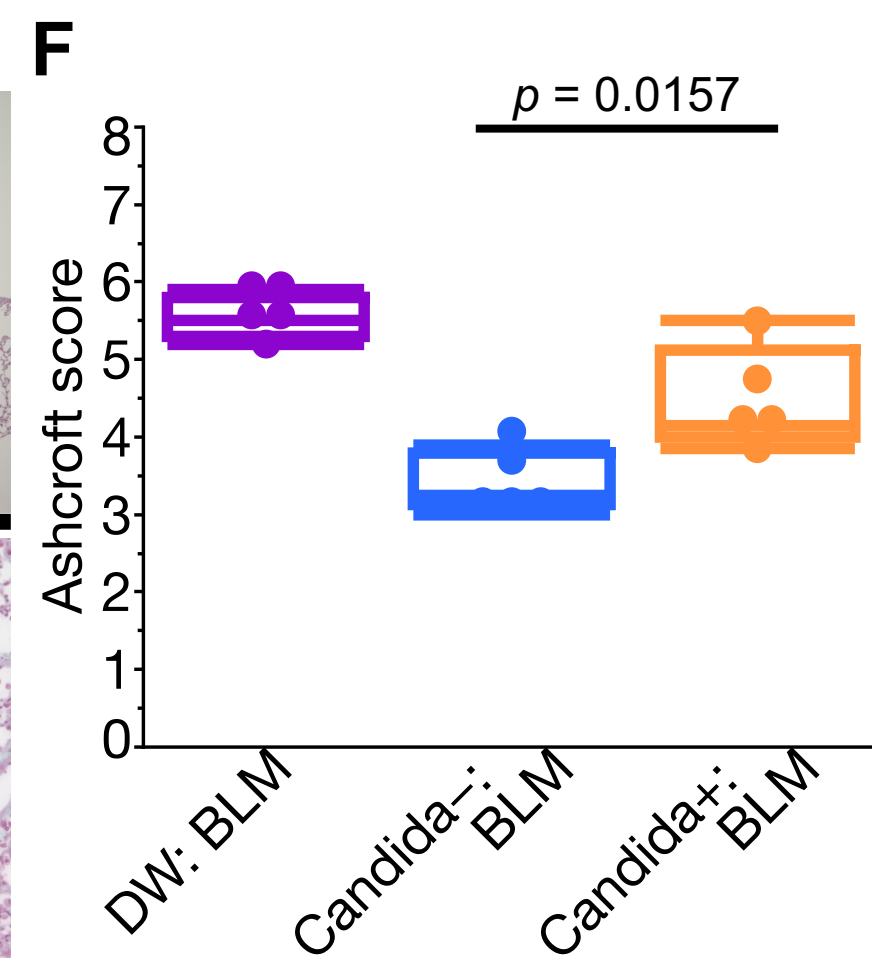
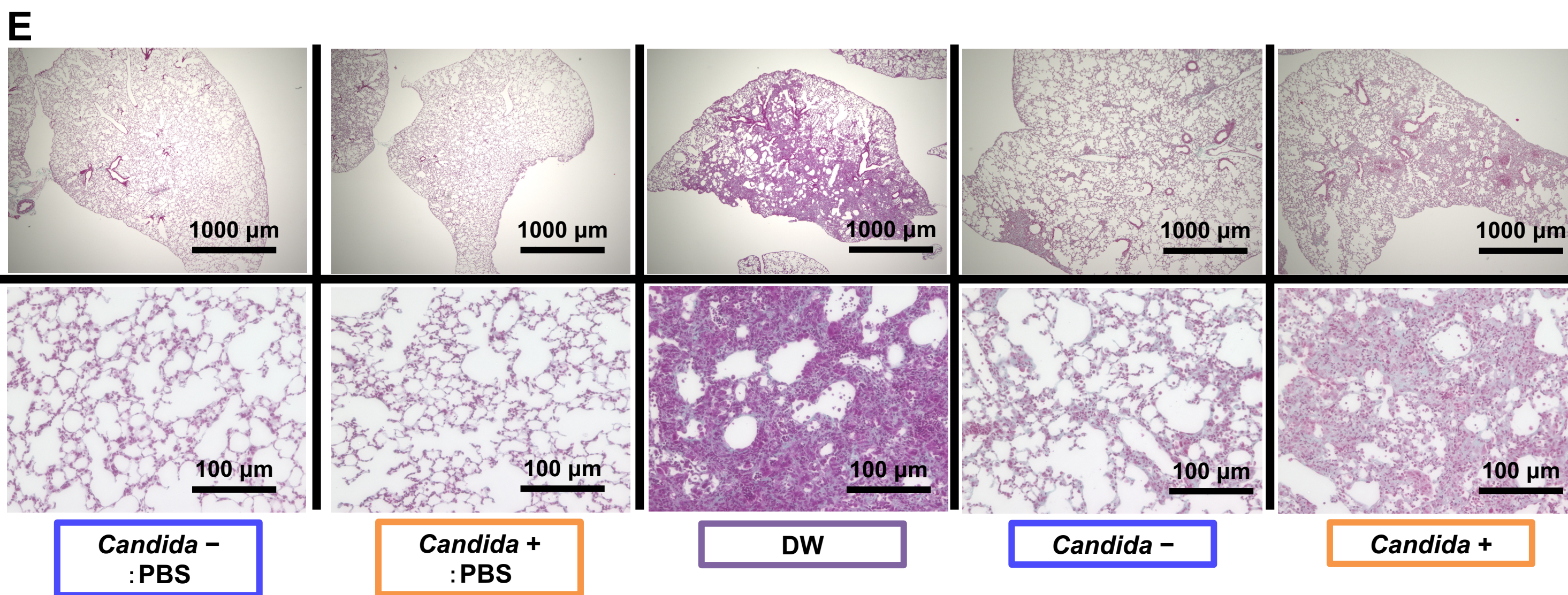
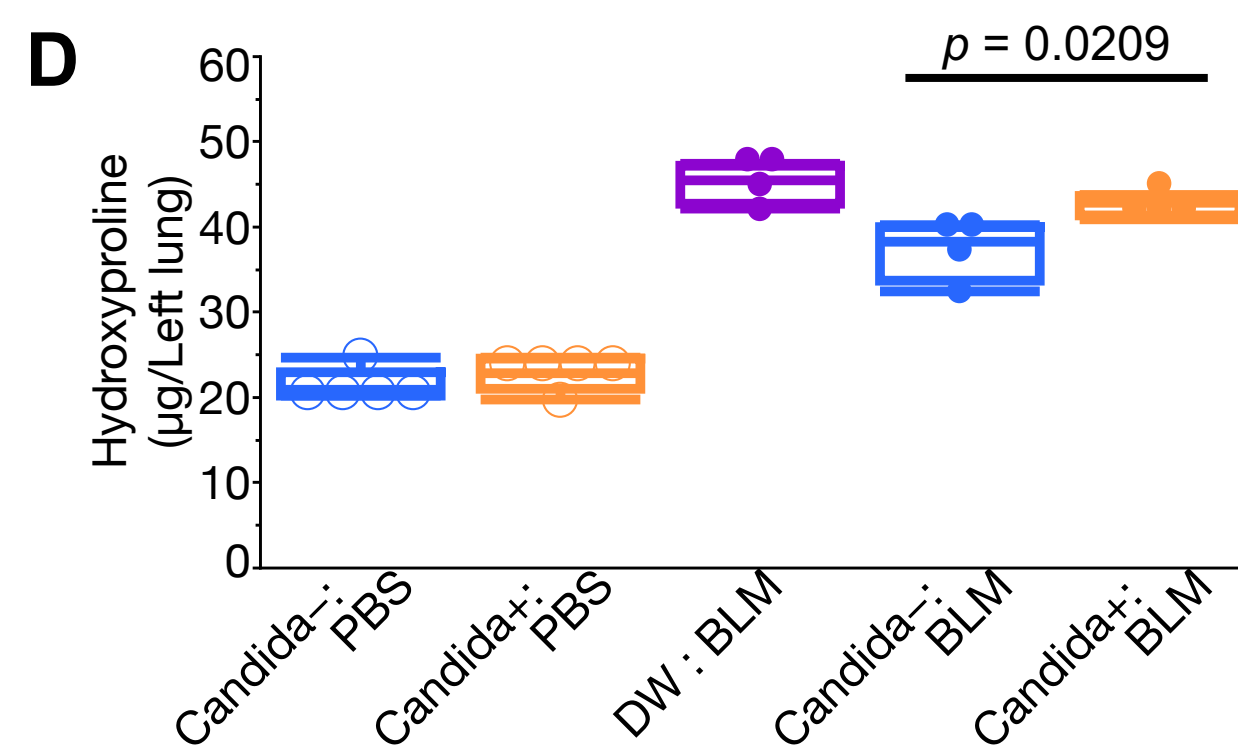
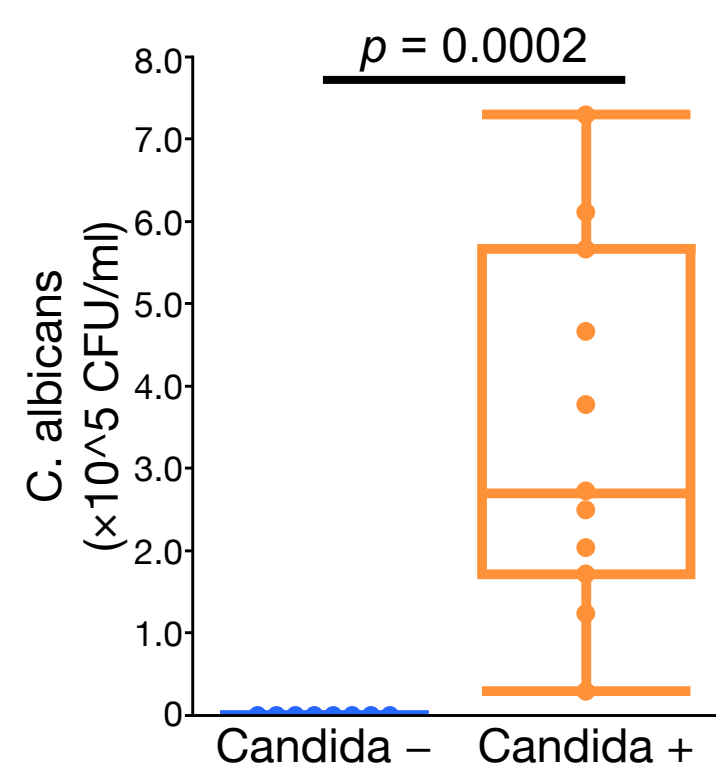
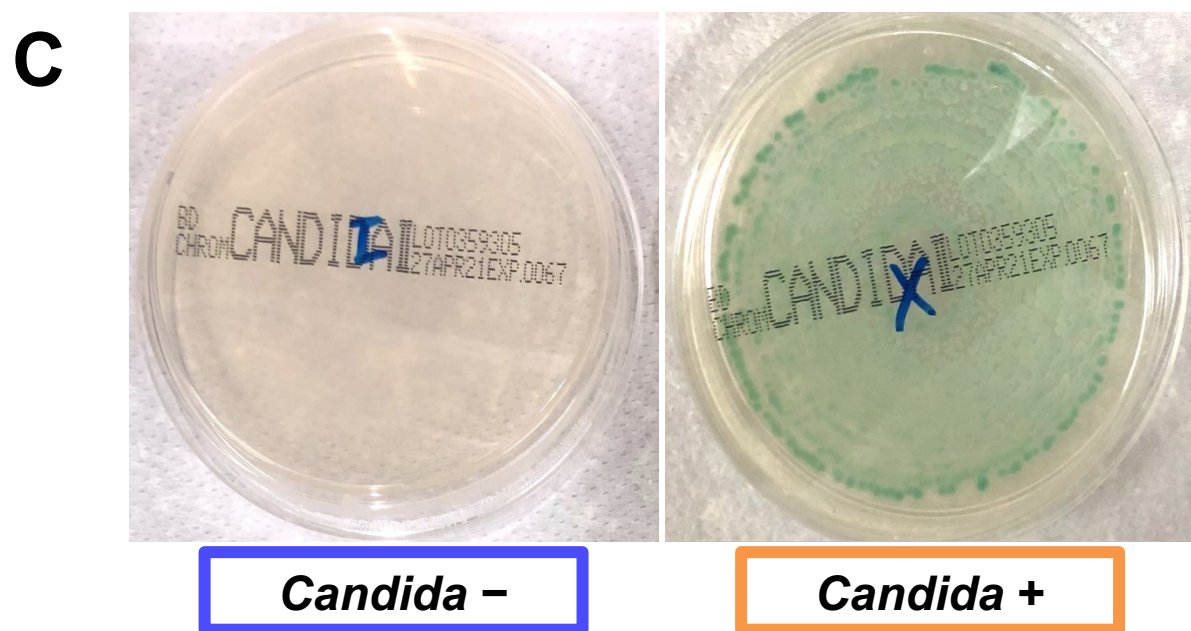
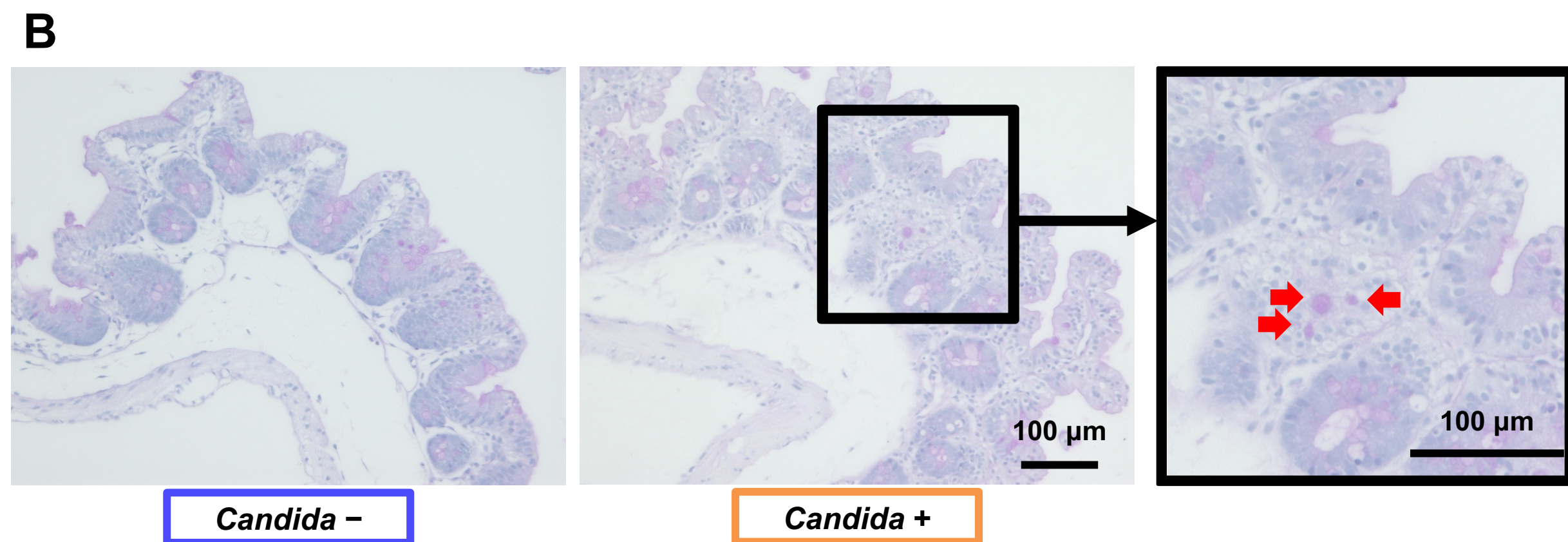
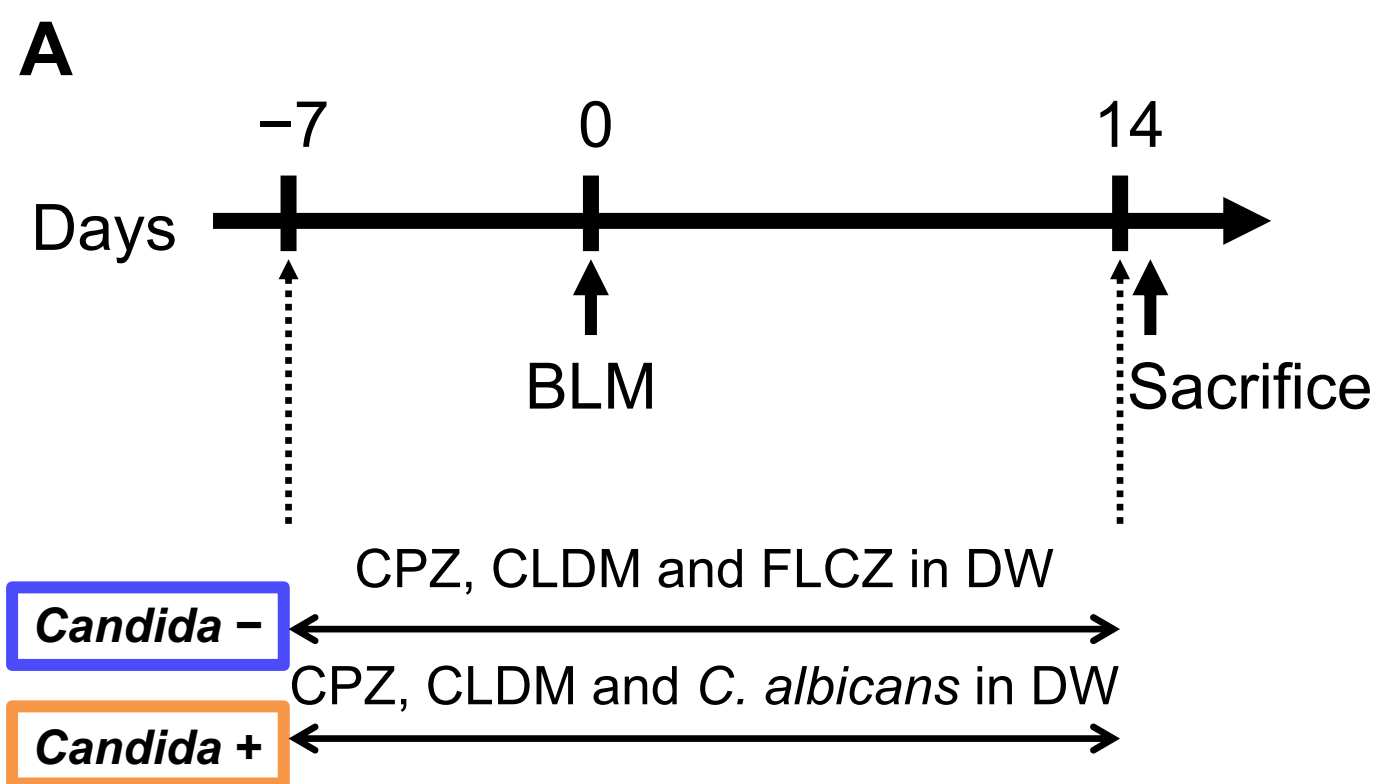
Primers	Company	Sequences
16S fwd	Thermo Fisher Scientific (Waltham, MA, USA)	TCGTCGGCAGCGTCAGATGTGTATAA GAGACAGTCGTCGGCAGCGTCAGATG TGTATAAGAGACAGCCTACGGGNGG CWGCAG
16S rev	Thermo Fisher Scientific	GTCTCGTGGGCTCGGAGATGTGTATA AGAGACAGGTCTCGTGGGCTCGGAG

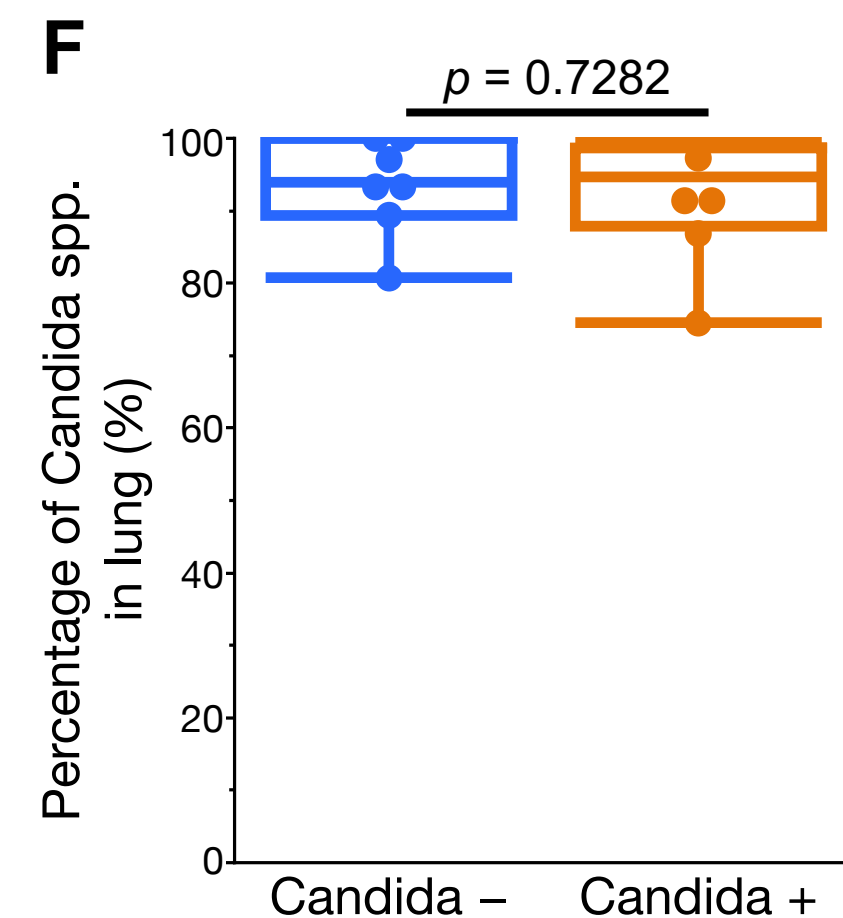
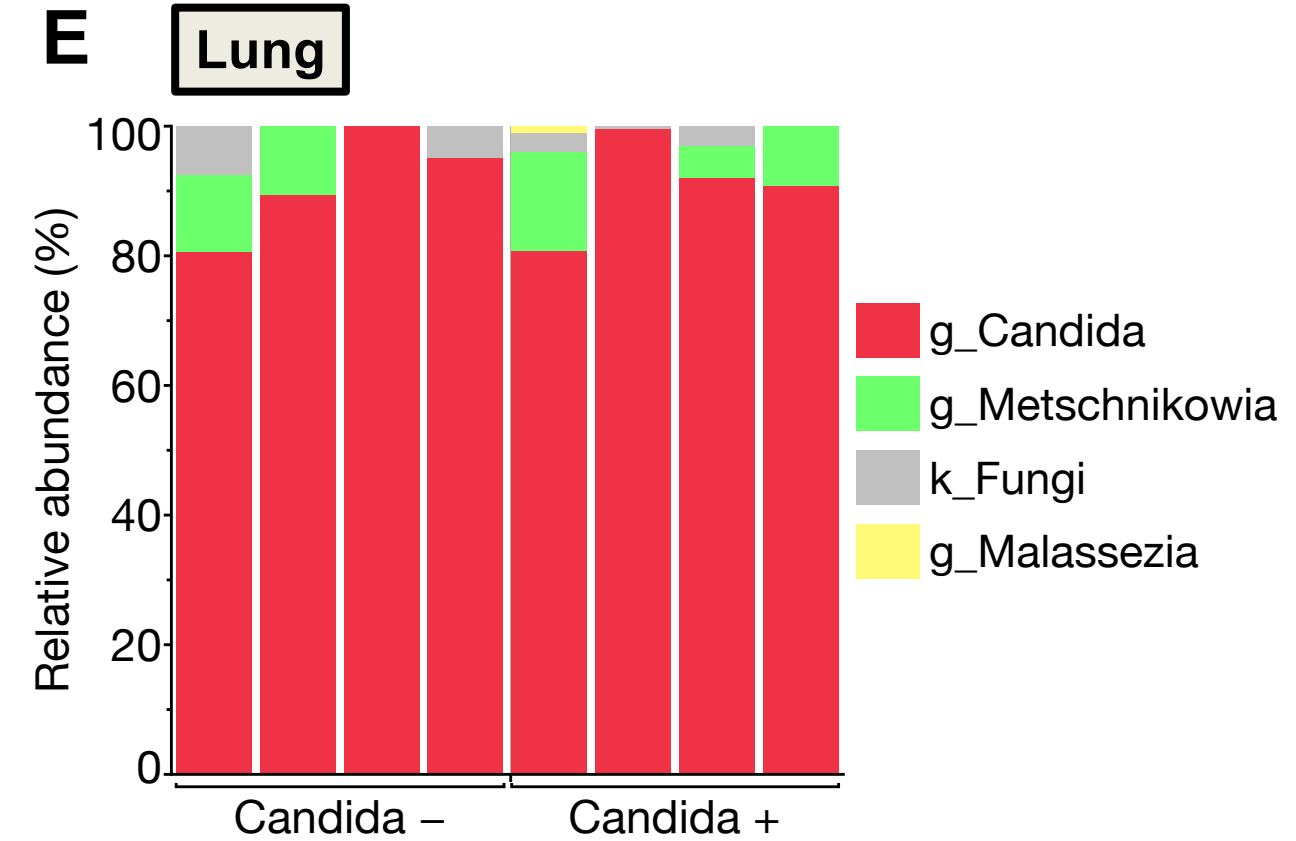
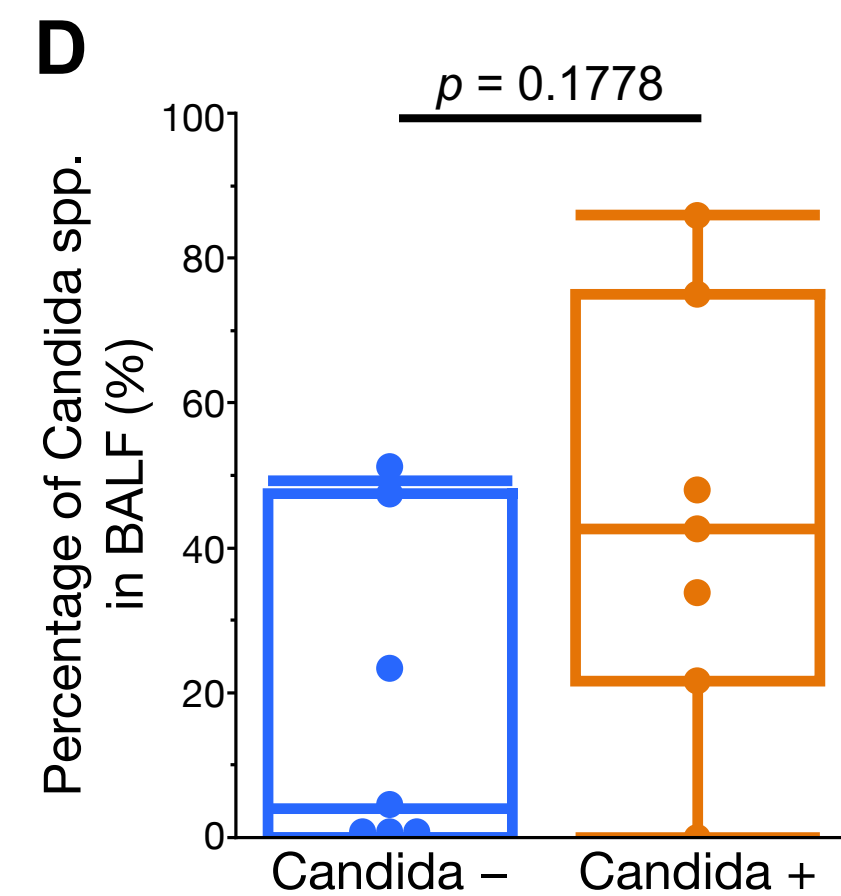
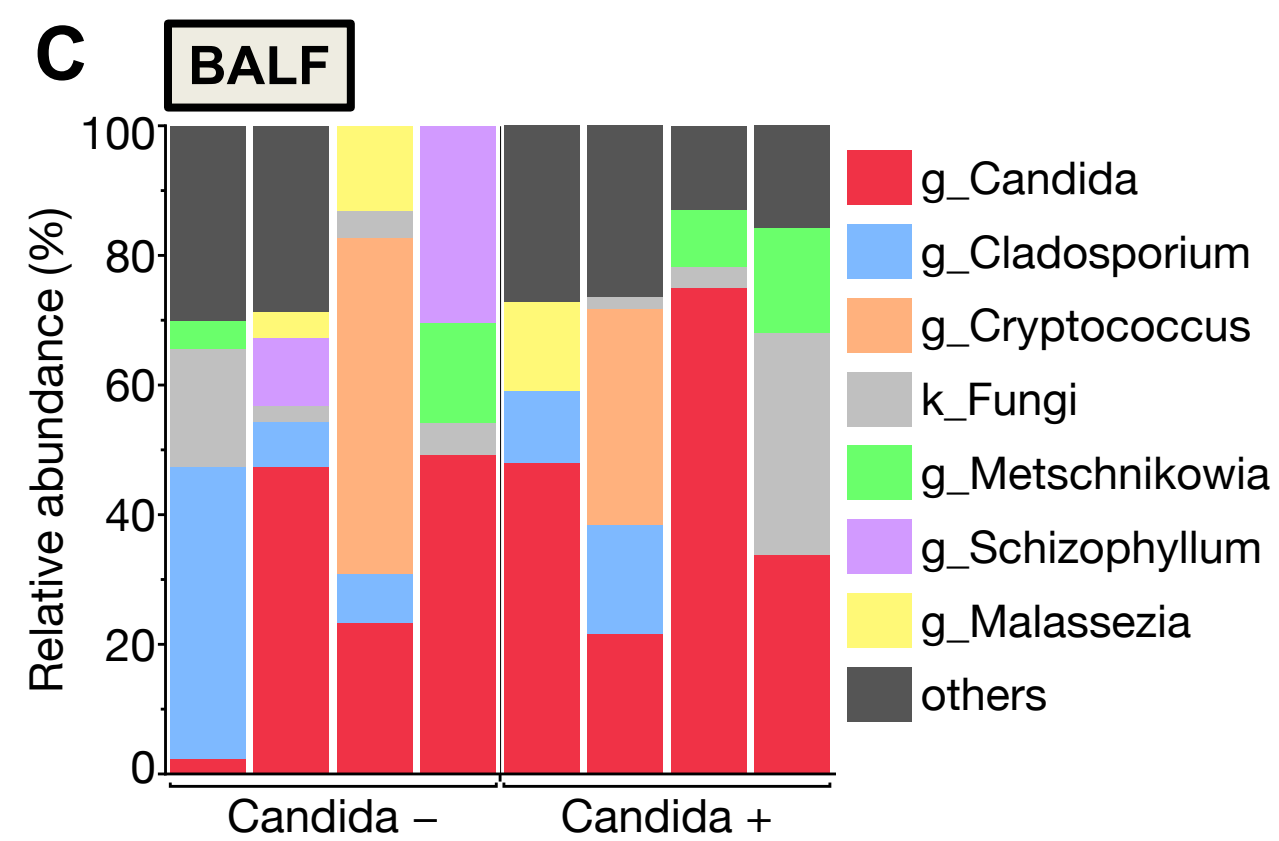
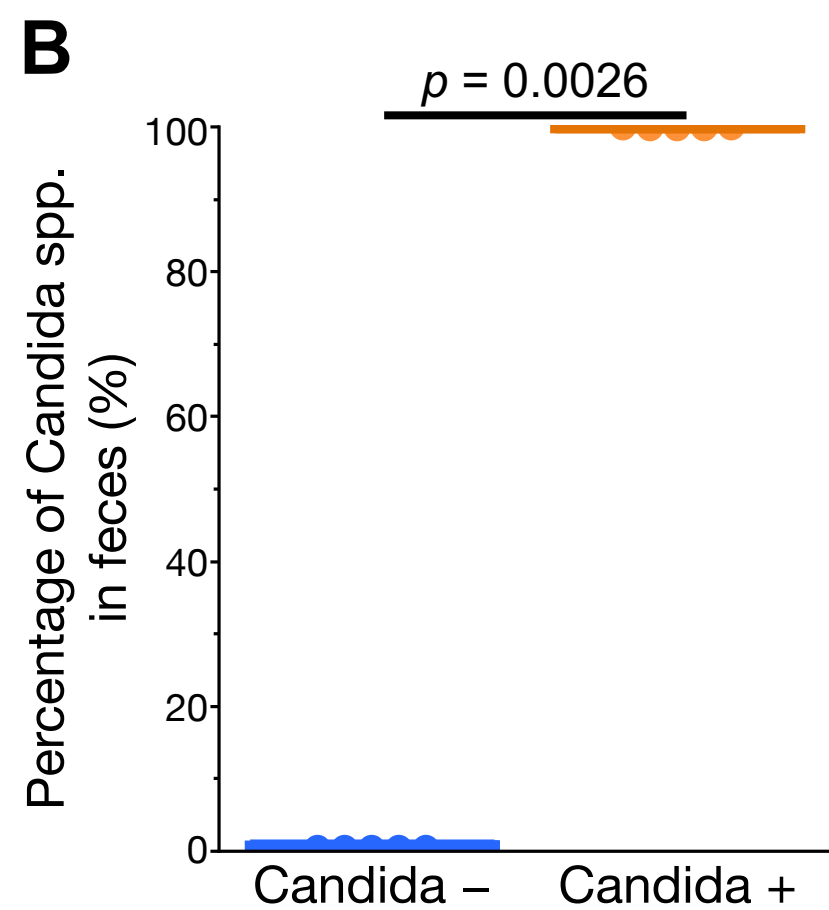
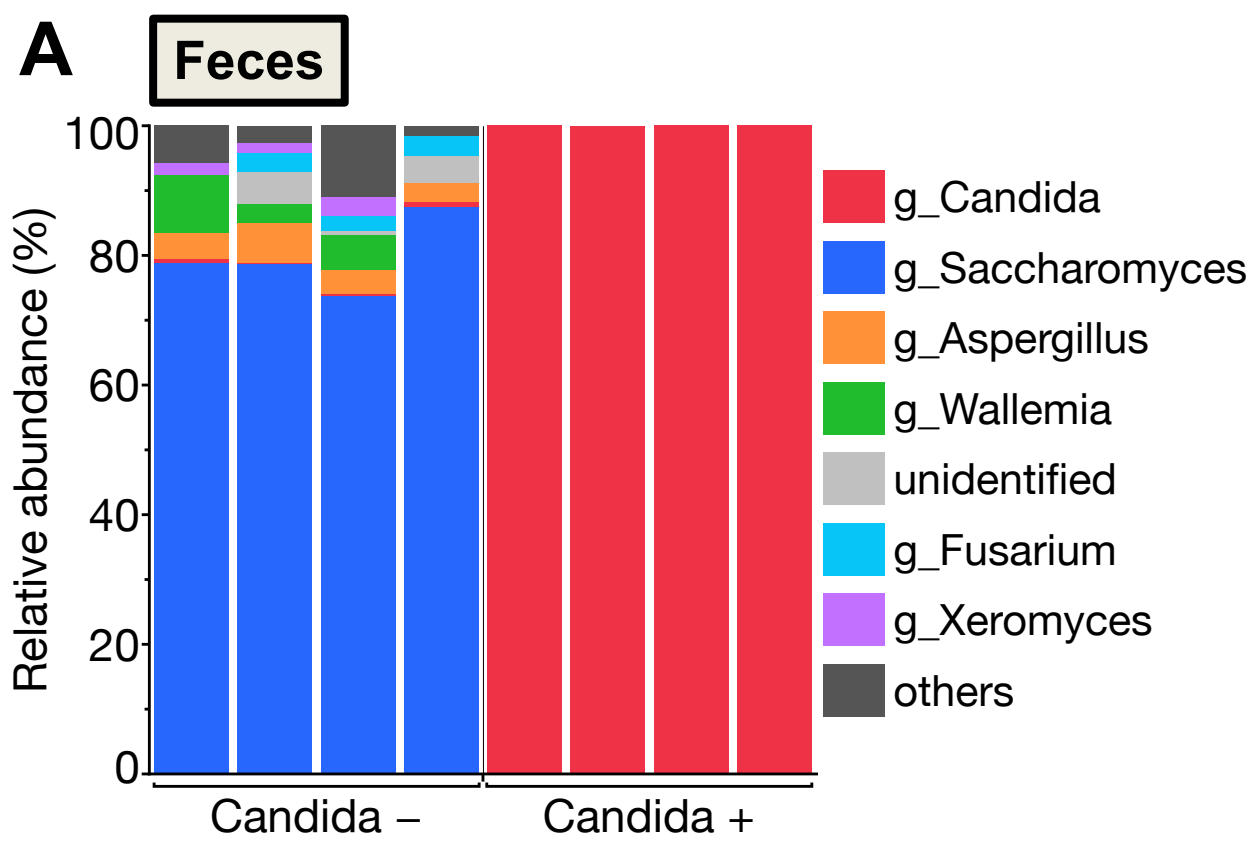
		ATGTGTATAAGAGACAGGACTACHV GGGTATCTAATCC
ITS_frd_1	Thermo Fisher Scientific	TCGTCGGCAGCGTCAGATGTGTATAA GAGACAGCTTGGTCATTTAGAGGAAG TAA
ITS_frd_2	Thermo Fisher Scientific	TCGTCGGCAGCGTCAGATGTGTATAA GAGACAGCTCGGTCATTTAGAGGAAG TAA
ITS_frd_3	Thermo Fisher Scientific	TCGTCGGCAGCGTCAGATGTGTATAA GAGACAGCTTGGTCATTTAGAGGAAC TAA
ITS_frd_4	Thermo Fisher Scientific	TCGTCGGCAGCGTCAGATGTGTATAA GAGACAGCCCGGTCATTTAGAGGAA GTAA

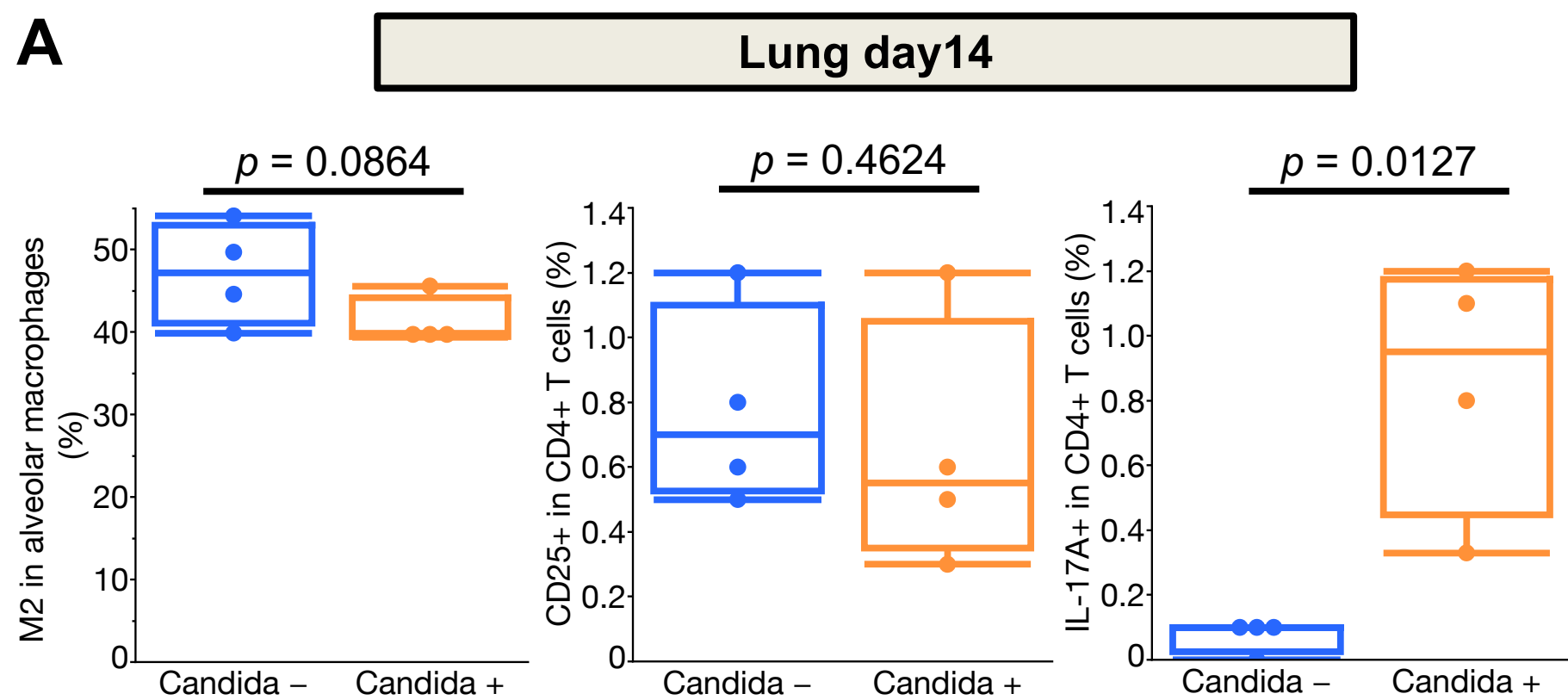
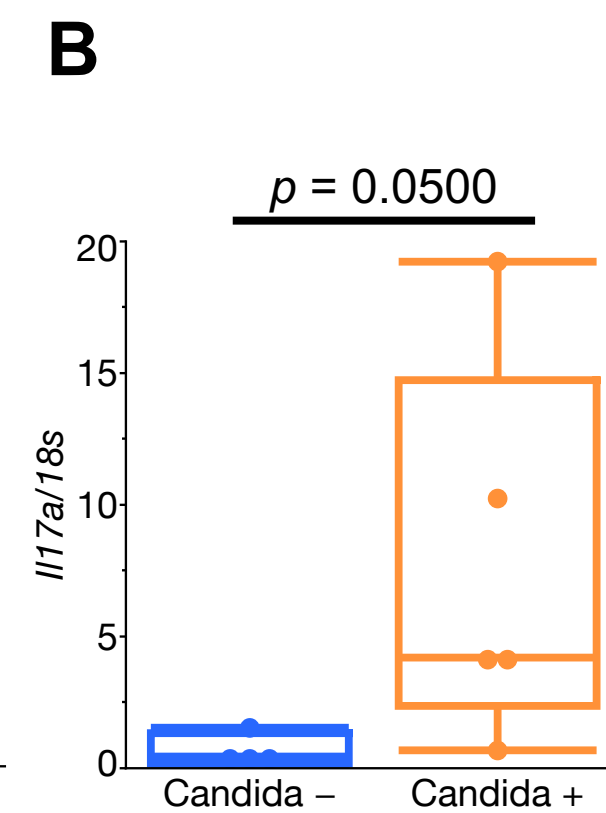
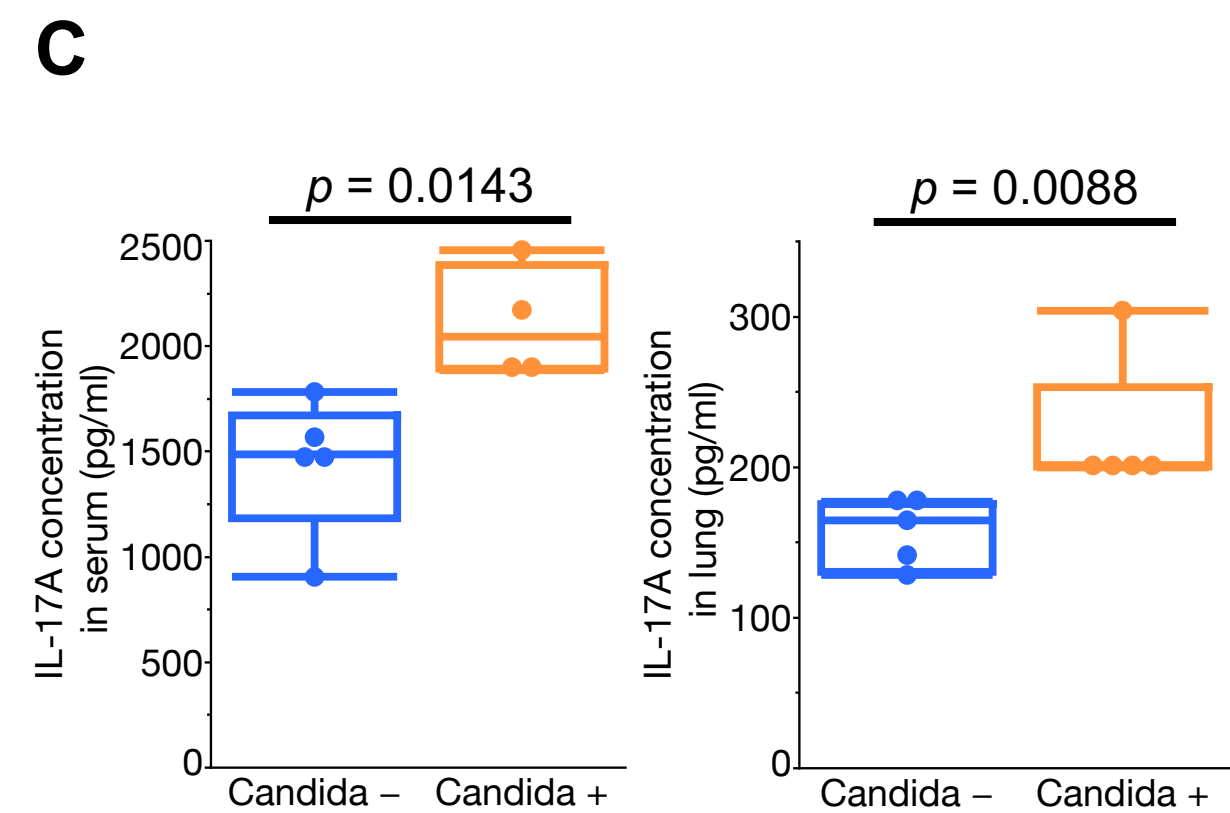
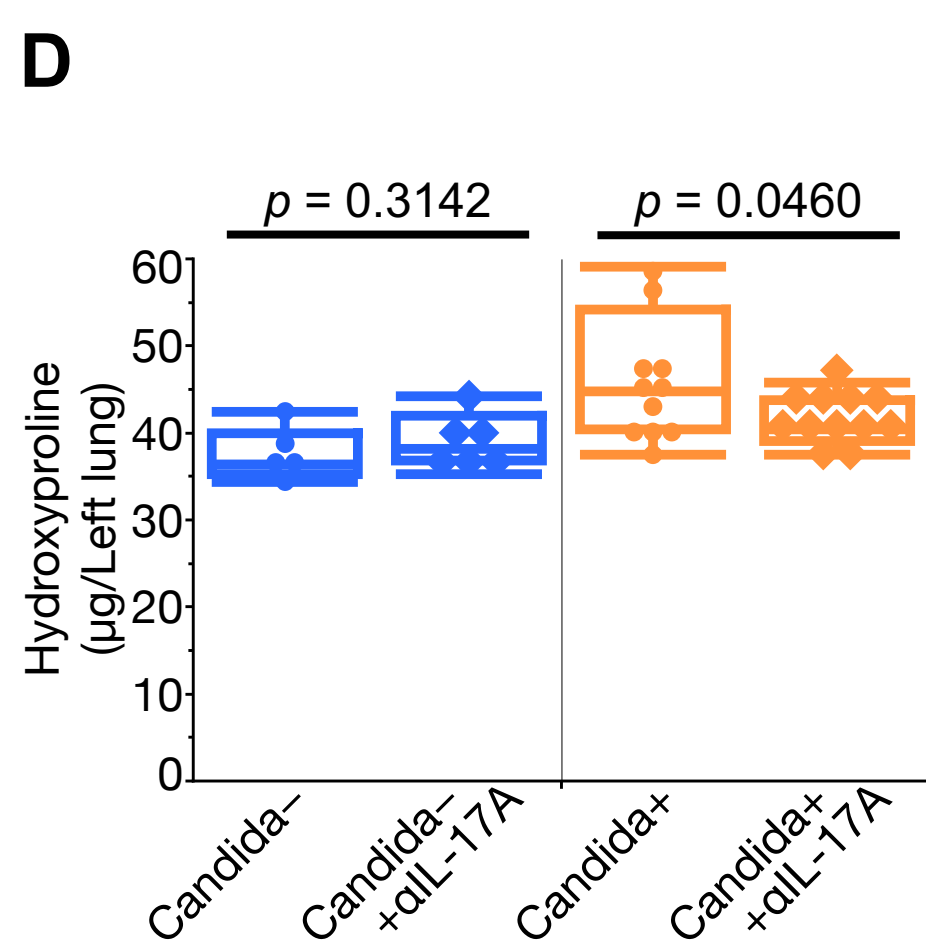
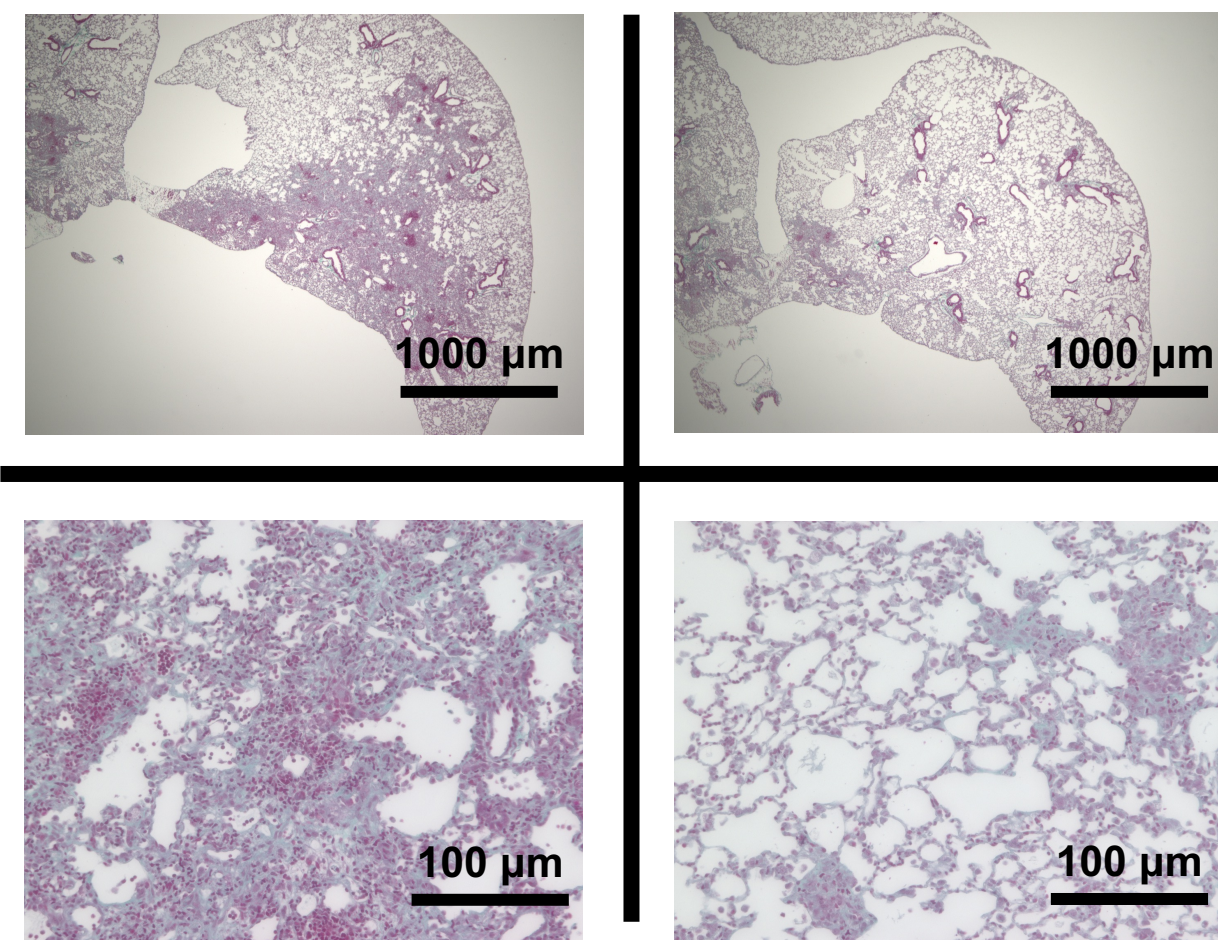
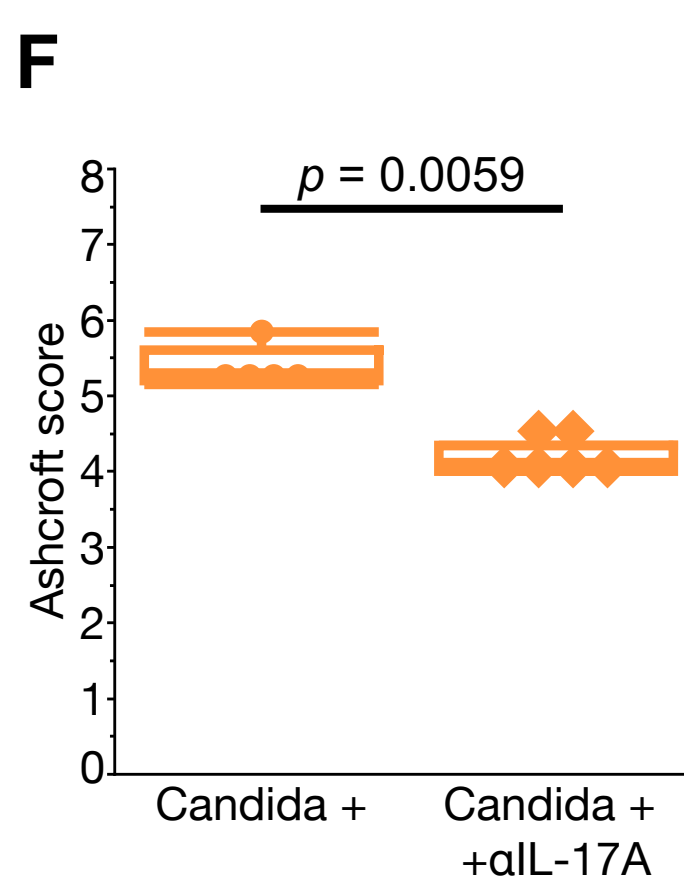
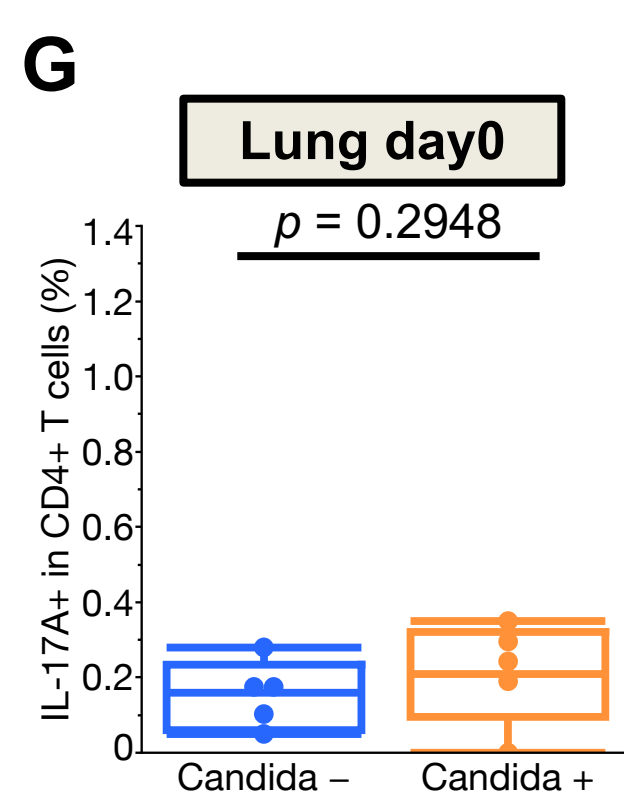
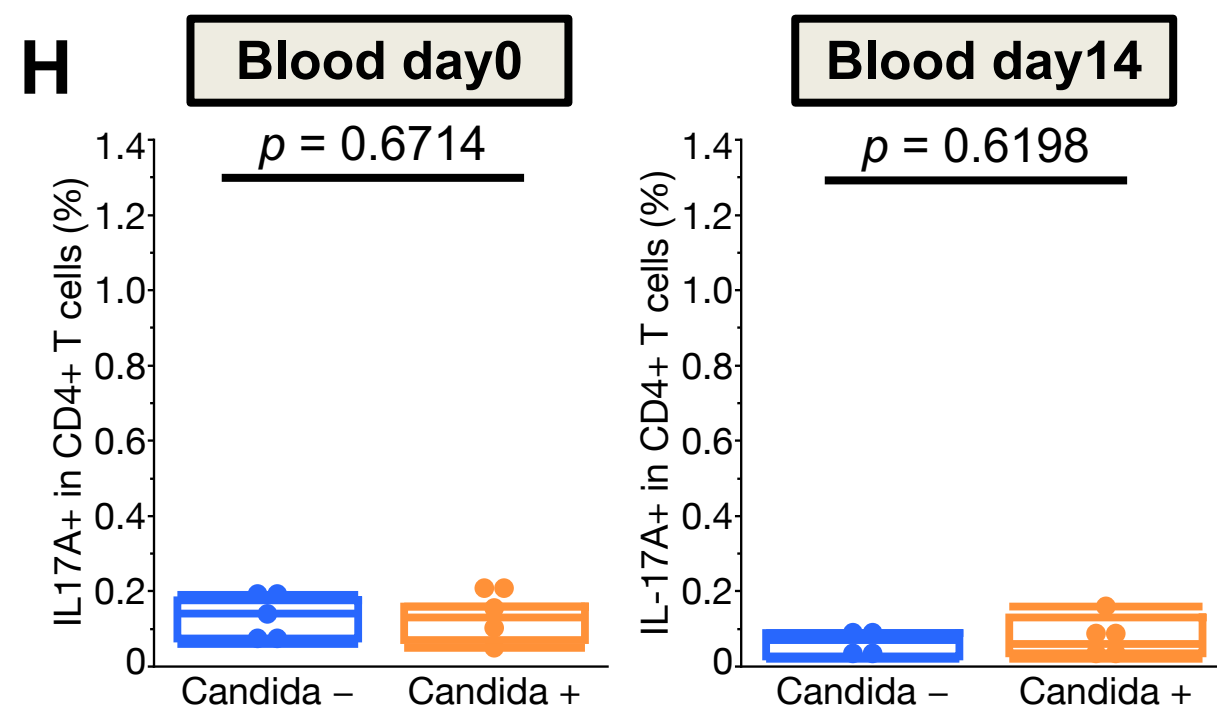
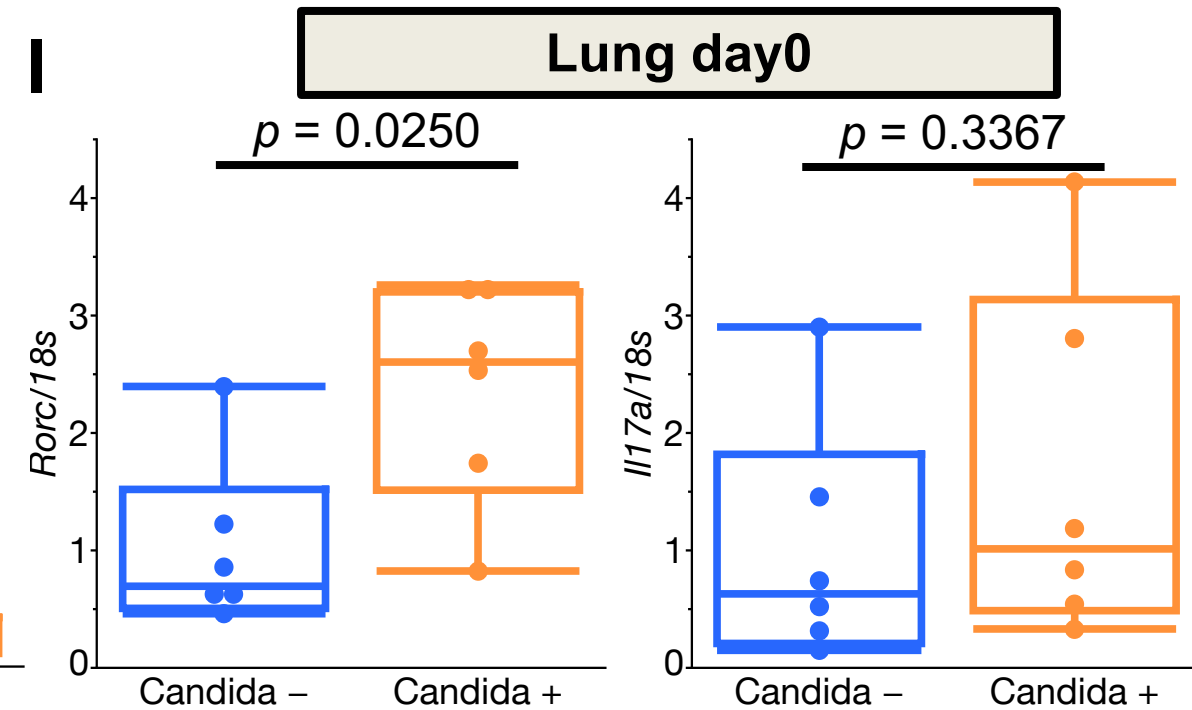
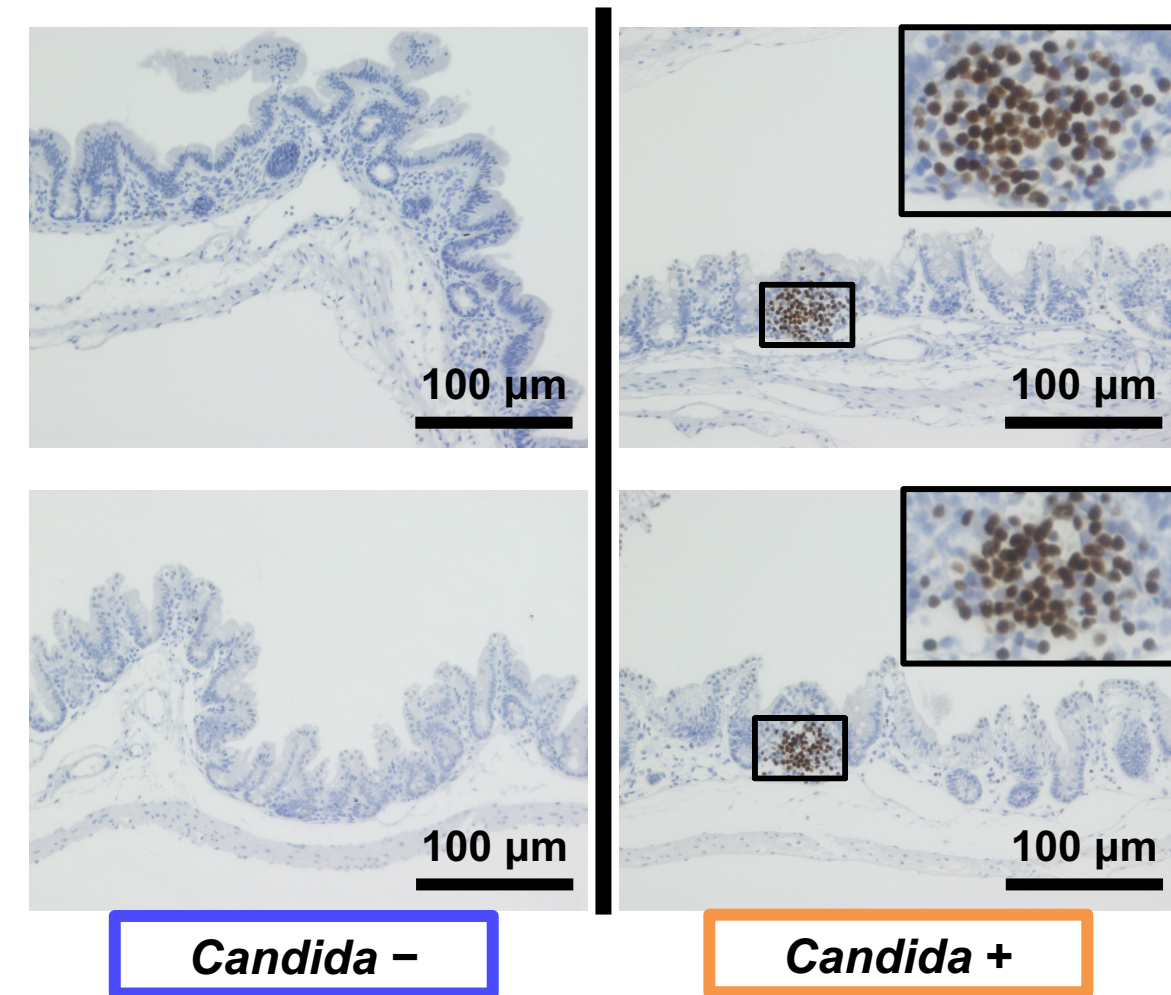
ITS_frd_5	Thermo Fisher Scientific	TCGTCGGCAGCGTCAGATGTGTATAA GAGACAGCTAGGCTATTTAGAGGAA GTAA
ITS_frd_6	Thermo Fisher Scientific	TCGTCGGCAGCGTCAGATGTGTATAA GAGACAGCTTAGTTATTTAGAGGAAG TAA
ITS_frd_7	Thermo Fisher Scientific	TCGTCGGCAGCGTCAGATGTGTATAA GAGACAGCTACGTCATTTAGAGGAAG TAA
ITS_frd_8	Thermo Fisher Scientific	TCGTCGGCAGCGTCAGATGTGTATAA GAGACAGCTTGGTCATTTAGAGGTCG TAA
ITS_rev_1	Thermo Fisher Scientific	GTCTCGTGGGCTCGGAGATGTGTATA AGAGACAGGCTGCGTTCTTCATCGAT GC

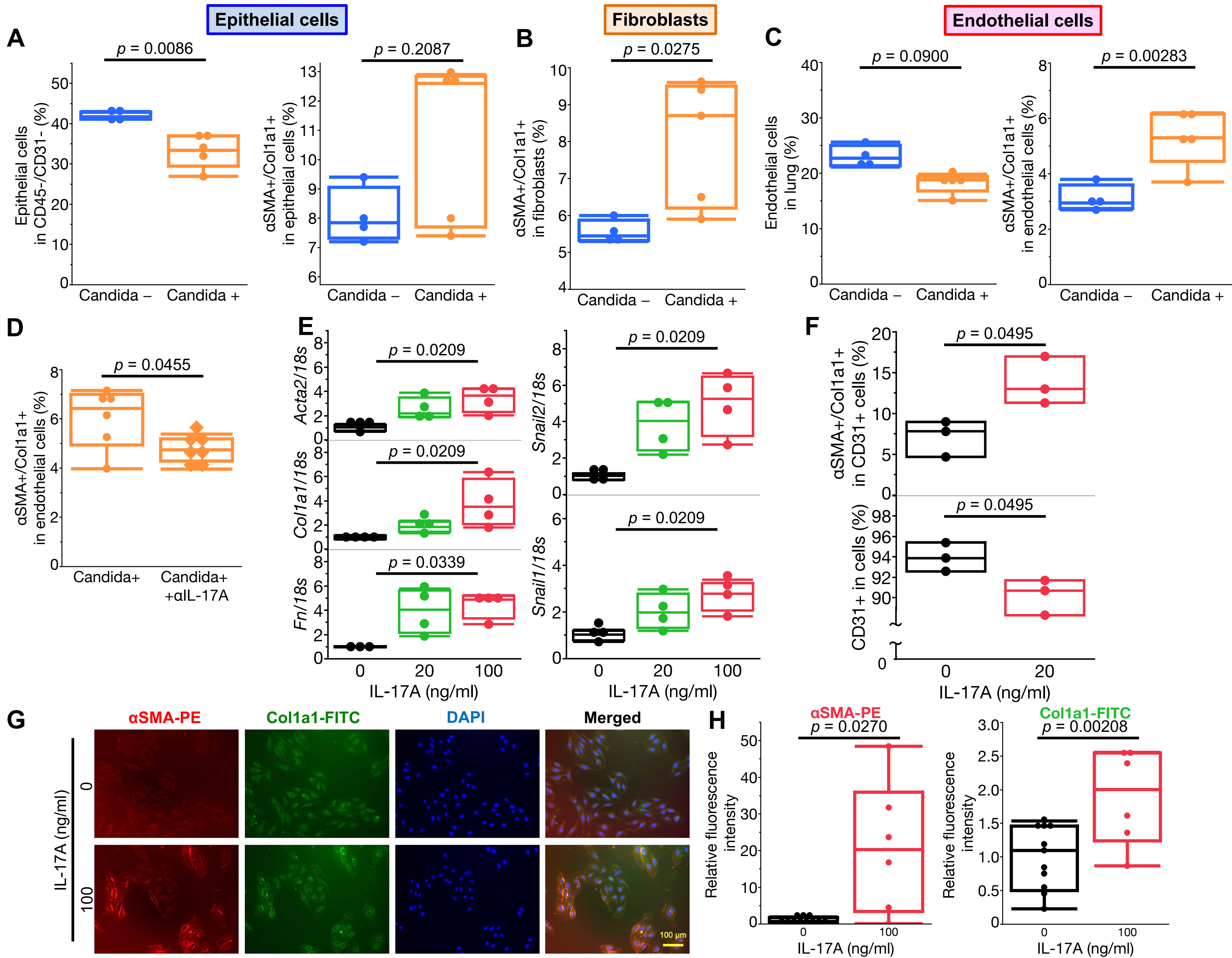
ITS_rev_2	Thermo Fisher Scientific	GTCTCGTGGGCTCGGAGATGTGTATA AGAGACAGGCTGCGTTCTTCATCGAT GG
ITS_rev_3	Thermo Fisher Scientific	GTCTCGTGGGCTCGGAGATGTGTATA AGAGACAGGCTACGTTCTTCATCGAT GC
ITS_rev_4	Thermo Fisher Scientific	GTCTCGTGGGCTCGGAGATGTGTATA AGAGACAGGCTGCGTTCTTCATCGAT GT
ITS_rev_5	Thermo Fisher Scientific	GTCTCGTGGGCTCGGAGATGTGTATA AGAGACAGACTGTGTTCTTCATCGAT GT
ITS_rev_6	Thermo Fisher Scientific	GTCTCGTGGGCTCGGAGATGTGTATA AGAGACAGGCTGCGTTCTTCATCGTT GC

ITS_rev_7	Thermo Fisher Scientific	GTCTCGTGGGCTCGGAGATGTGTATA AGAGACAGGCGTTCTTCATCGATGC
-----------	--------------------------	---





A**B****C****D****E****F****G****H****I****J**



Intestinal tract

Lung

Dysbiosis

+

C. albicans proliferation

Bleomycin

EMT

Fibroblast
activation

EndMT

IL-17A producing
Th17 cells
(IL-17A⁺/CD3⁺/CD4⁺)

Rorc expressing
Th17-skewed lymphocytes
(*Rorc*⁺/IL-17A⁻/CD3⁺/CD4⁺)

Naive T cells

Fibrosis ↑

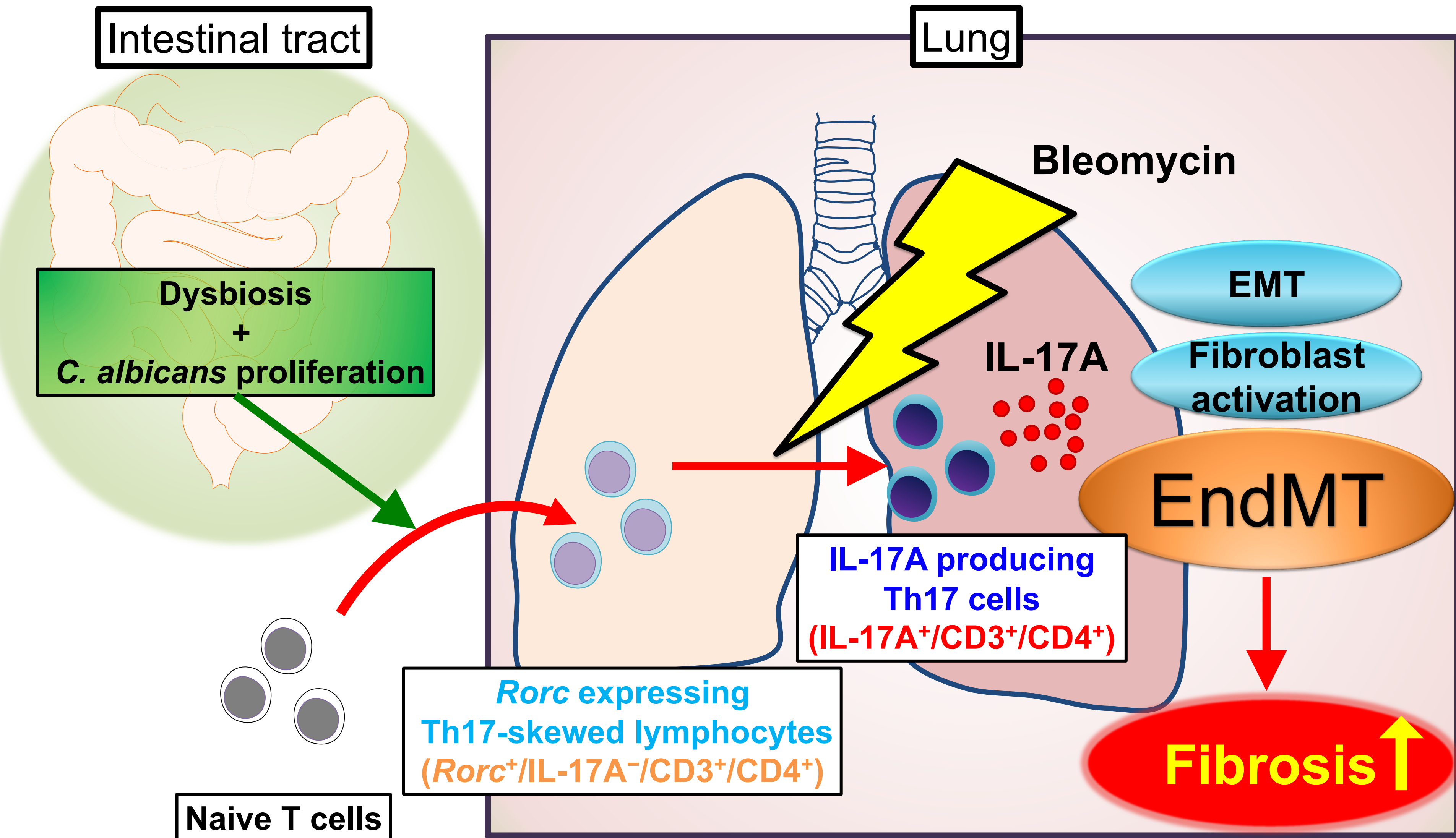
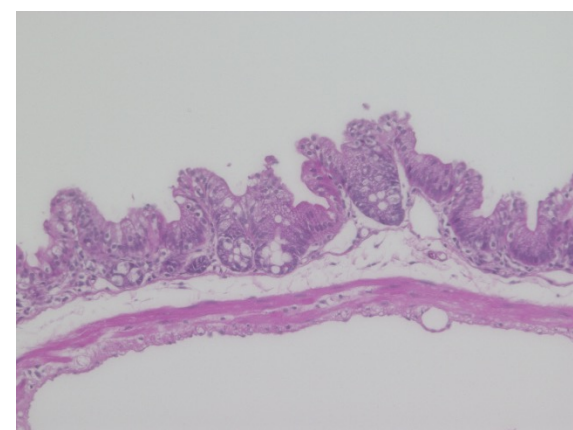
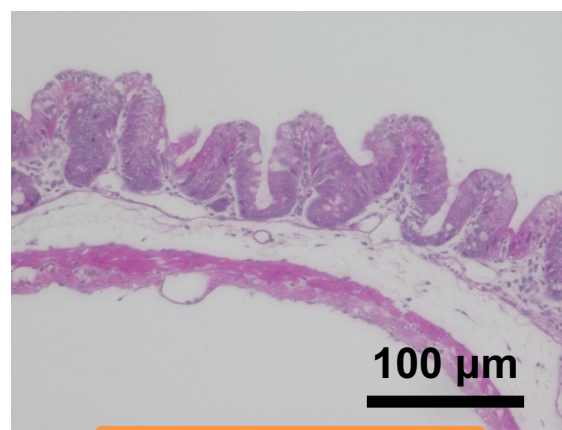


Fig. S1

A



Candida –



Candida +

B

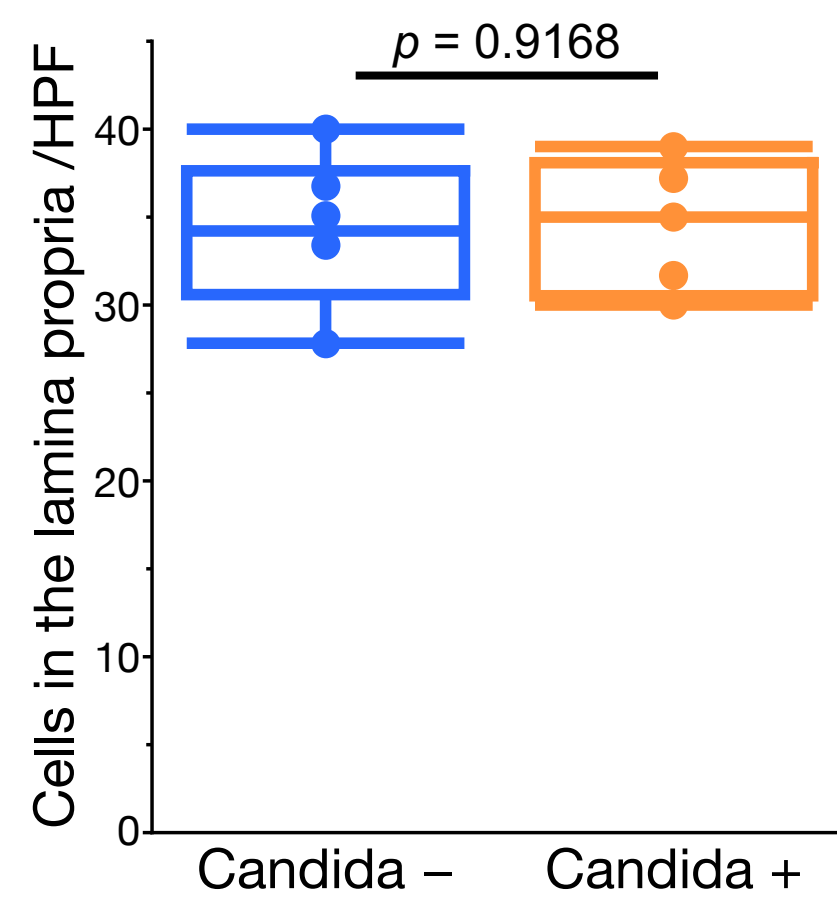
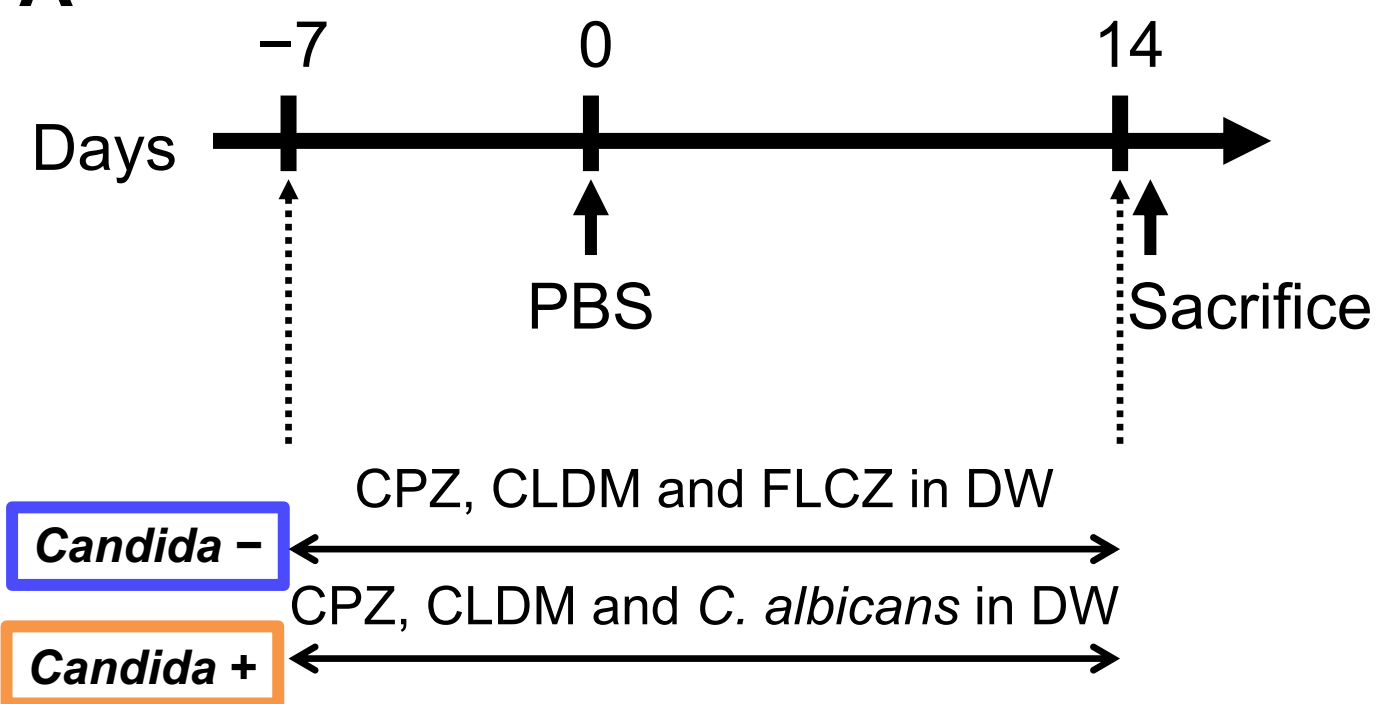
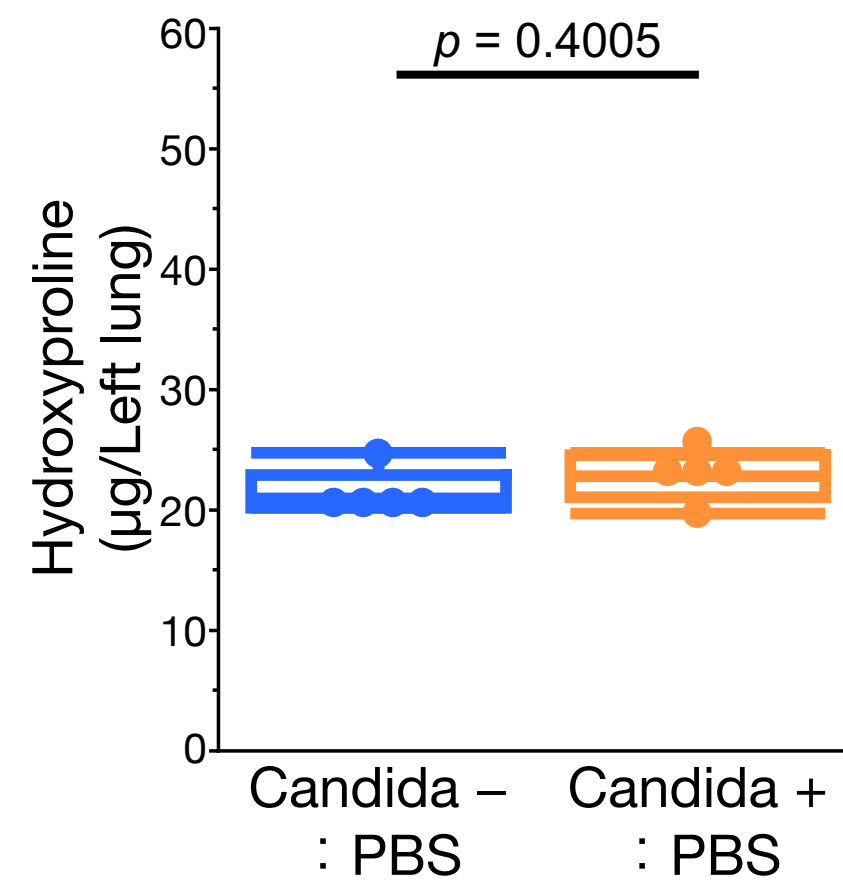


Fig. S2

A



B



C:

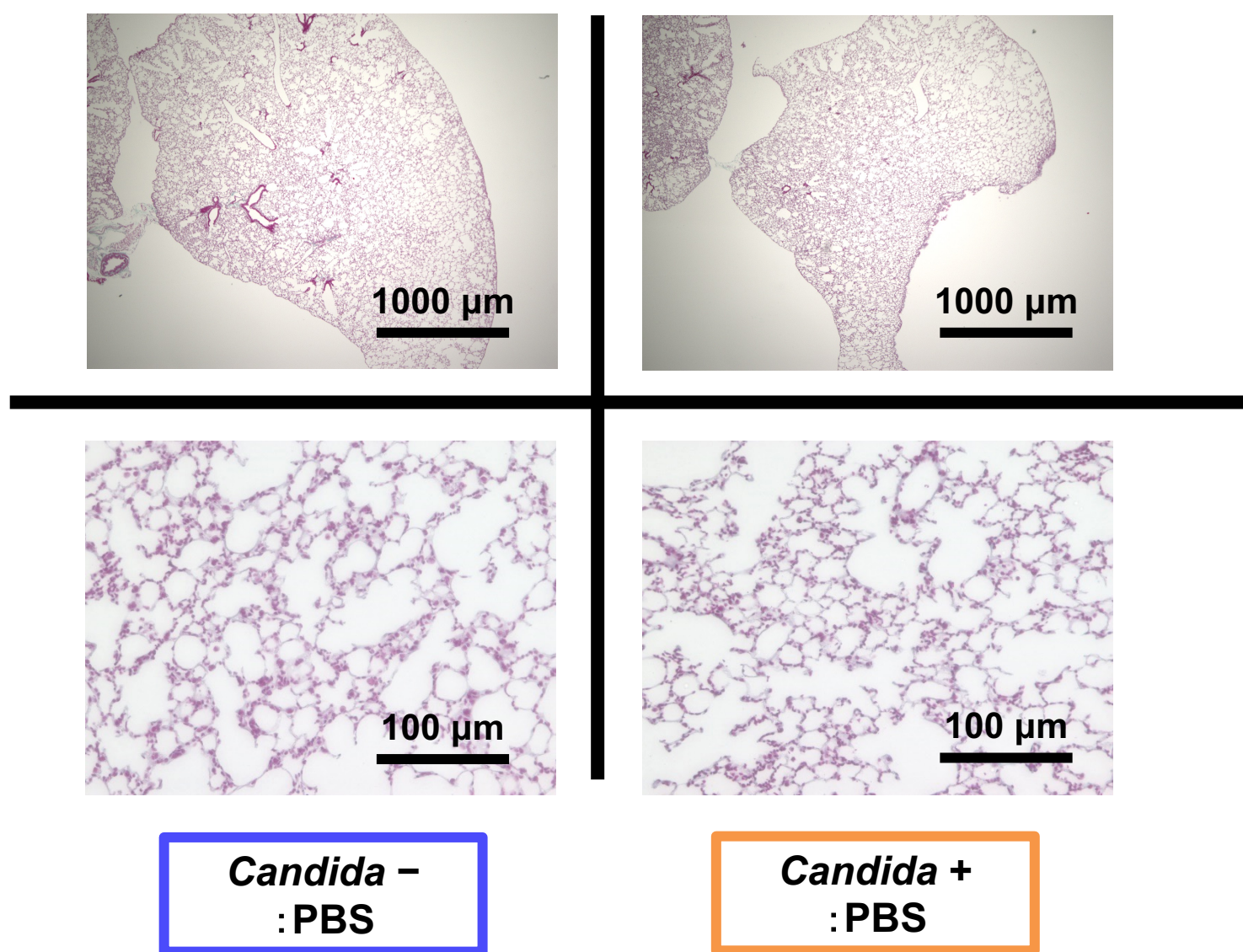
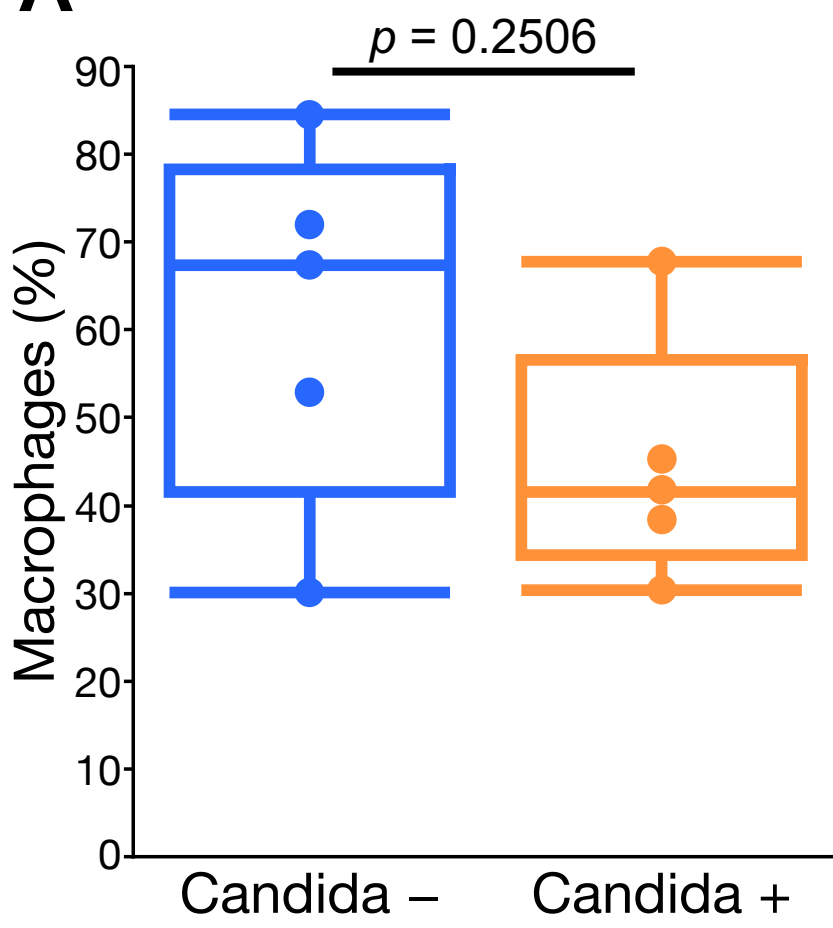
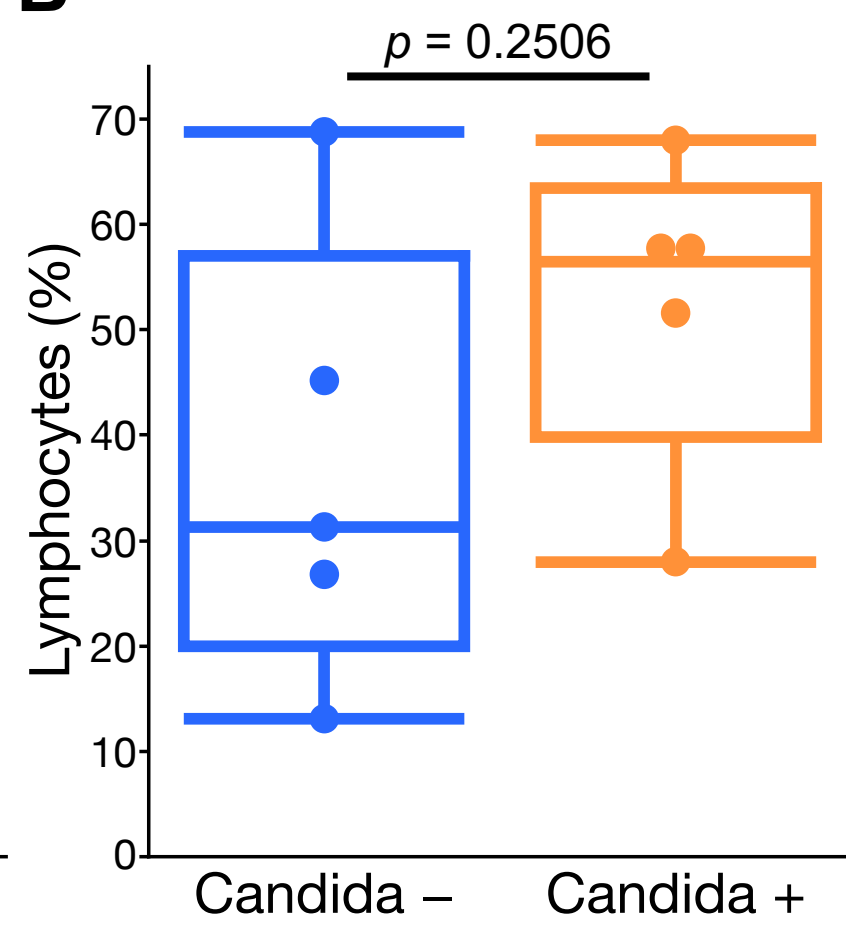


Fig. S3

A



B



C

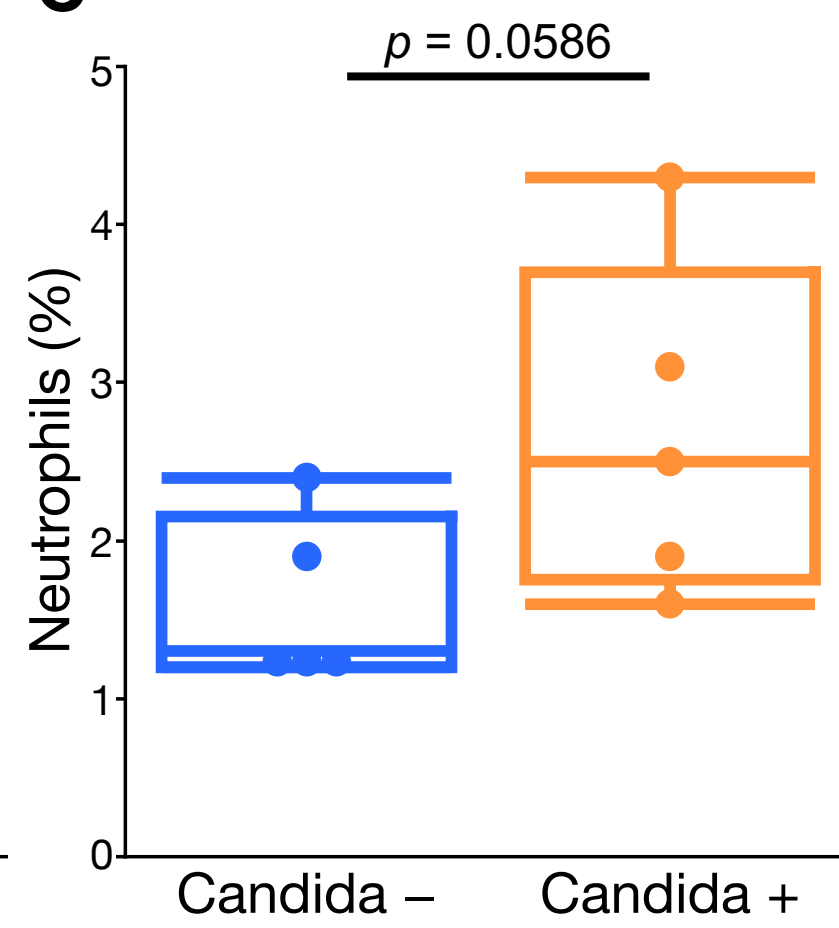
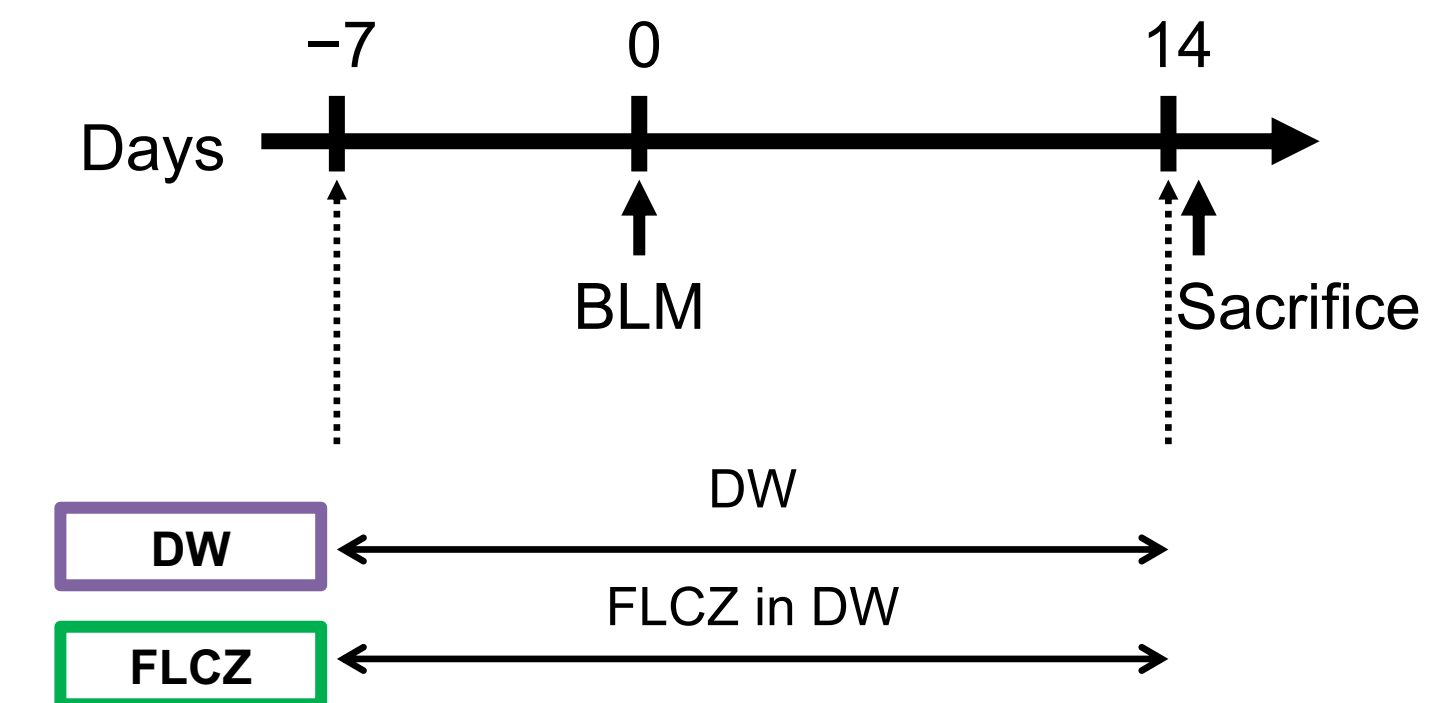


Fig. S4

A



B

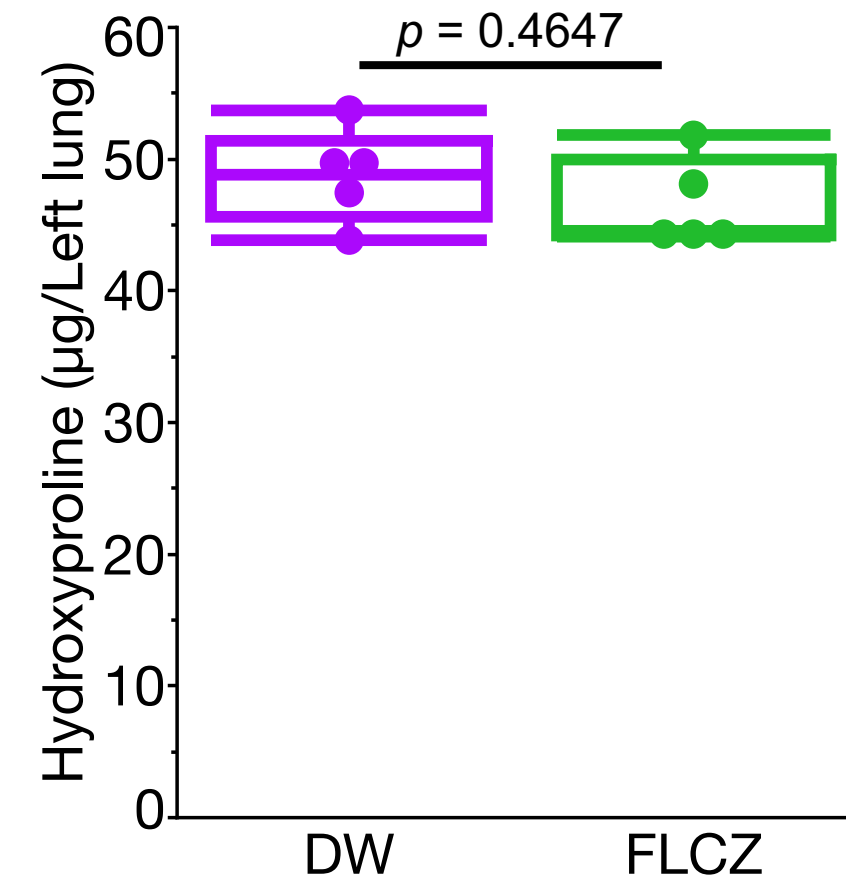


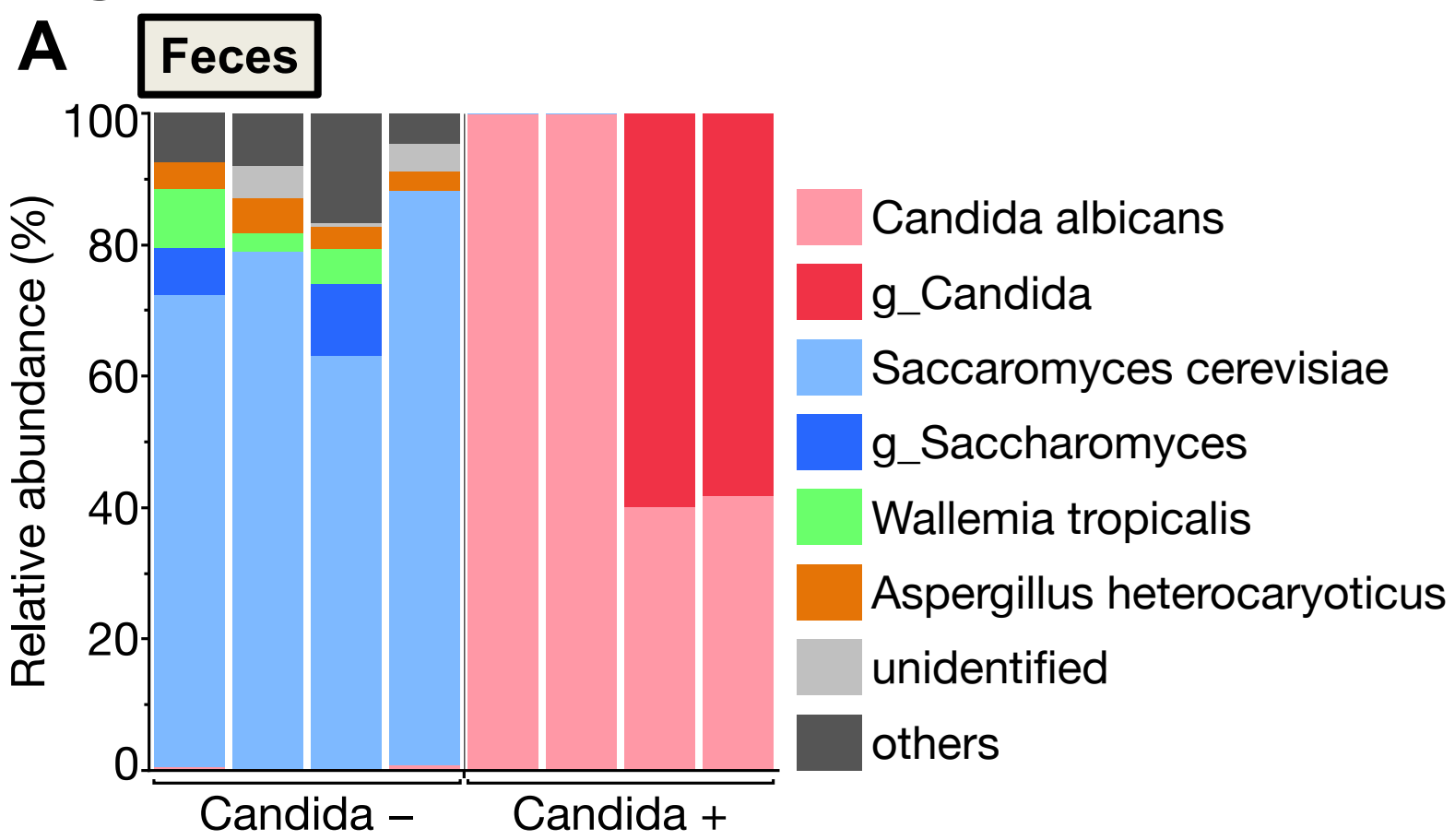
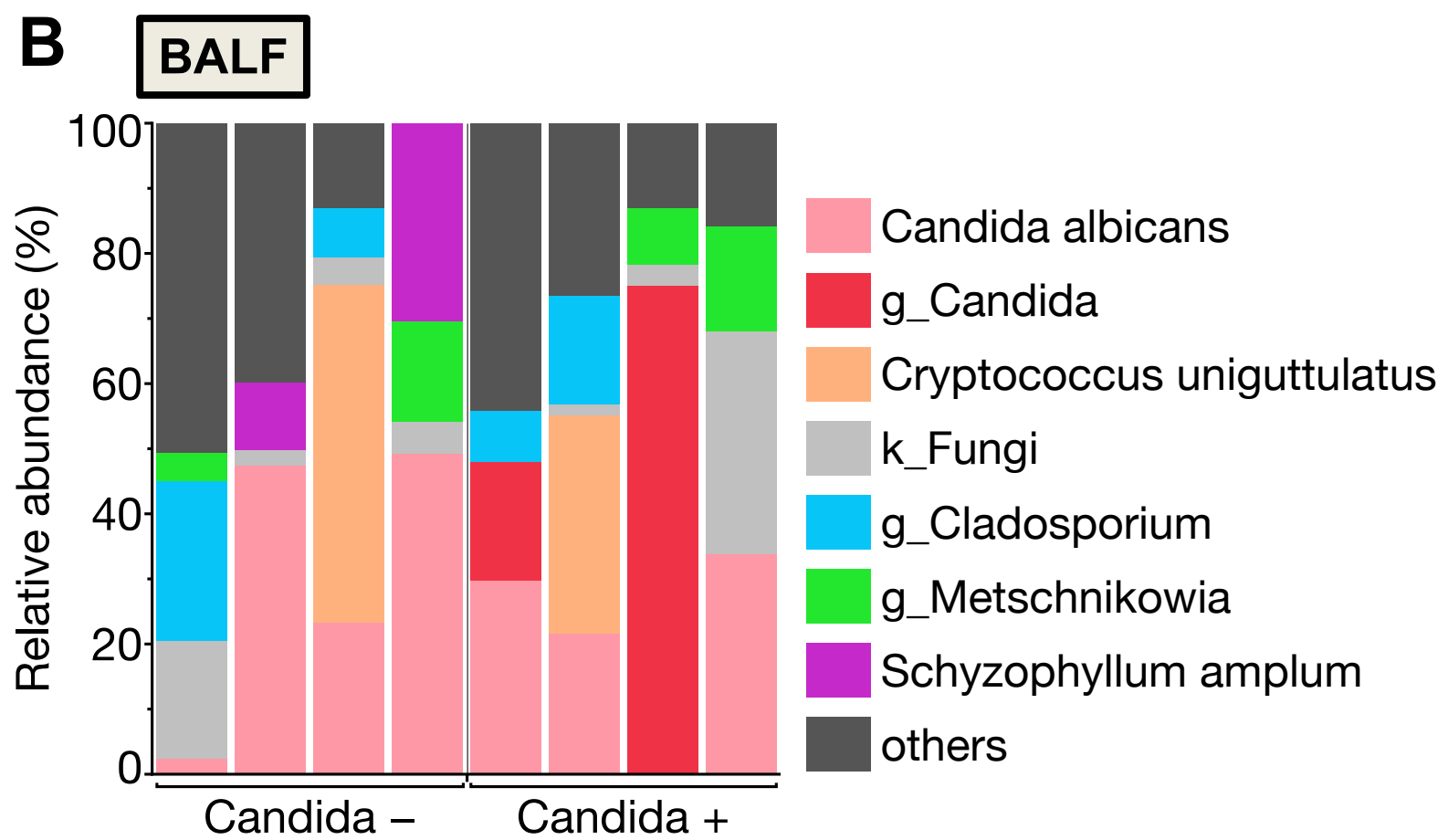
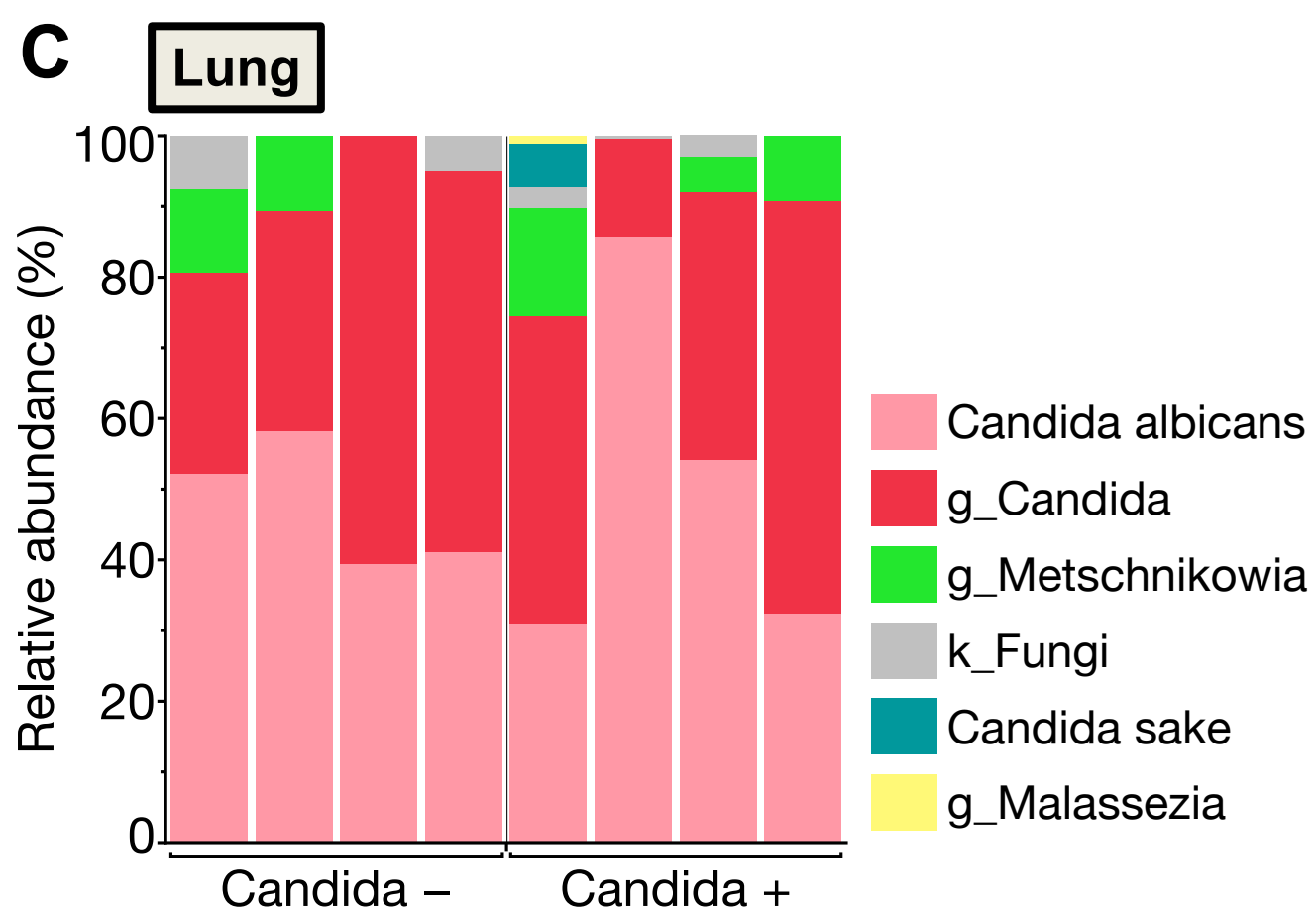
Fig. S5**A****B****C**

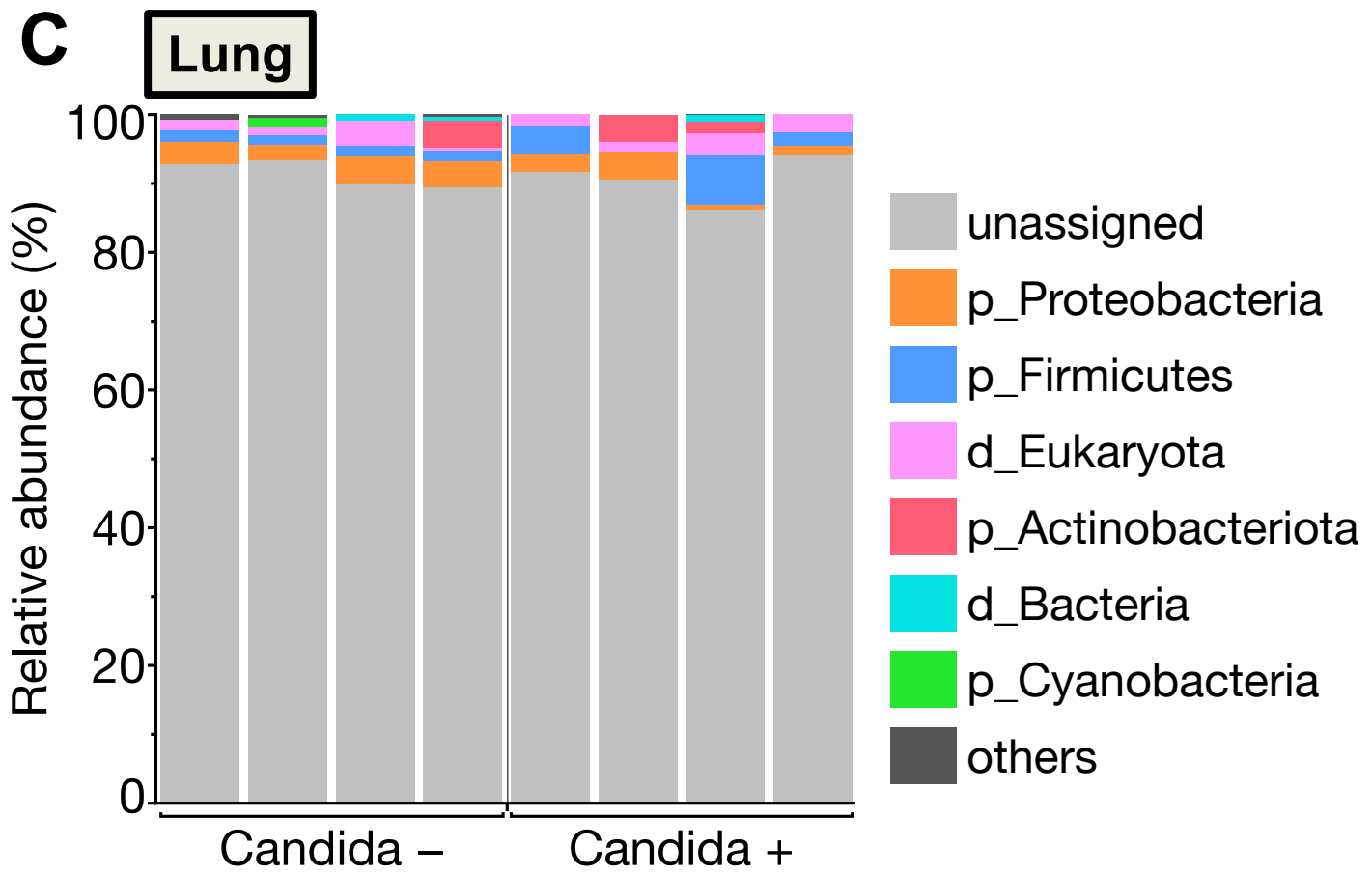
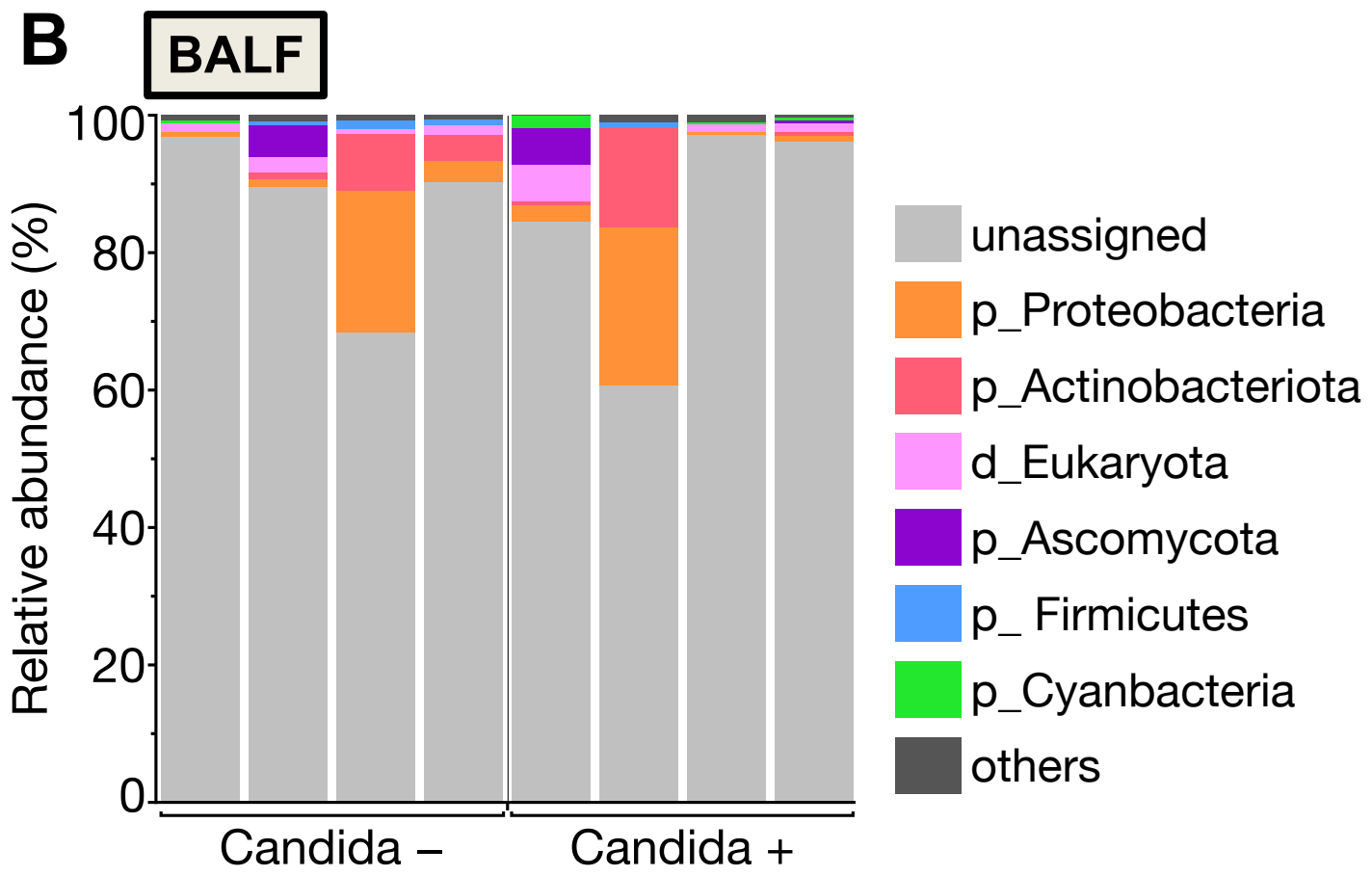
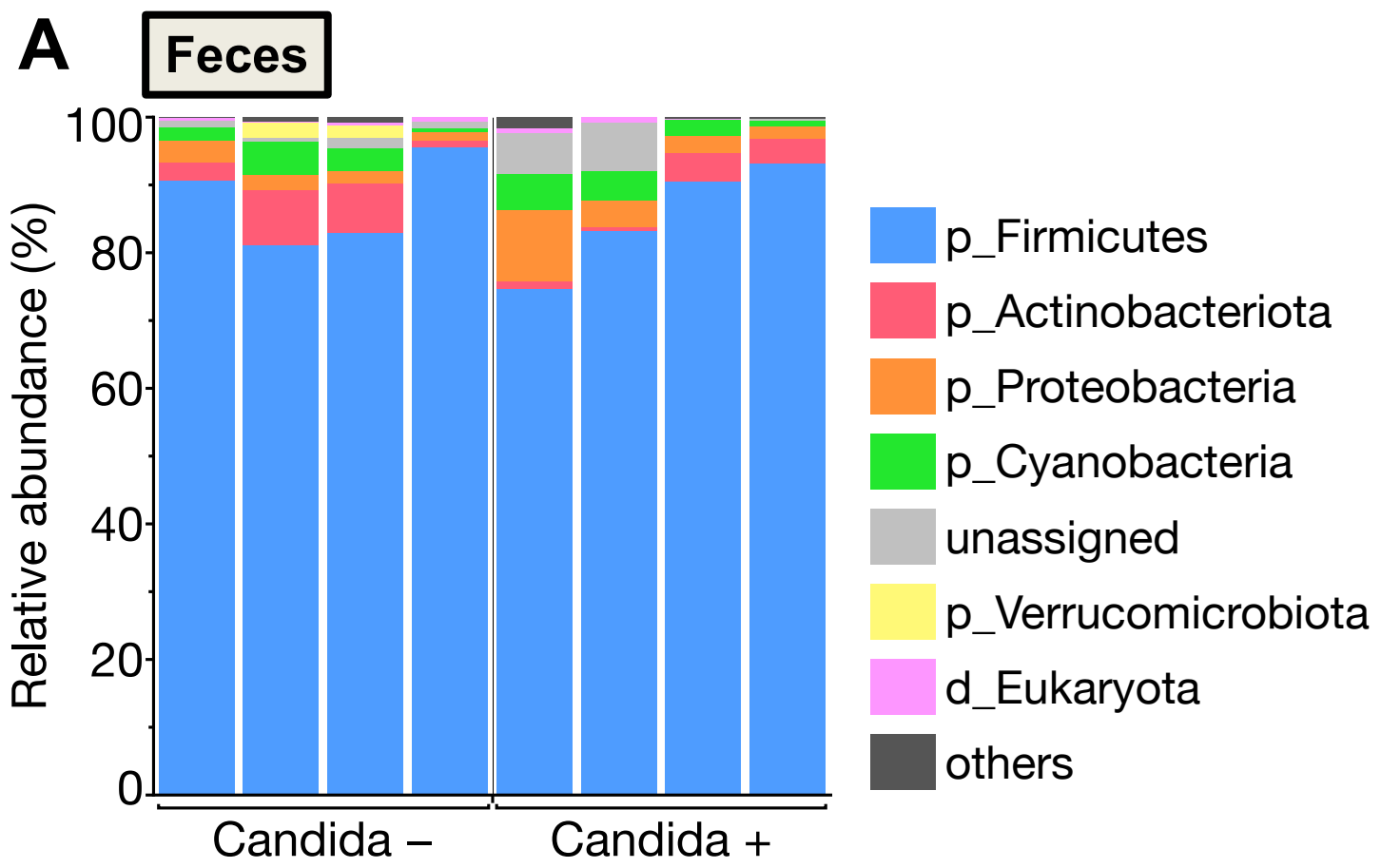
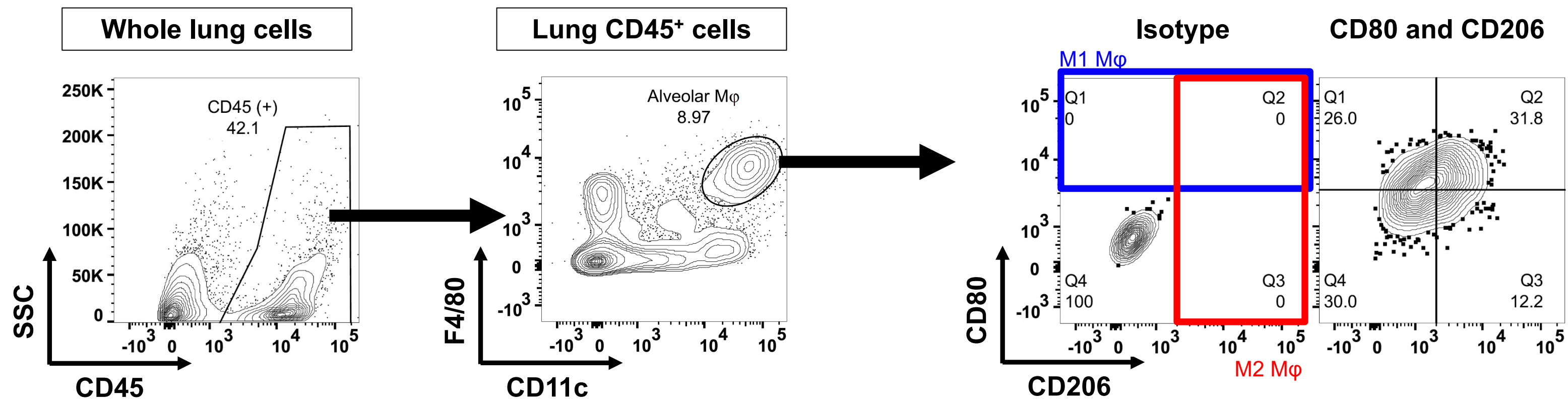
Fig. S6

Fig. S7

A



B

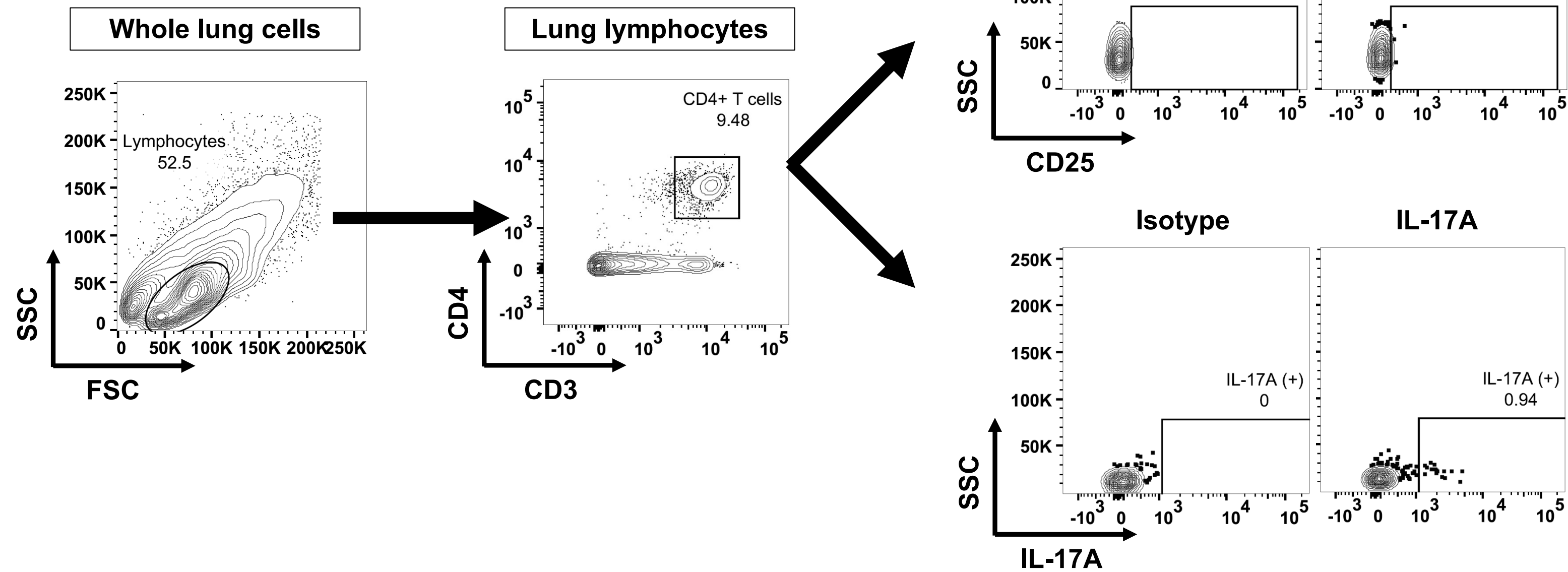


Fig. S8

A

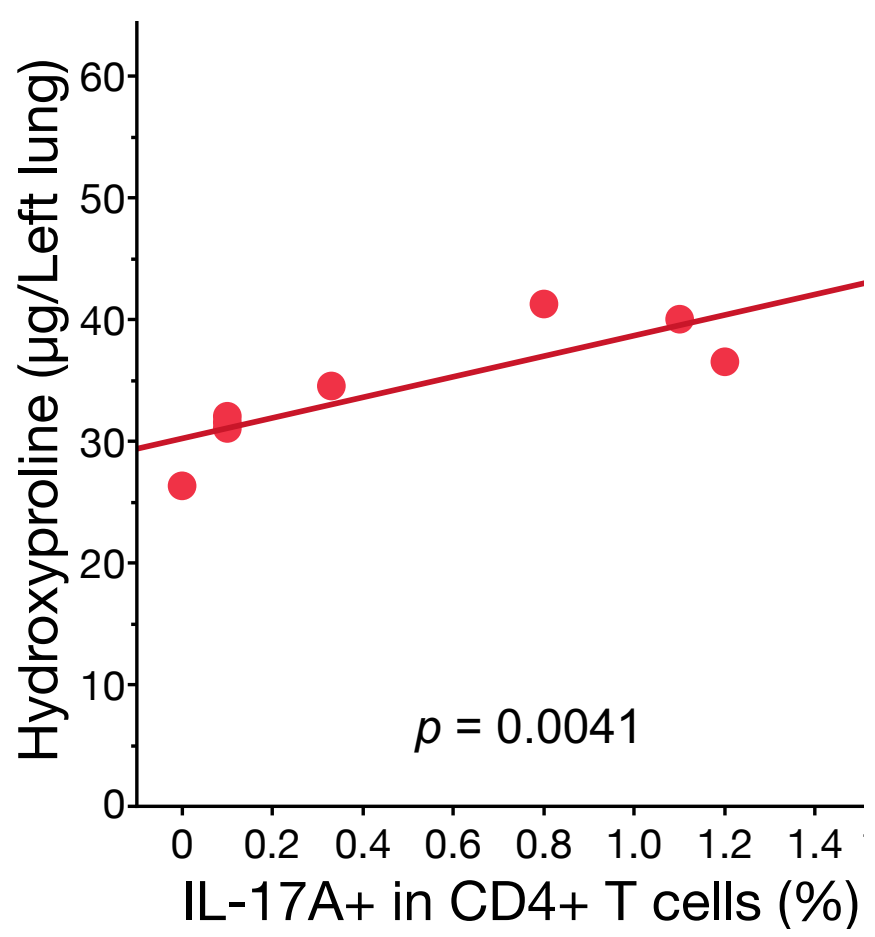
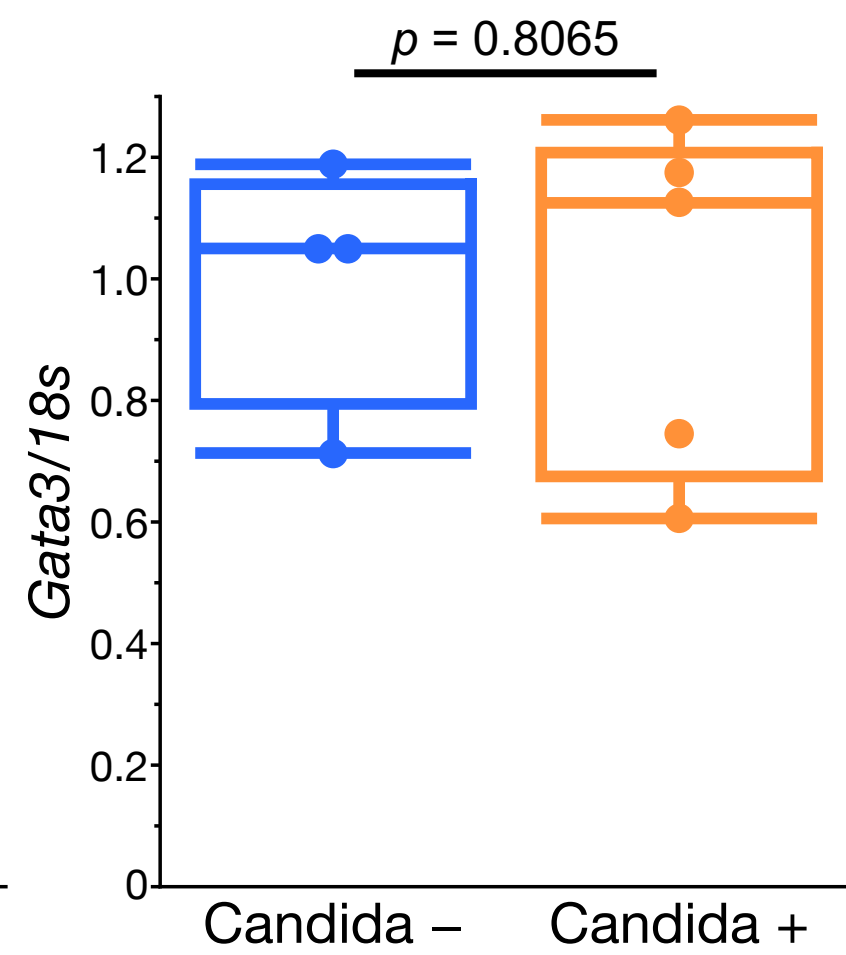
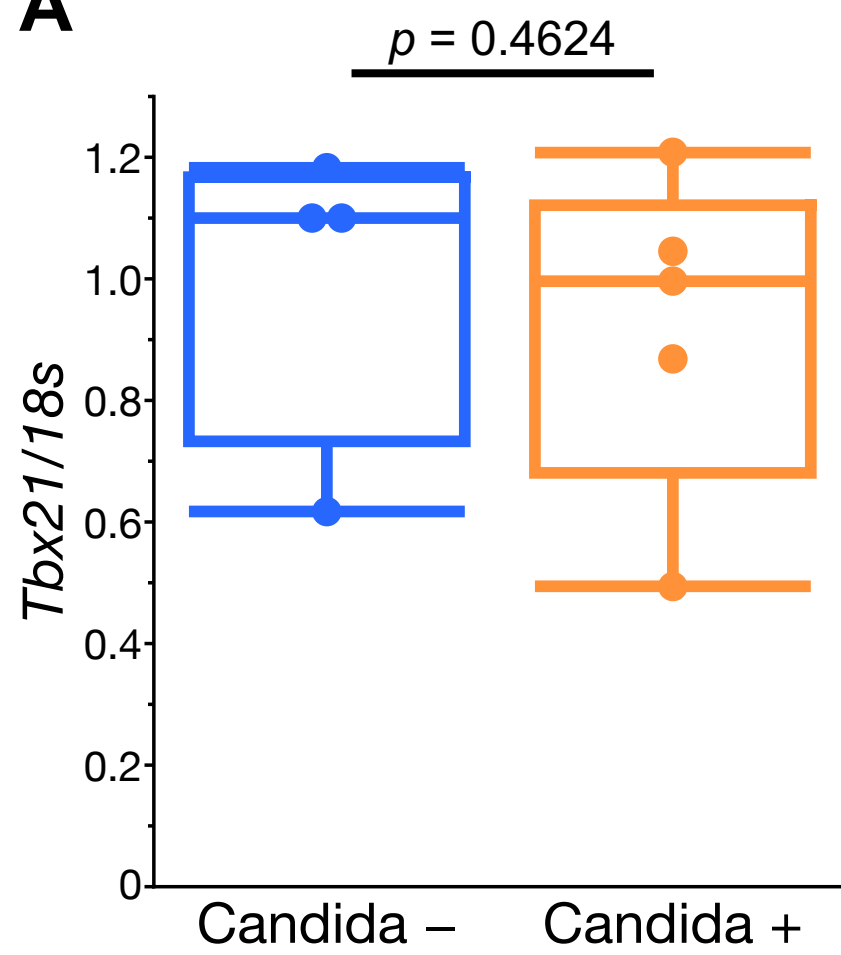
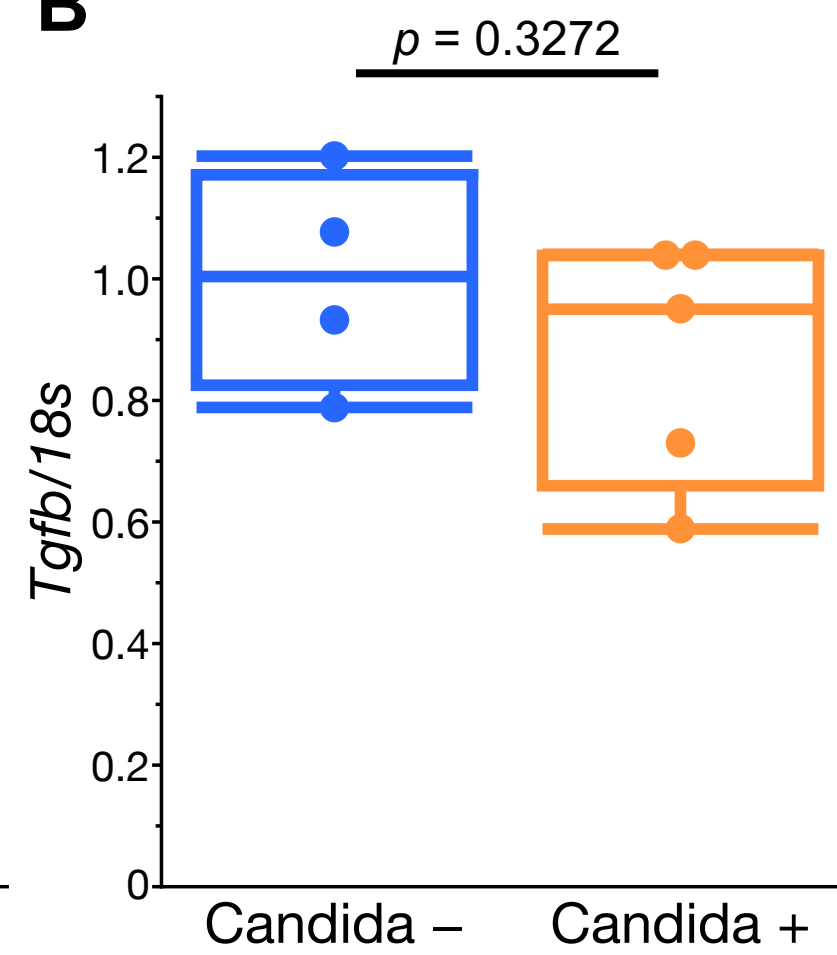


Fig. S9

A



B



C

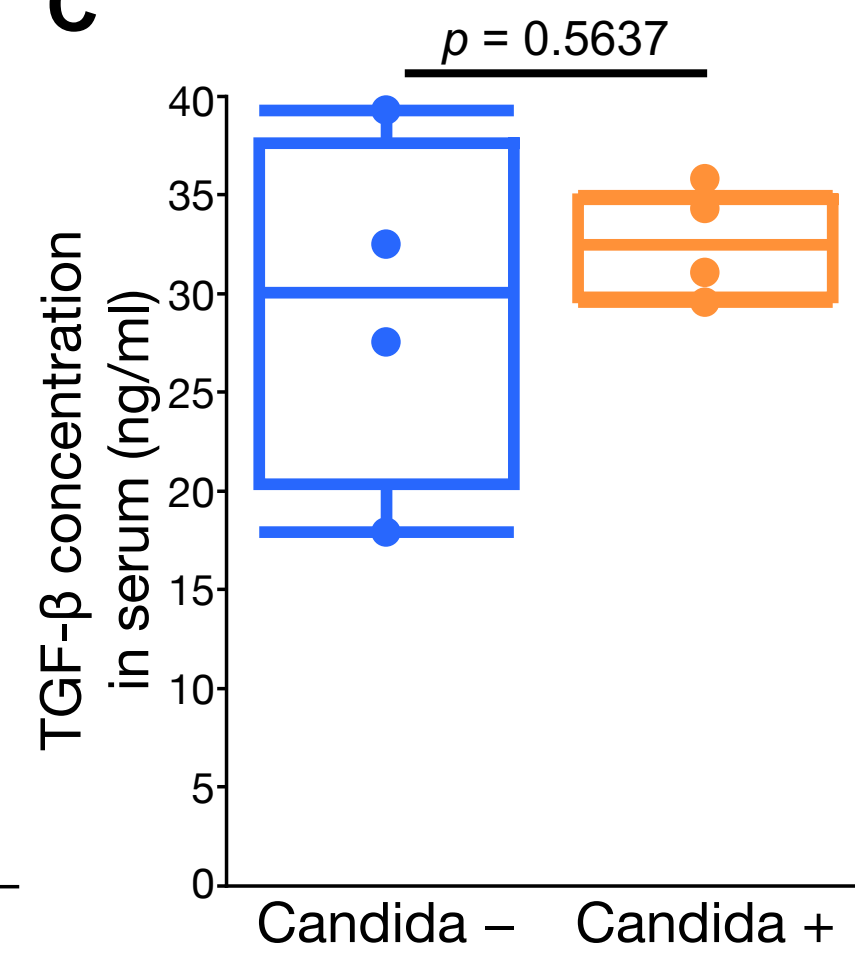


Fig. S10

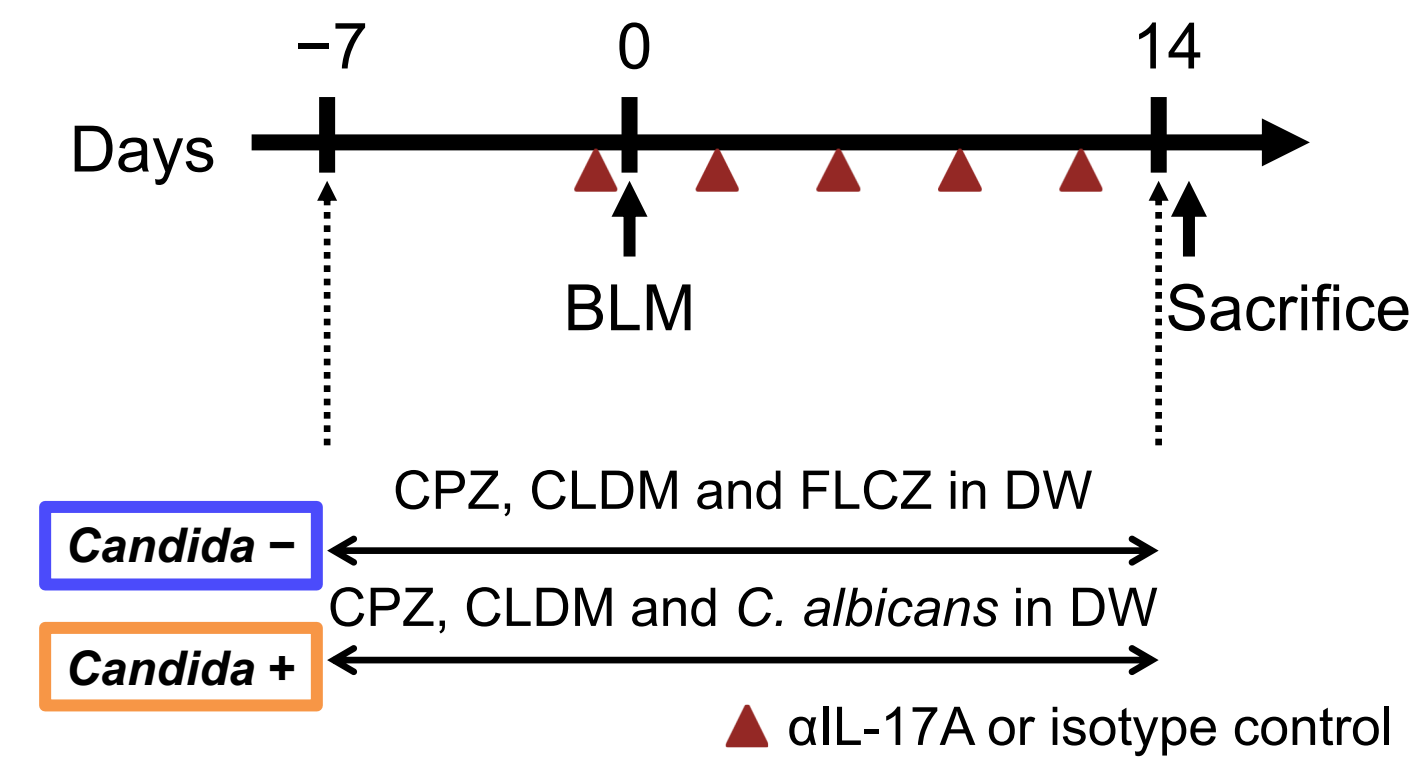


Fig. S11

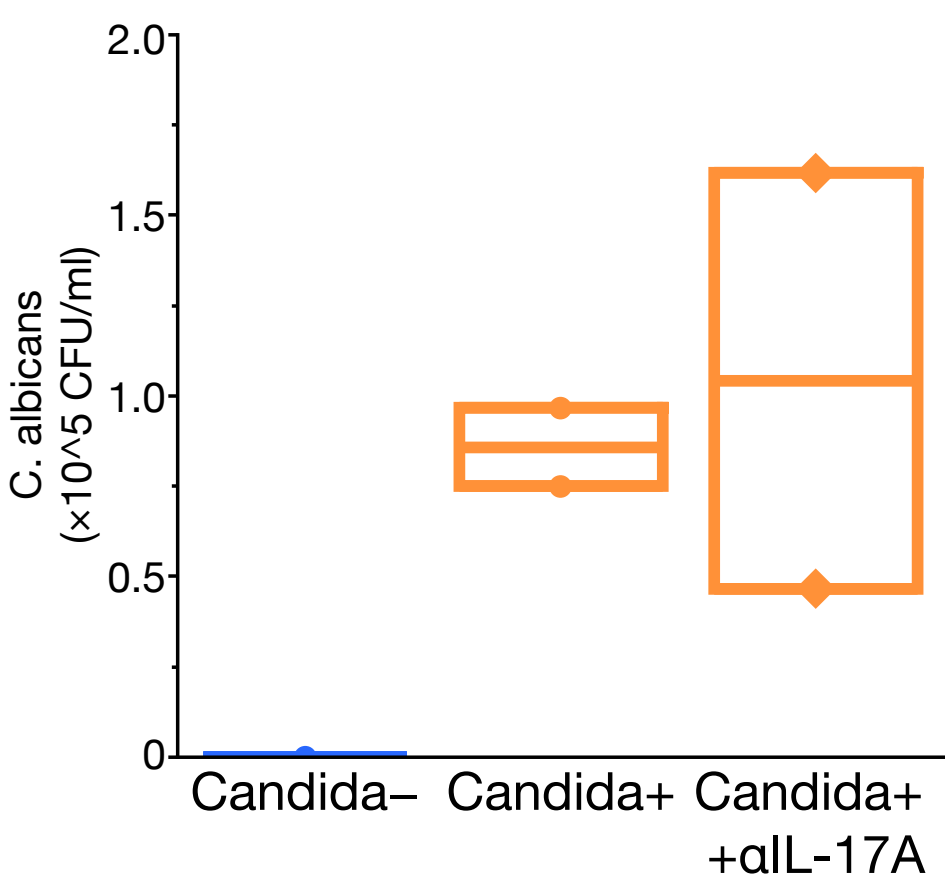
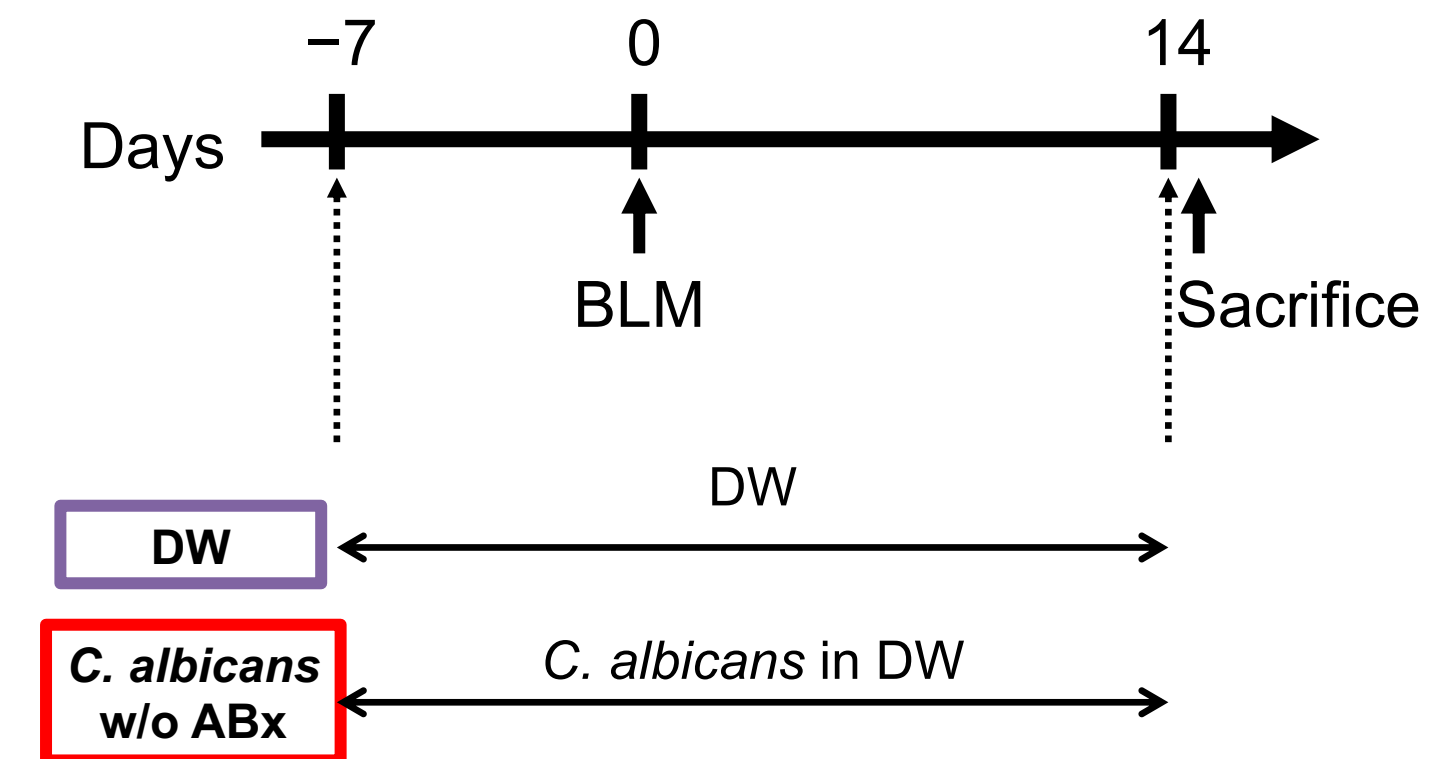
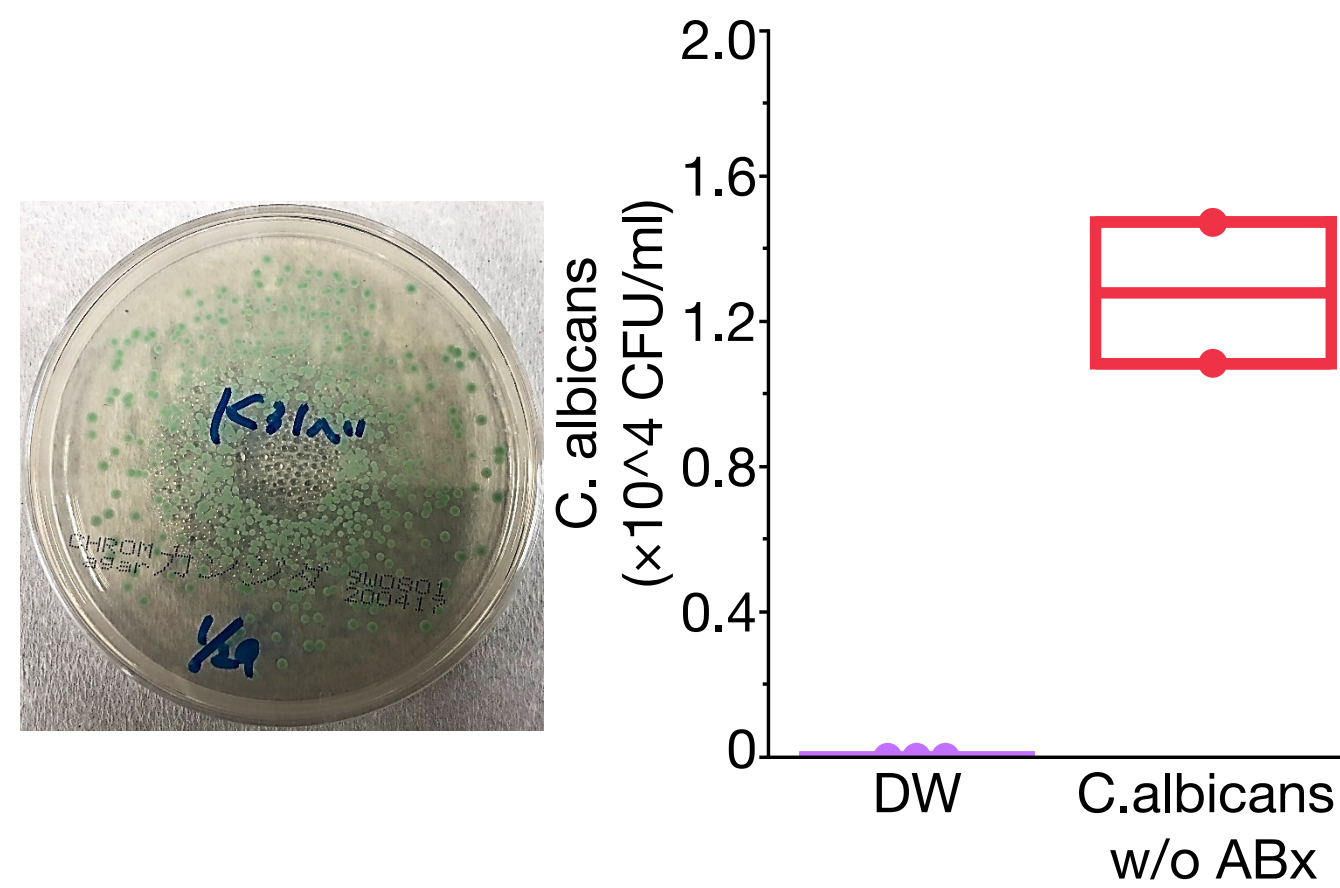


Fig. S12

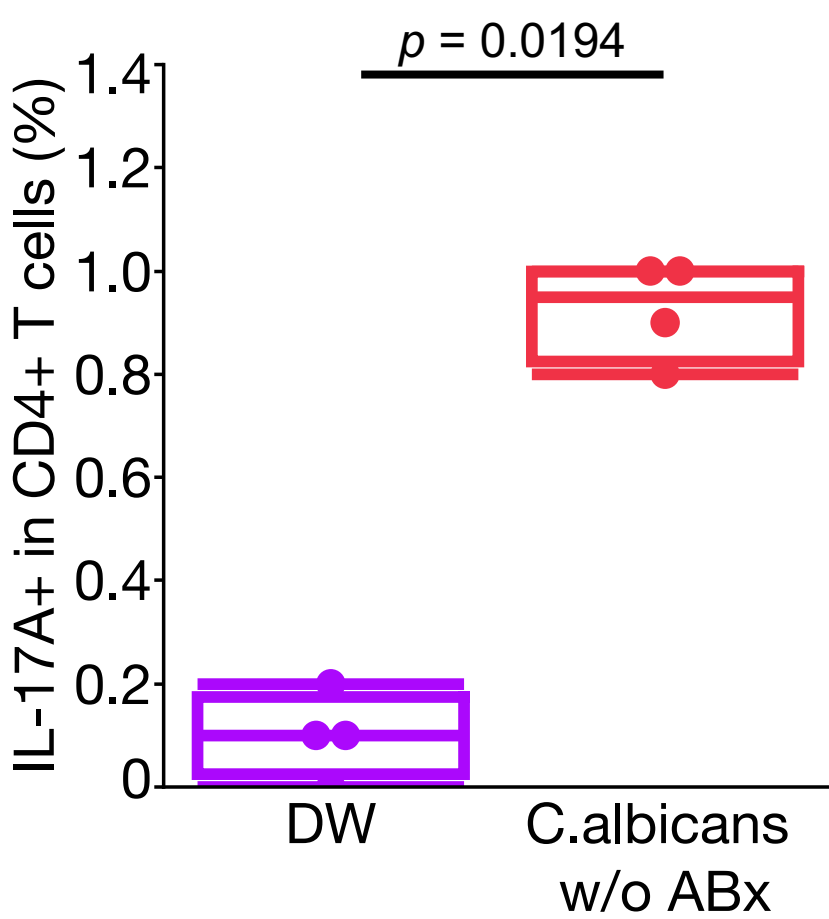
A



B



C



D

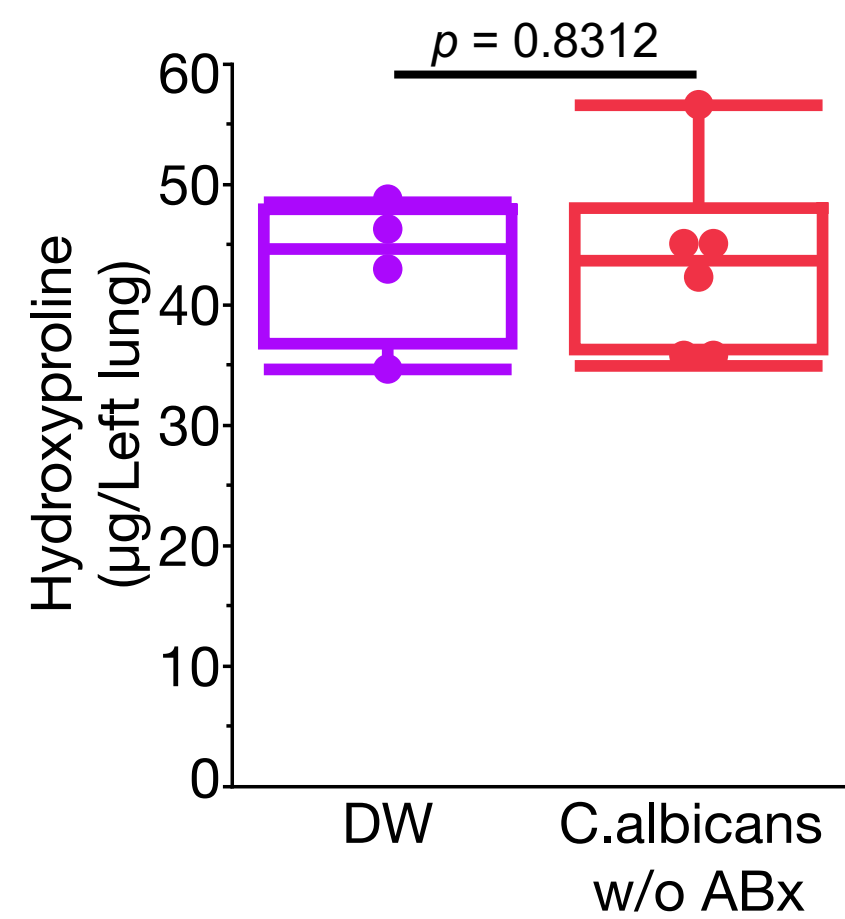
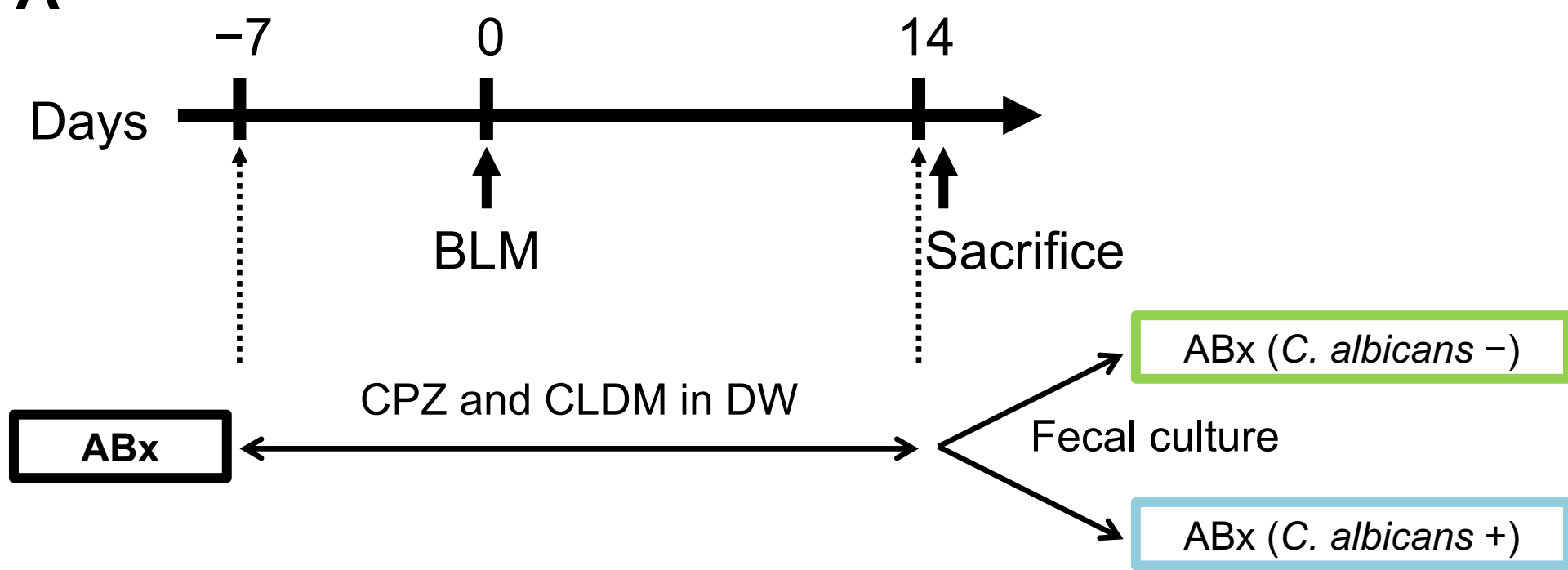


Fig. S13

A



B

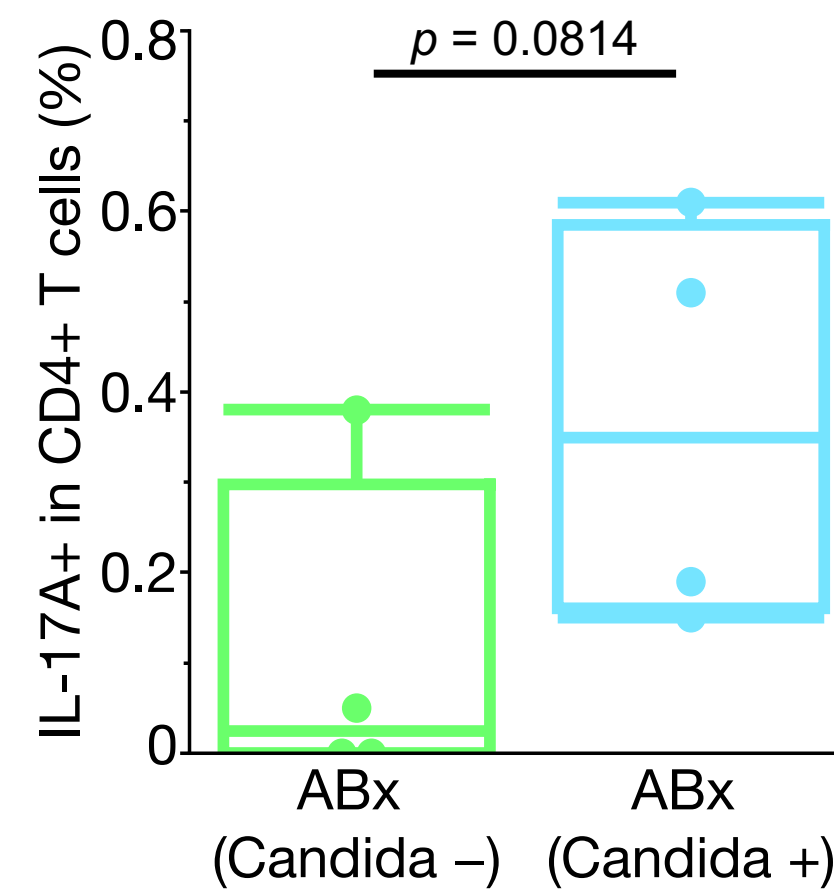
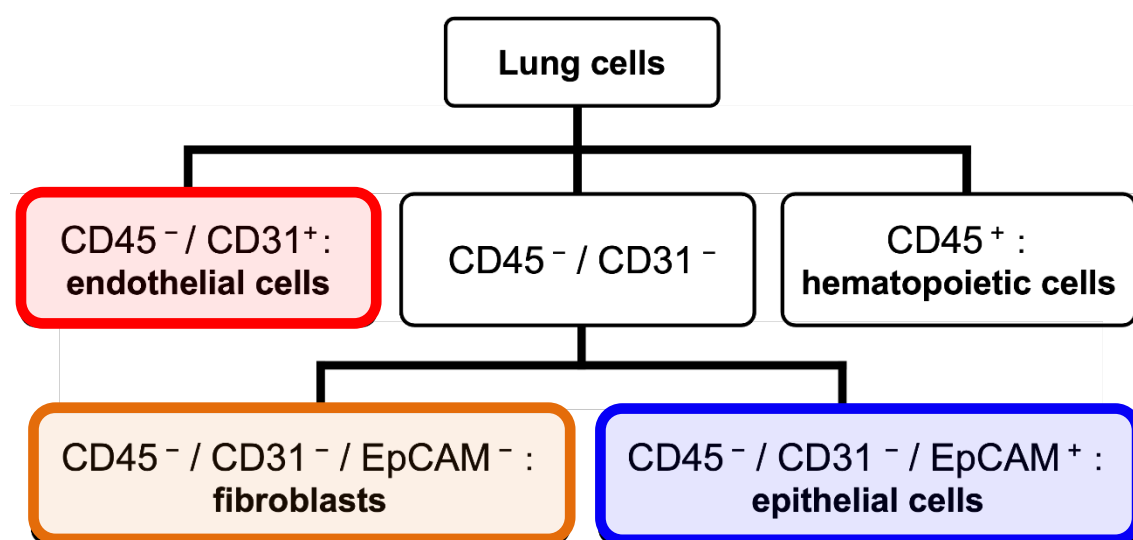
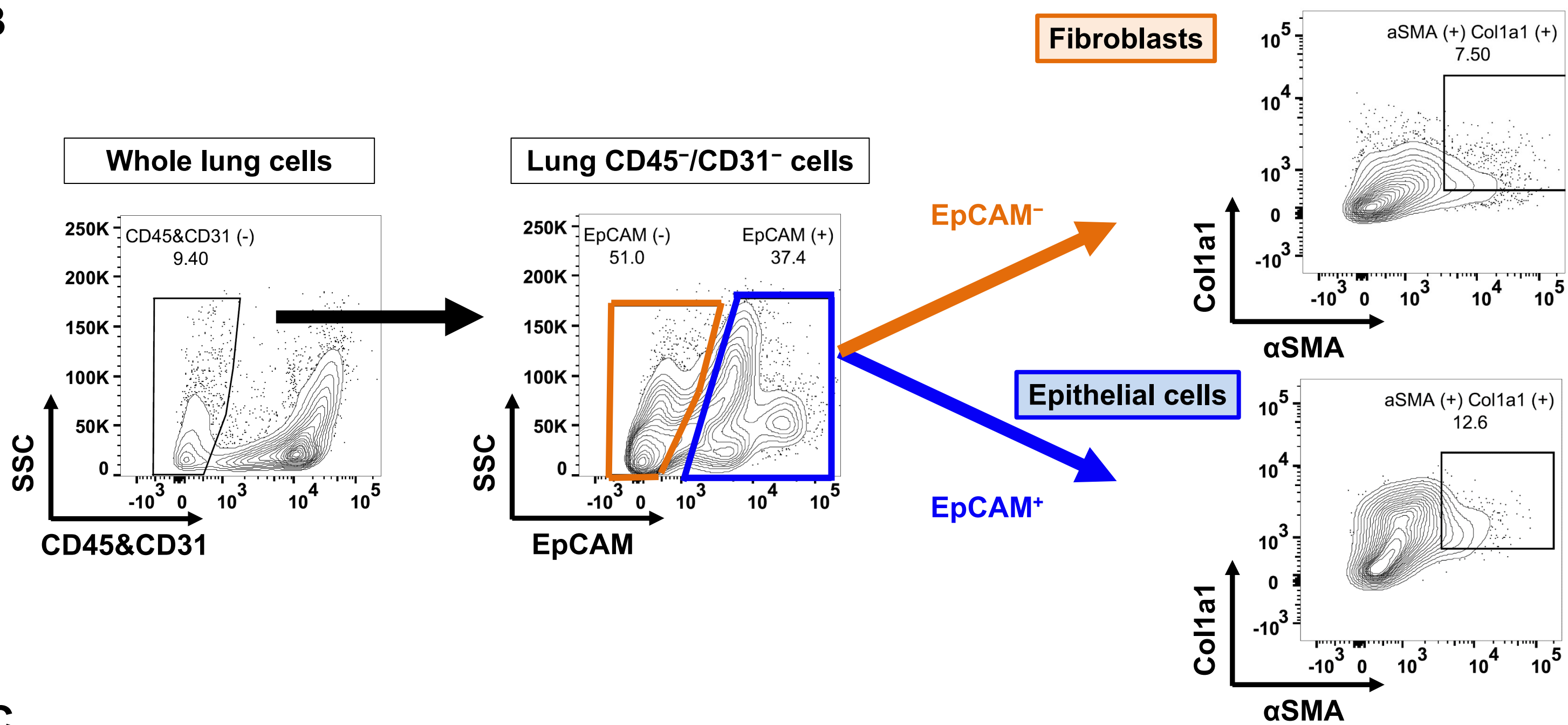


Fig. S14

A



B



C

